



Lawrence Berkeley Laboratory

UNIVERSITY OF CALIFORNIA

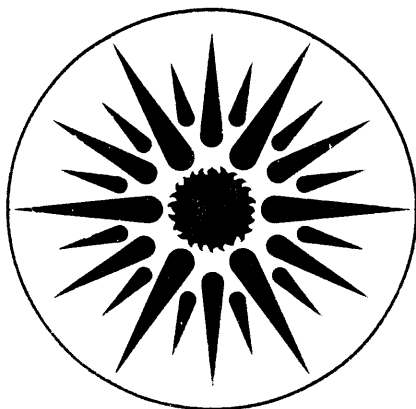
APPLIED SCIENCE DIVISION

Report No. LBL-2971

Improved Heat Recovery and High-Temperature Clean-Up for Coal-Gas Fired Combustion Turbines

N.M. Barthelemy* and S. Lynn
(*M.S. Thesis)

July 1991



APPLIED SCIENCE
DIVISION

DISTRIBUTION OF THIS DOCUMENT IS UNRESTRICTED

DISCLAIMER

This document was prepared as an account of work sponsored by the United States Government. Neither the United States Government nor any agency thereof, nor The Regents of the University of California, nor any of their employees, makes any warranty, express or implied, or assumes any legal liability or responsibility for the accuracy, completeness, or usefulness of any information, apparatus, product, or process disclosed, or represents that its use would not infringe privately owned rights. Reference herein to any specific commercial product, process, or service by its trade name, trademark, manufacturer, or otherwise, does not necessarily constitute or imply its endorsement, recommendation, or favoring by the United States Government or any agency thereof, or The Regents of the University of California. The views and opinions of authors expressed herein do not necessarily state or reflect those of the United States Government or any agency thereof or The Regents of the University of California and shall not be used for advertising or product endorsement purposes.

Lawrence Berkeley Laboratory is an equal opportunity employer.

LBL--31079

DE92 000841

**IMPROVED HEAT RECOVERY AND
HIGH-TEMPERATURE CLEAN-UP FOR
COAL-GAS FIRED COMBUSTION TURBINES**

by

Nicholas M. Barthelemy and Scott Lynn

Applied Science Division
Lawrence Berkeley Laboratory
University of California
Berkeley, California 94720

July 1991

This work was supported by the Morgantown Energy Technology Center, Assistant Secretary for Fossil Energy, Office of Coal Utilization, Advanced Research and Technology Development, Division of Surface Coal Gasification through the U.S. Department of Energy under Contract No. DE-AC03-76SF00098.

MASTER

DISTRIBUTION OF THIS DOCUMENT IS UNLIMITED



**Improved Heat Recovery and High-Temperature Clean-up for
Coal-Gas Fired Combustion Turbines**

Copyright © 1991

by

Nicolas M. Barthelemy

**The Government reserves for itself and
others acting on its behalf a royalty free,
nonexclusive, irrevocable, world-wide
license for governmental purposes to publish,
distribute, translate, duplicate, exhibit,
and perform any such data copyrighted by
the contractor.**

**The U.S. Department of Energy has the right to use this thesis
for any purpose whatsoever including the right to reproduce
all or any part thereof**

Improved Heat Recovery and High-Temperature Clean-up for Coal Gas Fired Combustion Turbines

Nicolas M. Barthelemy

ABSTRACT

This study investigates the performance of an Improved Heat Recovery Method (IHRM) applied to a coal-gas fired power-generating system using a high-temperature clean-up. This heat recovery process has been described by Higdon and Lynn (1990). The IHRM is an integrated heat-recovery network that significantly increases the thermal efficiency of a gas turbine in the generation of electric power. Its main feature is to recover both low- and high-temperature heat reclaimed from various gas streams by means of evaporating heated water into combustion air in an air saturation unit. This unit is a packed column where compressed air flows countercurrently to the heated water prior to being sent to the combustor, where it is mixed with coal-gas and burned. The high water content of the air stream thus obtained reduces the amount of excess air required to control the firing temperature of the combustor, which in turn lowers the total work of compression and results in a higher thermal efficiency.

Three designs of the IHRM were developed to accommodate three different gasifying processes. The performances of those designs were evaluated and compared using computer simulations. The highest thermal efficiency was obtained with an air-blown fluidized-bed gasifying process and is close to 46%. Efficiencies reached with oxygen-blown fluidized-bed and Texaco gasifying processes are respectively 45% and 42.2%. Those values are based on the High Heating Value for coal, and on an effective turbine inlet temperature of 2100°F. The efficiencies obtained with the IHRM are substantially higher those yielded by other heat-recovery technologies using the same gasifying processes. The study also revealed that the IHRM compares advantageously to most advanced power-generation technologies currently available or tested commercially. Cost estimations were not included in this study, since our main concern was to investigate the potential of the IHRM as an advanced power-generation technology. It would be necessary to deal with those considerations later in the investigation.

ACKNOWLEDGEMENTS

This research was supported by the Assistant Secretary for Fossil Energy, Office of Coal Utilization, Division of Surface Coal Gasification of the U.S. Department of Energy under Contract No. DE-AC03-76SF00098.

I am very grateful to my advisor, Professor Scott Lynn, who conceived the idea of the Improved Heat Recovery Method and was always available when I needed help. I greatly appreciated his wealth of knowledge and learned a lot about process design and power generation at his contact. I also appreciated his patience regarding the (hopefully improving!) quality of my English and the intensive editing that it induced.

Working with my fellow labmates Dave Koch, John Markels, Dr. Dan Newman, Andy Ting and Gavin Towler was a broadening experience from all points of view. I especially appreciated the generous assistance of Dr. Dan Newman, who showed me the way out of the computer mazes I got myself in several times.

TABLE OF CONTENTS

CHAPTER 1: INTRODUCTION	1
1.1 Coal, Gas Turbines and Power Generation	1
1.2 Coal Gasification	2
1.3 Coal-Gas Clean-Up	5
1.4 Heat-Recovery Methods	5
CHAPTER 2: RESEARCH OBJECTIVES AND TECHNICAL APPROACH	11
2.1 Research Objectives	11
2.2 Technical Approach	11
2.3 Convergence Procedure	13
2.4 Simulation Monitoring	14
2.5 Modules Overview	15
2.5.1 Thermodynamics Module	15
2.5.2 Shift Module	17
2.5.3 Compressor Module	18
2.5.4 Turbine Module	18
2.5.5 Combustion-Chamber Module	19
2.5.6 Air-Saturation-Unit Module	20
2.5.7 Heat-Exchanger Module	20
2.5.8 Boiler	21
2.5.9 Contactor Module	21
2.5.10 Clean-up Module	21
2.5.11 Partial-Quench Module	22
2.5.12 Total-Quench Module	22
2.5.13 Mixer and Splitter Modules	22
2.5.14 Coal Gasification	23
CHAPTER 3: DESIGN AND FLOW SHEET DESCRIPTIONS	24
3.1 "Core" Section	24
3.2 Clean-Up Section	26
3.3 Heat-Recovery Section	27
CHAPTER 4: PRELIMINARY STUDIES	31
4.1 Computation of the System Thermal Efficiency	31
4.2 Oxygen Plant Energy Requirements	32
4.3 Optimization of the cooling water flows	34
4.4 Optimization of the ASU Number of Theoretical Stages	36
4.5 Other Optimizations	37
4.6 Water-Gas-Shift Reaction	38
CHAPTER 5:	
ANALYSES OF THE RESULTS OBTAINED FOR EACH GASIFYING PROCESS	40
5.1 Assumptions and Approximations Used in the Simulations Base Cases	40
5.2 Design Based on a Texaco-Type Gasifier	40
5.3 Design Based on an Oxygen-Blown Fluidized-Bed Gasifier	46
5.4 Design Based on an Air-Blown Fluidized-Bed Gasifier	51
CHAPTER 6: SENSITIVITY ANALYSES	56

6.1	Efficiencies and Compression-Work Split	56
6.1.1	Design Based on the Texaco-Type Gasifying Processes	56
6.1.2	Design Based on the Air-Blown Fluidized-Bed Gasifying Process	58
6.1.3	Design Based on the Oxygen-Blown Fluidized-Bed Gasifying Process	60
6.1.4	Comparison of the Results for the Three Designs	62
6.2	Efficiency and System Pressure	64
6.2.1	Design Based on The Texaco Gasifying Process	64
6.2.2	Designs Based on the Fluidized-Bed Gasifying Processes	66
6.2.3	Comparison of the Results Obtained for the Different Designs	69
6.3	Efficiency and Clean-Up Temperature	69
6.3.1	Design Based on the Texaco-Type Gasifying Process	71
6.3.2	Designs Based on the Fluidized-Bed Gasifying Processes	71
6.3.3	Comparison of the Results Obtained for the Three Designs	75
6.4	Efficiencies and Effective Turbine-Inlet Temperature	77
CHAPTER 7: OTHER SENSITIVITY ANALYSES		80
7.1	Efficiency and Pressure Drops	80
7.2	Efficiency and Compressor C-3 Outlet Pressure	84
7.3	Efficiency and Minor Design Modifications	84
7.4	Is the Presence of HX-1 Justified?	87
CHAPTER 8: CONCLUSIONS		89
REFERENCES		93
APPENDIX		94

CHAPTER 1: INTRODUCTION

The object of this work is to present the results of the analysis and preliminary process design of the Improved Heat Recovery Method (IHRM). This new heat recovery process has been described by Higdon and Lynn (1990). The present study is more specifically concerned by the application of the IHRM to coal-gas fired power plants involving high-temperature clean-up.

The purpose of this chapter is to provide the necessary background to understand the work presented in the following chapters.

1.1 Coal, Gas Turbines and Power Generation

Coal is often associated with the industrial revolution and the heavy industries, which accounts for the "obsolete" connotation commonly attached to it. It is less known that coal is also the fossil fuel of the future. It will indeed outlast oil and natural gas by several centuries, since the world reserves of coal are simply tremendous in addition to being much better distributed (Fulkerson, 1990). Coal has moreover the advantage of being much better accepted than nuclear energy. This accounts for the sustained interest of the power industry in this fuel and the enormous investments made in research and development.

Coal has nonetheless important drawbacks along with these remarkable advantages, its main inconvenience being the by-products of its combustion. Among them are the substantial amounts of pollutants (such as H_2S , NO_x , NH_3 , and HCl) that will have to be removed. Because of increasingly strict pollution-control regulations, these emissions are and will be a dominant concern in the design of the future power plants. In the power plants investigated in this work, coal is gasified prior to its combustion and is therefore not directly used as a fuel. One major advantage of coal gasification is to ease the removal of pollutants since it is more simple to clean a gas than it is for a solid. Besides, the coal-gas clean-up can

be achieved before combustion, which is much more cost effective than removing diluted pollutants from the flue gases as it is commonly done in traditional coal-fired power plants. Another major advantage of coal-gasification is to allow the use of gas turbines instead of steam turbines.

The main advantage of gas turbines is to have a higher allowable inlet temperature than steam-turbines, and therefore enable a greater power output. Till recently, technical difficulties have limited the size, the efficiency, and the reliability of gas turbines. This accounts for their restricted use in power industry, where they are mainly used for peak power generation. These problems were making the long-known steam turbines more attractive. Recent technological developments (especially in material science, which allows much higher inlet temperatures) has increased the efficiency of gas-turbines to a point where they are competitive with steam-turbine technology. Reliability has also been greatly enhanced. The higher turbine inlet temperatures increase the incentive to add heat-recovery systems to reclaim the large amount of energy available in the stack gas, which leads to still more efficient and integrated power generating systems.

1.2 Coal Gasification

Coal gasification consists of converting solid coal into a gaseous mixture called coal-gas. CO , H_2 , H_2O and CO_2 are the main constituents of this mixture, CO and H_2 being the fuel components of the gas. Several gasifying processes are either available commercially or currently under development, three of which have been considered in the present study. The purpose of this section is to give an overview of those processes.

The Texaco O_2 coal gasifier, which is commercially available, is an entrained-flow gasifier that uses O_2 to accomplish the gasification of the solid coal to gaseous compounds, including the fuel components CO and H_2O . The coal is fed to the gasifier as an aqueous slurry with a water content of roughly 34 percent. Water used to make the coal slurry is

preheated in the process to around 250°F before being added to the coal, and is added to allow the coal to be pumped into the gasifier. Prior to adding the slurry water, the coal is pulverized to a particle size of less than 0.1 mm. The oxidant used is 95 percent O₂, which is produced by cryogenic separation of air. The coal slurry is sprayed into the gasifier and entrained into the O₂ stream, resulting in a cocurrent type of gasification. Typical exit temperatures from this type of gasifier are normally 2400-2600°F. The mineral content of the coal melts and forms a slag in the gasifier exit stream.

In this study of coal-gas turbine systems, two other types of gasifiers were considered because of their potentially different impacts on system thermal efficiency. Both of the additional gasifiers were fluid-bed gasifiers, in which the coal is pulverized and added dry to the gasifier. Two sources of oxygen were considered: simple compressed air and 95 percent O₂ from cryogenic separation. Both gasifiers inject a stream of high-temperature steam (950°F) into the gasifier to supply H₂O that is consumed by direct reaction with carbon and in the water-gas shift reaction. Coal is typically ground to a particle size of less than 8 mm for proper fluidization. Fluidized-bed Gasifiers are still being developed and are not currently available commercially.

Fluid-bed gasifiers, unlike the Texaco gasifier, do not add water to the coal and thus do not suffer the thermal penalty for vaporizing the water. Additionally, fluid-bed gasifiers have a much lower exit temperature than entrained-flow gasifiers, 1850°F instead of the 2400°F for the Texaco-type gasifier. This lower temperature of the coal gas leaves more of the original energy content of the coal in chemical form rather than in sensible heat form. Gasification occurs at a lower temperature in a fluid-bed gasifier due to the countercurrent flow of the coal and hot gases, unlike the entrained-flow gasifier where the flow is cocurrent. The mineral content of the coal is not melted to form slag in a fluidized-bed gasifier, due to the lower gasifier temperature, and hence leaves the gasifier as ash, which poses an environmental problem that would have to be dealt with. Furthermore, fluid-bed gasifiers

Table 1-1**Comparison of Coal-Gas Streams Produced by Three Different Types of Gasifiers**

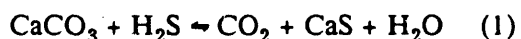
Gasifier:	<u>Texaco</u>	<u>Fluidized-bed</u>	<u>Fluidized-bed</u>
Oxidant:	95% O ₂	95% O ₂	Air
Exit Temperature :	2400°F	1850°F	1850°F
Pressure:	500 psia	500 psia	500 psia
Coal-Gas Flow Rate (lb-mol / 23.15 lb of coal):	2.625	2.048	4.200
Water-to-Coal Ratio (w/w):	0.50	--	--
Steam-to-Coal Ratio (w/w):	--	0.12	0.18
Oxygen-to-Coal Ratio (w/w):	0.65	0.58	--
Air-to-Coal Ratio (w/w):	--	--	3.3
Coal-Gas Composition (mole fraction):			
CO	0.396	0.544	0.268
H ₂	0.303	0.276	0.156
CH ₄	0.001	0.058	0.010
CO ₂	0.108	0.047	0.038
H ₂ O	0.165	0.044	0.041
N ₂ + Ar	0.016	0.017	0.481
H ₂ S	0.010	0.013	0.006
NH ₃	0.002	--*	--*

* Not known, assumed negligible

are dependent on a local source of high-temperature steam. Table 1.1 shows the important characteristics of the three different types of coal-gas streams which are produced by the three different methods of coal gasification that were used in this study.

1.3 Coal-Gas Clean-Up

One of the major difficulties that arise when using coal gas as a fuel is that the gasified product contains particulate and gaseous pollutants that must be removed prior to the combustion of the gas, hence the importance of the clean-up step. Particulates have to be removed mainly to prevent damage to the turbine blades. In the designs used in the study, particulates are removed prior to the coal-gas entrance into the clean-up section. This is achieved by processing the gas through a set of cyclones in parallel. Gaseous pollutants consist mainly of H_2S , COS and NH_3 . H_2S predominates and we are chiefly concerned by its removal. Different methods are currently either available or under investigation, from low to high-temperatures clean-ups. High-temperature clean-up is desirable from a thermal-efficiency standpoint. This study involves a proposed high-temperature clean-up method using limestone as the main reactant. H_2S reacts with limestone as follows:



A light iron oxide coating would catalyse the decomposition NH_3 into N_2 and H_2 . This clean-up method is currently under investigation, so that the details of its implementation are not yet available.

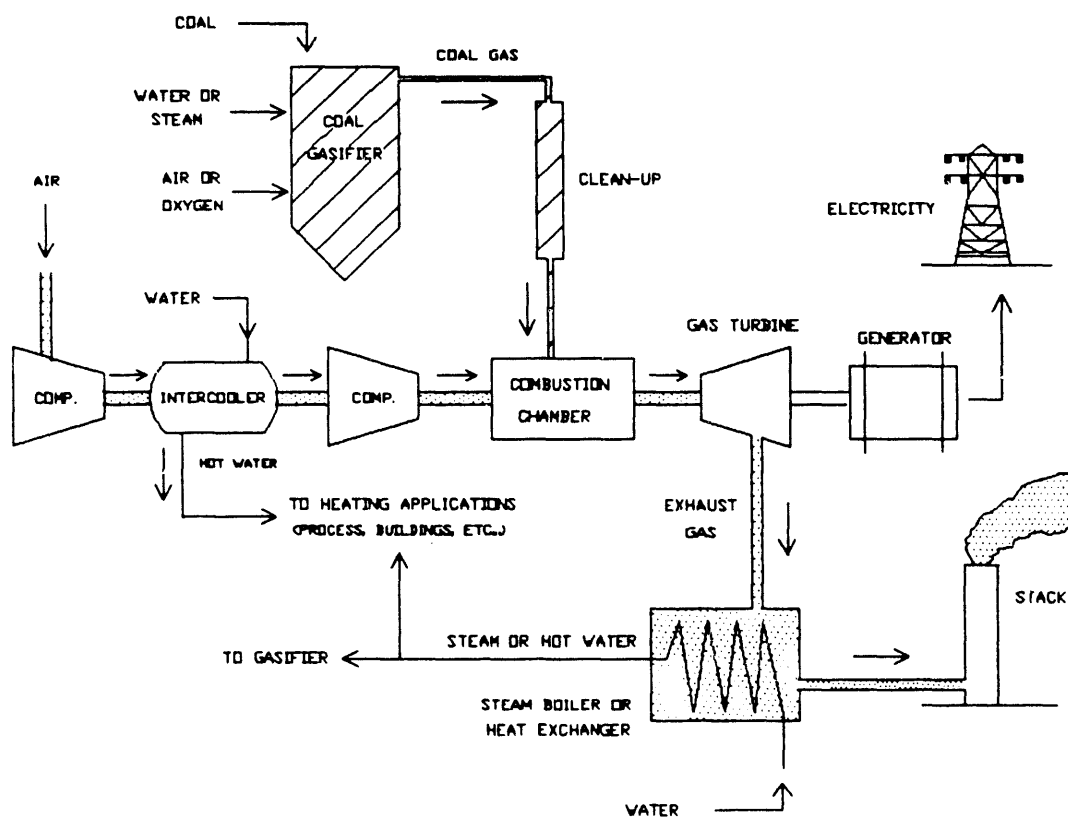
1.4 Heat-Recovery Methods

A common and efficient way to improve the thermal efficiency of a power plant is to recover heat from the turbine exhaust, which can be done in different manners. The purpose of this section is to give an overview of the main heat-recovery methods available or currently developed as well as the principles of the IHRM (Improved Heat-Recovery Method)

studied in this work.

Cogeneration is the most efficient of all the heat-recovery methods. Figure 1-1 shows a very simplified cogeneration design for a coal-gas-fired power plant. Coal is converted to

Figure 1-1: Cogeneration



a gaseous mixture by reaction with steam (or water) and air (or oxygen) into the gasifier. Pollutants are then removed in the clean-up unit and the "clean" coal gas is fed to the combustion chamber, where it is burned. Compressed air is also fed to the combustion chamber and has two functions: it provides the amount of oxygen necessary for the combustion reaction and helps controlling the temperature of the gas sent to the turbine. The hot gases thus produced expand through the turbine, the exhaust of which is the main heat source for heat recovery. In order to reduce the work of compression, the air is cooled

between the two main compression stages. This feature is called "intercooling" and produces hot water and (or) steam that are also available for heat recovery. Except for the intercooling scheme, the part of the process described so far is independent of the heat-recovery method selected and is common to all of the four methods to be described. Cogeneration itself consists of recovering the heat available in the turbine exhaust gases and in the intercooling water to produce steam or hot water that are used directly for various heating applications (for process and buildings mainly). This method is the most efficient because it uses all of the low-level heat generated by the power plant without any further transformation. Low-level heat can be defined as an energy available at too low of a temperature to permit the generation of steam under the operating pressure. In the present case, this energy would have to be produced by other means if it was not available, and hence represents a sheer energy saving. Cogeneration therefore represents a very efficient way to increase the thermal efficiency of the power plant.

Thermal efficiency is defined as the fraction of the energy content of the coal that is converted to electricity. The energy content of the coal is actually a "chemical energy" usually expressed in terms of Higher or Lower Heating Values (HHV or LHV). These heating values differ by the latent heat of evaporation of the water produced by the combustion; the HHV assumes that this water has been condensed, whereas the LHV does not, which accounts for the fact that HHV of the coal exceeds its LHV by a few percent (typically 4%).

Cogeneration cannot usually be incorporated into large power plants since they would generate much more low-level heat than the plants and their surroundings could use. Besides, power generation systems are usually quite remote from urbanized areas, which decreases the number of potential users of the heat recovered (an exception to this large generalization is found in some large chemical plants).

The Integrated Coal-Gasification Combined Cycle (IGCC) is an advanced heat-recovery method that is now available commercially while still being actively developed.

Figure 1-2: Combined Cycle

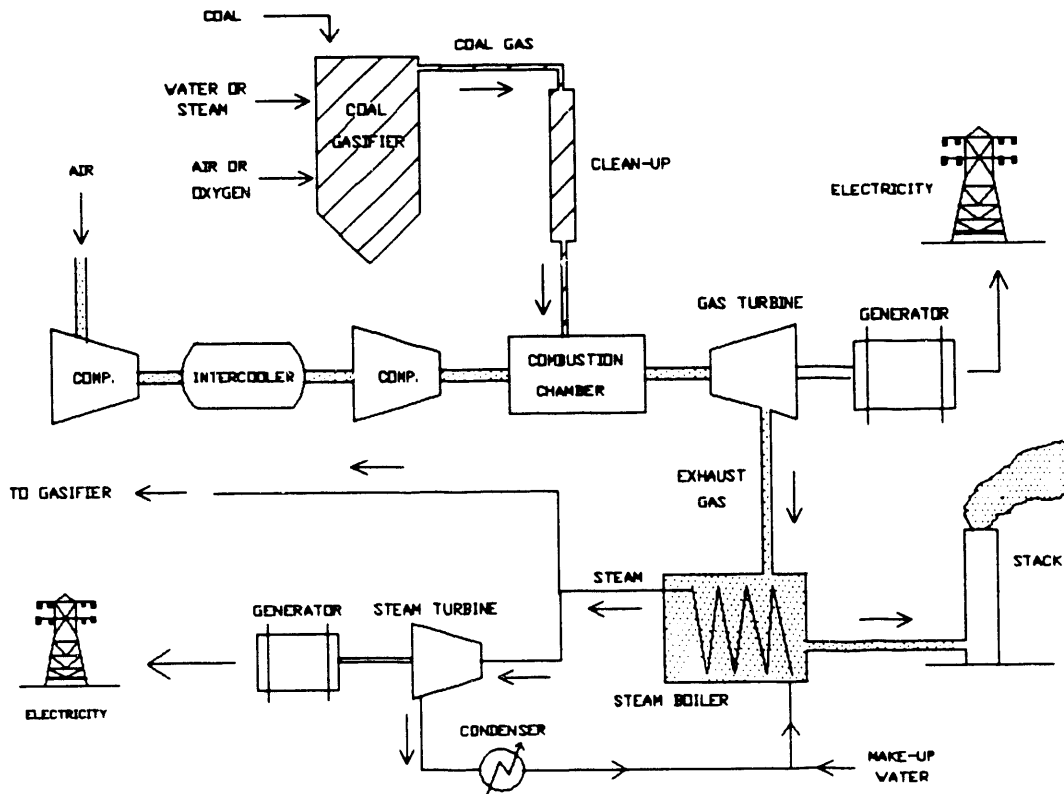
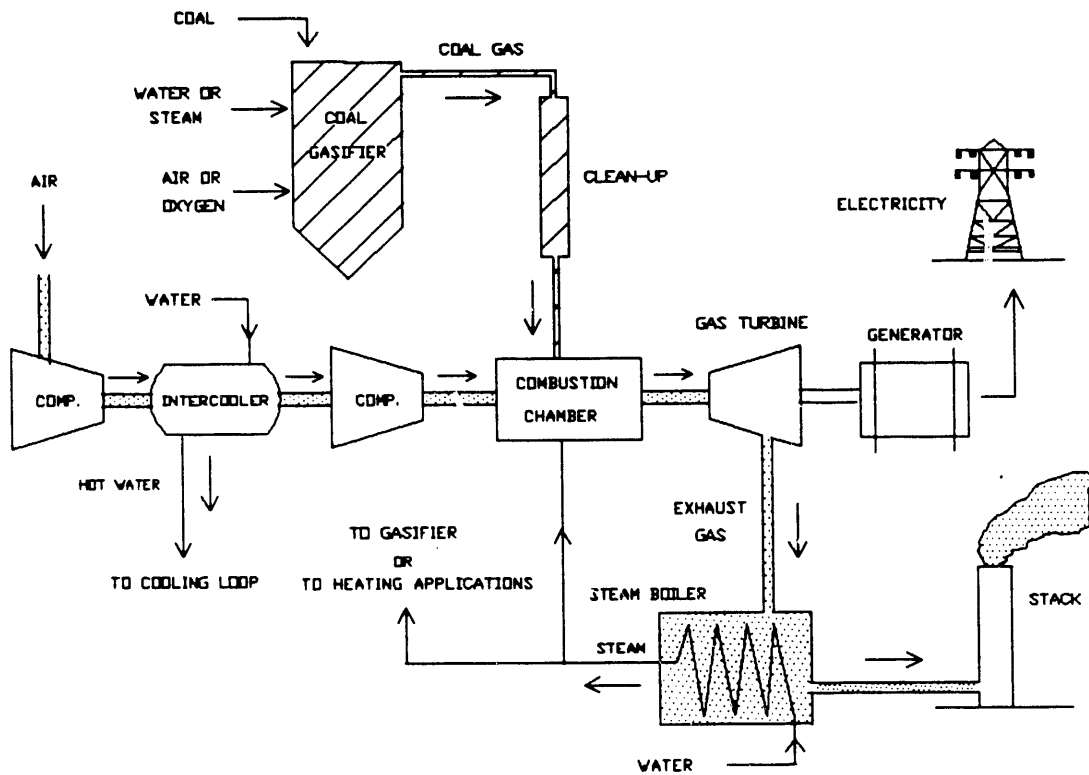


Figure 1-2 shows the main features of the IGCC. Intercooling might be used to maintain the temperature of the compressed air below the maximum operating temperature of the compressor. The primary feature of the IGCC is that the heat recovered from the turbine exhaust gases is used to generate steam to run a steam turbine. Electricity is thus generated within the heat recovery process itself. Combined cycles are more efficient than conventional power plants because they extract more energy per unit of coal burned by means of the heat-recovery loop. Literature currently available indicates that the IGCC concept has a very good potential for improving the thermal efficiency of coal-fired power plants (Fulkerson, 1990).

Figure 1-3 shows a simplified view of the Intercooled Steam-Injected Gas (ISTIG) Turbine System. The ISTIG design is similar to the IGCC in the way the heat from the turbine exhaust gases is used to generate steam in a boiler. However, the final use of this

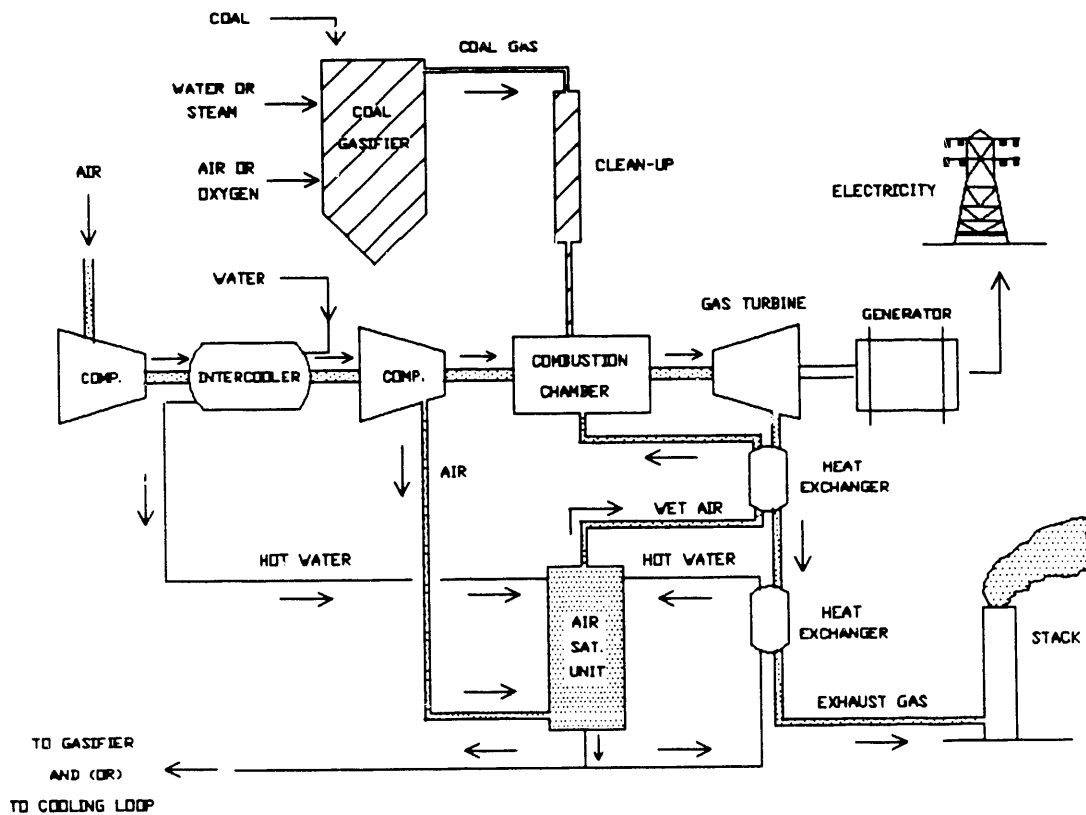
Figure 1-3: Intercooled Steam-Injected Gas (ISTIG) Turbine System



steam is very different. In the ISTIG turbine system, the steam is channeled to the combustion chamber where it reduces the excess compressed air needed to control the firing temperature, which increases the net power output and improves the thermal efficiency of the system. The heat recovered is therefore not directly used to generate electricity (via a steam turbine) as in the IGCC scheme, but is instead recycled in the system to reduce the work of compression. As in the previous design, intercooling can also be used as a way to control the temperature of the compressed air.

Figure 1-4 gives a simplified description of the Improved Heat-Recovery Method (IHRM). At this point of the discussion, our purpose is to give a brief introduction to the method, since it will be dealt with in much greater depth in the rest of the study. We can immediately notice the similarity of the IHRM and the ISTIG designs. Both are indeed based

Figure 1-4: Improved Heat Recovery Method (IHRM)



on a "heat recycling" pattern (unlike the IGCC) since they use the heat recovered from the process to increase the net power output by reducing the amount of excess compressed air needed to control the firing temperature. The particularity of the IHRM is that it involves no steam generation. Instead, the hot water available is sent to an Air Saturation Unit (ASU), where part of it is vaporized into the stream of compressed air bound for the combustion chamber. The air leaving the ASU is saturated with water vapor. The IHRM could be described as a way to produce "low-temperature steam" through water evaporation. This method has the advantage of making better use of the cooling water available, since the water leaving the system (if any) has a significantly lower temperature (and heat content) than the same stream in the ISTIG design. A later part of the study will be devoted to a comparison of the performances of the heat-recovery methods presented.

CHAPTER 2: RESEARCH OBJECTIVES AND TECHNICAL APPROACH

This section describes the initial goals of the research and details the technical approach selected to achieve those goals. Important approximations and simplifying assumptions used in the technical approach will be emphasized throughout the chapter.

2.1 Research Objectives

Our objective was to assess the potential of a new method of heat recovery for gas turbines as a way to improve the efficiency of coal-gas-fired power plants involving high-temperature clean-up. This new method is the Improved Heat Recovery Method (IHRM) mentioned in section 1.4. It will be examined in greater detail in Chapter 3, since it constitutes the core of the present work. Along with the development of an effective design of the IHRM, the investigation of the new heat recovery method involved several goals. One goal was to quantify the thermal efficiency of the new design, and to explore various operating conditions in order to estimate its optimum performance. Another goal was to compare the performances obtained for coal-gas fired power plants based on the three gasifying processes mentioned in section 1.2. Lastly, we wanted to compare the IHRM with other heat recovery methods, such as the methods described in section 1.4.

The results exposed in the present study should give a basis for deciding whether further research is justified or not. To a certain extent, this work could be envisioned as a "preliminary study" of the implementation of the IHRM into coal-gas-fired power plants.

2.2 Technical Approach

We chose to pursue the objectives described above by means of computer simulations. This technical approach enables us to solve accurately the large and complex set of equations that describe the problem in an effective, convenient and inexpensive fashion. We therefore

started with the development of computer models for a coal-gas-fired power plant. The constraints considered in the elaboration of these models were the following:

- Necessity to obtain results of sufficient accuracy to enable a comparison of the performances of the IHRM with other methods.
- Need for a very adaptable model, since we wanted to simulate the response of different designs.
- Need for a convenient simulation structure in terms of computer hardware and computing time.

The first constraint was met by using a quite elaborate set of programs that will be reviewed later in this section. We can mention for instance the fact that thermodynamic non-idealities were taken into account everywhere in the process, and that complex numerical methods were used to solve heat and mass balances simultaneously where necessary. This constraint was also met by determining the system efficiency in a quite accurate way, as will be explained later (Section 4.2.1).

The second constraint was met by the use of a modular simulation structure. Each piece of equipment involved in the process is described by an independent module (or set of computer programs), which gives the simulation great flexibility since a different design can be accommodated by only changing the way these modules are connected. This is made possible by the use of a "Drive program", the function of which will be described shortly.

To meet the third constraint, the programs were written in Microsoft FORTRAN (version 5.1) and run on an 80486-based Personal Computer. The simulation can be run on this PC in a typical computing time of six minutes. However, on less-advanced microprocessors the computing time can be more of a problem since it is, respectively, 25 and 100 minutes on 80386- and 80286-based computers. Moreover, certain "difficult" simulation runs might require up to five-fold the average computing time.

The next sections (2.3 and 2.4) are devoted to the presentation of the simulation

procedure and monitoring as well as to the description of the different modules involved in the computations. The objective of these sections is to give the reader enough information to understand the simulation structure without getting too much into technicalities. Very detailed information regarding the structure of the programs, the codes themselves, and the way for running the simulation can be found in the Appendix.

2.3 Convergence Procedure

The process can be described by a certain number of equations or relations, such as the heat and mass balances and the thermodynamic equilibria. The process simulation actually consists of solving these equations sequentially (*i.e.*, successively for each piece of equipment) in an iterative fashion. Results for a particular iteration are then used as the starting points for the next one. This procedure eventually leads to the final solution if the initial values were chosen carefully. The solution is reached when the different process variables are stable from one iteration to the other, since the equations involved have a "reasonable" (*i.e.*, non singular) behavior. The simulation is then said to have converged.

Two problems had to be solved to make this convergence scheme operational. The first one had to do with the initialization procedure. If the values used for the first iteration are too far from the solution, the simulation will either converge very slowly (*i.e.*, a great number of iterations will be necessary) or might not even converge at all. Mathematically, the problem can be envisioned as the determination of the minimum of a multi variable function. Each stream is fully described by 16 process parameters (temperature, pressure, flow rate, enthalpy, and 12 composition-related terms). Since a typical process involves 40 streams, it is described by 640 parameters and the multi variable function depends on that many variables (which are not independent however). If the initial guess is far from the solution, the search for a minimum might experience a secondary minimum, a saddle-like extremum, or even no minimum at all. To get what we call a "careful choice", one can use the

results of previous computations or a trial-and-error procedure. The determination of an efficient set of initial values can be very tedious, especially if no runs of a similar design are available. It is an essential step however, since it greatly affects the computing time, and prevent the crash of the simulation.

The second problem is related to the choice of convergence criterion. In other words, we had to decide when the results generated by the computations can be considered to be a "good approximation" of the actual solution (*i.e.*, solution attained after an infinite number of iterations). A 0.01% convergence criterion was finally selected. The simulation is terminated when the difference between successive values of each process parameter is less than the prescribed allowable error (0.01% in the present situation). A sensitivity analysis showed that this value provides sufficient accuracy for the computation of the system efficiency.

Another important aspect of the simulation procedure is the way computations are monitored, and adapted to a given flow-sheet.

2.4 Simulation Monitoring

The process simulation involves 25 subroutines that are divided in 13 modules. This clearly indicates the need for a program that would monitor the work of the different subroutines involved and compute the final results of the simulation. More specifically, the function of this program, called "DRIVETEX", is to set the order of execution of the different modules, to process the results generated by each program, to monitor the convergence of the simulation, and finally to compute the efficiency and produce the different outputs. The drive program has therefore a very important role in the simulation, since it provides an interface between the user and the computer programs. Once the codes involved in the different modules are written, debugged and running, DRIVETEX is the only program that has to be modified to accommodate changes in the flow sheet or in the process.

The following procedure is followed in performing the computations to simulate the behavior of the power plant shown on a given flowsheet. First a data file named "UNIT.DAT" is called by DRIVETEX. UNIT.DAT sets the order of execution of the different modules and provides the values of a certain number of important parameters (such as the system pressure, the compressors efficiency, etc...). Most of all, it provides each module with the number of each stream entering and exiting the piece of equipment modelled, thus offering a translation of the flow sheet in "computer language". It is true that there many possibilities for the order of execution of the different modules, since it is an iterative procedure, but some configurations are definitely more efficient and convenient than others in terms of computing time and initial guesses. Initial guesses and process parameters are provided by a second data file named "STREAM.DAT". This file is essential since it initializes the convergence procedure; section 2.3 emphasized the importance of this phase of the simulation. STREAM.DAT is called by DRIVETEX at the beginning of each run (*i.e.*, for the first iteration). An overview of the simulation structure is given in Figure 2.1.

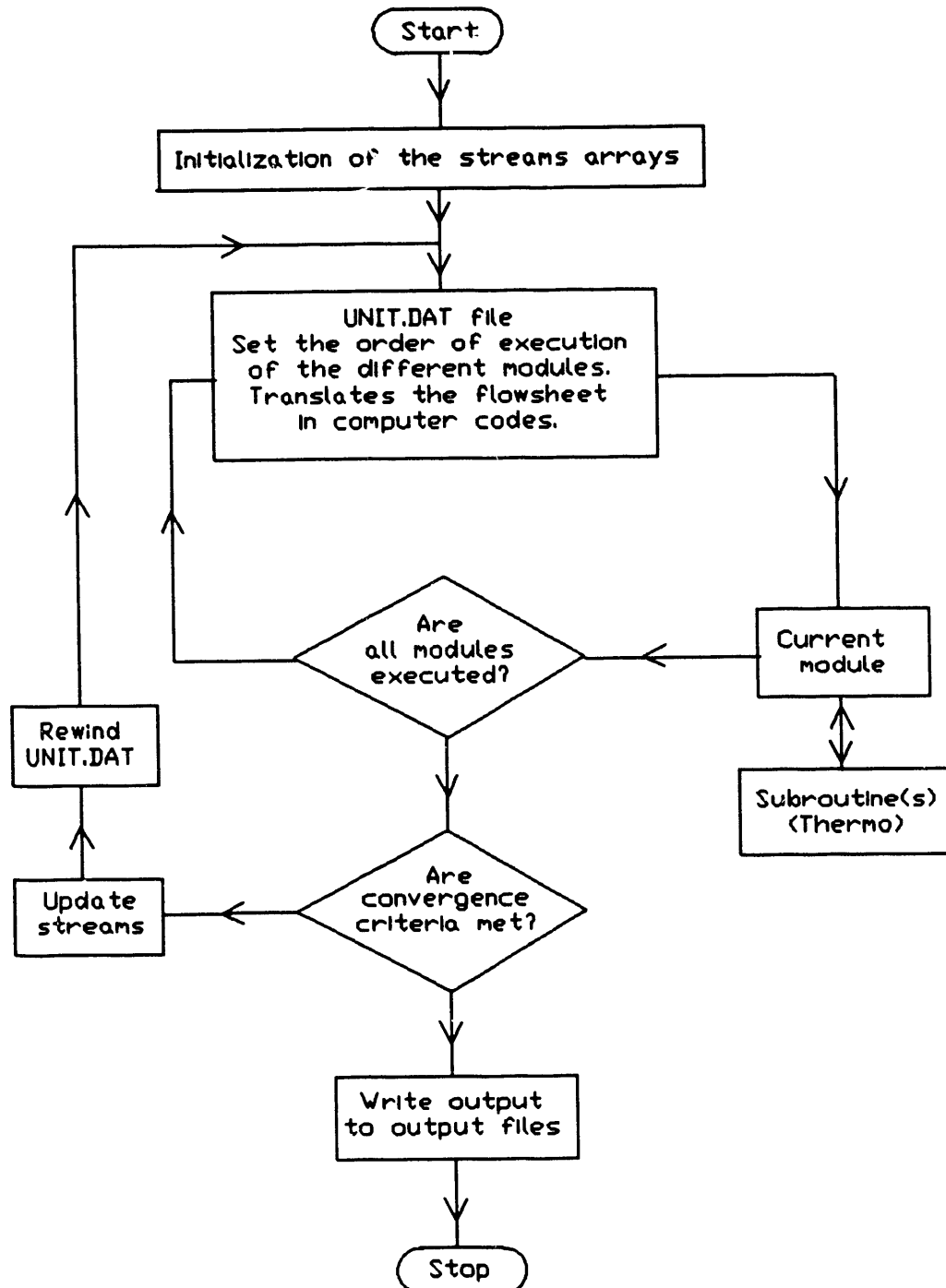
2.5 Modules Overview

The objective of this section is to give an overview of each of the modules involved in the simulation along with the important assumptions made for each one of them. It is not our intention to design each of the different pieces of equipment involved in the process since modelling was our primary goal. Equipment design is for the most part outside the scope of the study defined in the Research Objectives (Section, 2.1). The structure of the simulation and a certain number of subroutines were conceived by Higdon (1988) and Russell (1989)

2.5.1 Thermodynamics Module

Thermodynamic properties are required over a wide range of temperature and pressure, from ambient conditions to a maximum of 2400°F and 720 psia. Non-idealities in the vapor phase are important, particularly for higher-pressure streams with significant

Figure 2-1
SIMULATION STRUCTURE



concentrations of water vapor. The virial equation is used to correct ideal-gas enthalpies and heat capacities for real-gas effects, following the method suggested by Prausnitz³. All liquid phases in the calculations are predominantly water (>99.9 mole%), and liquid properties are based on a correlation of water properties based on the steam tables.

Vapor-liquid equilibria in the air saturation unit are calculated using Henry's law for air (nitrogen, oxygen, argon and carbon dioxide) and Raoult's law for water; temperature-dependent Henry's law constants are used. The vapor-phase non ideality is accounted for with fugacity coefficients calculated from the virial equation.

2.5.2 Shift Module

The purpose of this module is to include the effects of the gas-shift reaction in the simulation. This reaction can be written:



Since CO and H₂ are present in large proportion in the coal-gas entering the system, and the coal-gas temperature and water content vary greatly during the quenching steps (thus changing the equilibrium composition), this reaction has a significant effect on the process modelling and must be included in the simulation. The effect of Shift module on the coal-gas stream is to modify the composition and the temperature of this stream in such a way that they are compatible with the water-gas-shift equilibrium. The heat effects of the reaction are accounted for adiabatically, since the kinetics of the reaction is usually quite fast. The vapor-phase non ideality is dealt with by the means of fugacity coefficients obtained from thermodynamic subroutines. Shift module is called by either the Drive program or other modules (such as Partial Quench) every time the coal-gas composition and temperature need to be known accurately, such as the inlets of the clean-up section and of the combustion chamber.

2.5.3 Compressor Module

The compressor module calculates the net work of compression and exit temperature of the compressed gas based on the specified pressure ratio and polytropic efficiency. Compressor efficiencies are assumed to be 86.8%, based on EPRI recommendations. The calculation is done in stages (not necessarily corresponding to actual compressor stages) to account for the change in heat capacities (and specific heat ratios) with temperature and pressure; a sensitivity analysis study showed that breaking the calculation into fifty stages is necessary for simulating the compression of a gas over a maximum pressure ratio of 50 to 1 with a good accuracy, and this was done in the present work. Along with the characteristics of the air stream before compression, it is necessary to provide the desired compressor-outlet pressure to the module.

2.5.4 Turbine Module

The turbine module is modeled in an analogous manner to the compressor, with staged calculations used to more accurately reflect the temperature-dependent properties. For turbines, a polytropic efficiency of 88 percent was suggested by EPRI (Louks, 1988) and the same number of calculation stages (*i.e.*, 50) was found to be sufficiently accurate. As in the compressor module, it is necessary to input the process parameters of the stream entering the turbine as well as the final pressure (*i.e.*, pressure after expansion). The allowable turbine inlet temperature is an extra parameter that has to be set as well.

Modeling the turbine used in each design as a simple turbine with an allowable inlet temperature of 2100°F is an approximation that greatly eased the turbine calculations. Modern turbines have allowable inlet temperatures that are as high as 2400°F, but such turbines also have elaborate internal cooling of the turbine blades (Brandt, 1987). Cooling of the turbine blades is accomplished by bypassing some of the compressed air or steam from upstream of the combustion chamber into complex passageways within the blades. The calculations involved in determining the actual flows of coolant through the turbine blades

and the true turbine performance parameters is very laborious, therefore an effective inlet-temperature approach is used in this study to facilitate ease of calculation. An effective inlet temperature is that temperature which, when used in a simple (*i.e.*, uncooled) turbine model, results in the same system performance as would be obtained with a combustion gas at its actual inlet temperature that is fed to an actual turbine having the same efficiency but with blade cooling. The effective inlet temperature of 2100°F, which is used in this study with the simple turbine model, corresponds approximately to an actual inlet temperature of 2400°F (Louks, 1988). It will however be subject to a sensitivity analysis that will be discussed later.

2.5.5 Combustion-Chamber Module

The combustion-chamber module is designed to calculate the exit-stream composition which results from fuel combustion and the air flow required to meet an exit temperature criterion. Complete, adiabatic combustion of the fuel components is assumed (CH_4 , CO and H_2 going to the stoichiometric amounts of CO_2 and H_2O). It is assumed that no appreciable amounts of NO_x are formed.

The exit-temperature criterion is important because the exit stream from the combustor passes directly to the turbine, which has a maximum allowable inlet temperature as noted above. To achieve the maximum thermal efficiency in a gas-turbine system it would be desirable to use only the stoichiometric amount of compressed air needed for combustion, but doing so would produce a turbine inlet temperature that would destroy the turbine. Accordingly, an excess of compressed air is added to the combustion products to bring the combustor exit temperature down to the maximum temperature allowable in the turbine. As turbine technology improves, the maximum allowable inlet temperature will rise, but the currently feasible effective value of 2100°F is used in this study. The air and fuel stream process parameters are provided to the module, along with the outlet temperature and the pressure penalty assigned to the combustor.

2.5.6 Air-Saturation-Unit Module

The air-saturation unit is modelled as a countercurrent gas/liquid contacting column with a variable number of theoretical stages and options for multiple feeds and a side-stream withdrawal. The equations describing the heat and mass balances and the phase equilibria are solved using the simultaneous convergence method developed by Newman (1968). This method is well-suited to separation problems with few components, such as the air-saturation unit. Convergence is normally fast and reliable. Tray efficiencies are set at 100%, since the actual column would most likely use random packing rather than trays. Inputs to the module include the number of theoretical stages, the pressure drop and the process parameters of the air and water streams fed to the unit. Theoretical stages are converted to packing heights outside the program, as discussed in Section 7 (below).

2.5.7 Heat-Exchanger Module

The heat-exchanger module models a simple, countercurrent-flow heat exchanger with no phase change and constant heat-transfer coefficients. A minimum temperature approach of 25°F was chosen as a general value for all heat exchangers. This value would need to be modified in a more detailed study, depending on how critical the temperature approach used in a specific heat exchanger is to the system efficiency or on how the economics of the process is affected by the heat-exchanger design. The heat-exchanger module determines exit temperatures by first determining at which end of the heat exchanger the temperature pinch occurs and then calculating the temperature of the exit stream at the other end using an enthalpy balance. The heat-exchanger module also calculates UA , the product of the heat-exchange area (A) and the overall heat-transfer coefficient (U), which can be used for sizing heat exchangers. The values of U which were used were 70 for gas-liquid, 60 for boiler and 50 for gas-gas heat exchange in units of Btu per hour square-foot°F (Louks, 1988). These values are based on the inside area of tubes with external extended area (fins). High-pressure gas or liquid would flow on the tube side; low-pressure air or turbine exhaust would flow on

the shell side of the heat exchangers. Pressure drops are specified for both sides.

2.5.8 Boiler

Boiler module models the water-cooling of a hot air stream in a heat-exchanger configuration similar to the one described in the previous paragraph. If enough heat is transferred to the water in the cooling process to generate steam, the module simulates a boiler. Otherwise, the unit simulates, the unit simulates a regular heat exchanger. Boiler module sets the cooling-water flow and computes the outlet temperatures in such a way that the thermal pinch occurs at the cold end of the exchanger, since cooling the air is our main purpose. The amount of saturated steam generated (if any) is also calculated in the process. The characteristics of the air and water streams entering the unit are provided as an input to the unit. Approach temperature and pressure drops on both sides also have to be specified.

2.5.9 Contactor Module

The function of this unit is to model the cooling of a hot solid stream by a cool gas in direct-contact flow. We assumed that the solid stream exits the contactor at the temperature of the cool gas entering the unit (*i.e.*, the approach temperature is set to zero). The cool-gas flow and outlet temperature are computed in such a way that the thermal pinch occurs at the cold end of the exchanger. The inputs required by this module are the characteristics of the streams entering the contactor.

2.5.10 Clean-up Module

This unit models the H_2S and NH_3 removal from the coal gas. In the present study, it is assumed that H_2S removal is achieved by reacting with limestone to give CaS , H_2O and CO_2 , while NH_3 is catalytically degraded into N_2 and H_2 . Both reactions are endothermic. This process is assumed to have a 100% efficiency, which means that the coal-gas exiting the module is supposed to be free of hydrogen sulfide and ammonia. The clean-up temperature is imposed by thermodynamic, kinetic and physical (*e.g.* possibility of sintering of the limestone particles) considerations, and should be input to the module. The other inputs

required are the characteristics of the coal-gas and limestone streams entering the unit, the limestone-to-H₂S ratio and the pressure-drop penalty assigned to the clean-up process. Composition and temperature effects are computed to yield the process parameters of the exiting "clean" coal-gas stream. The clean-up method itself is outside the scope of this work and will therefore not be discussed further.

2.5.11 Partial-Quench Module

The purpose of this module is to model the quenching of the coal-gas entering the system to a specified temperature. In the present study, this temperature is imposed by the clean-up section. The module computes the amount of water required to achieve the cooling. Under the process conditions, the gas exiting the quench is not saturated in water, hence the term "partial quench". The effects of the water gas-shift reaction are taken into account, since this reaction has an important impact on the quench-water requirements and on the characteristics of the exiting stream. The inputs required by this module are the process parameters of the coal-gas and the water streams, as well as the desired outlet temperature. The pressure drop through this module was assumed to be negligible.

2.5.12 Total-Quench Module

The function of this module is to cool a specified gas stream to its adiabatic saturation temperature by quenching. The aim of the total quench is to provide a cold source for the gas-solid heat-exchange process mentioned in the Contactor Module. The inputs required are the gas and water process parameters and, as in the case of the partial quench, the pressure drop through the quench was neglected.

2.5.13 Mixer and Splitter Modules

The functions of these modules are to accommodate any merger or split of streams in the process flow-sheet. Mixer module is used to compute the properties of a stream resulting from the mixing of two streams. The only inputs required by this module are the characteristics of the two incoming streams. Splitter module's purpose is to compute the

process parameters of two streams resulting from the split of a single original one. The properties of the source stream and the flow of one of the resulting streams should be input to the module.

2.5.14 Coal Gasification

No module is developed for the coal-gasification process. Doing so would have required a different module for each type of gasifier that is used. Instead, the coal-gas streams produced by each type of gasifier (listed in Table 1.1) were used as feeds to the system simulated. Modifications were made in each design to accommodate the utilities required for each type of gasification.

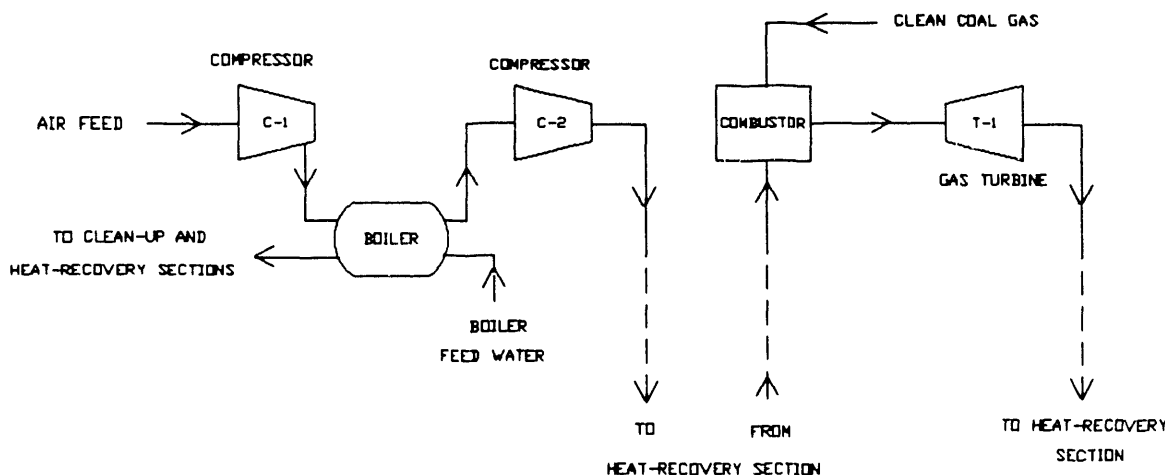
CHAPTER 3: DESIGN AND FLOW SHEET DESCRIPTIONS

The purpose of this chapter is to discuss the implementation of the Improved Heat Recovery Method (IHRM) and the present the designs selected in the study. To do so, it was convenient to divide the process flow sheet into the three sections examined in detail below.

3.1 "Core" Section

The core section of the design involves the essential parts of a gas-turbine power plants, *i.e.*, compressors, turbine and combustion chamber. The design of this section is

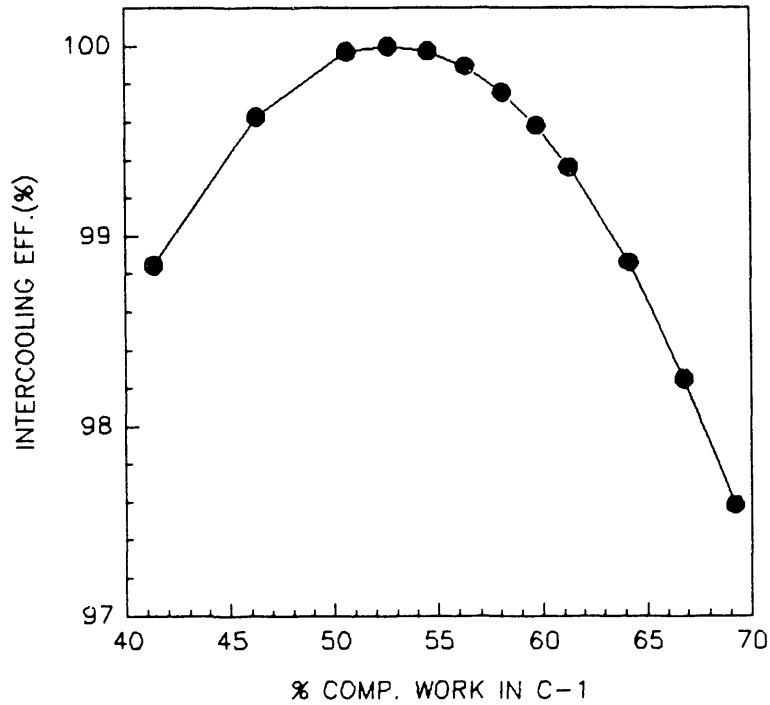
Figure 3-1: Core Section



shown in Figure 3-1. Air is compressed in a two-stage, water-intercooled compressor and directed to the heat-recovery section, where it is heated and humidified. The air stream obtained is sent to the combustor and mixed with coal gas prior to combustion. Hot gases thus produced are used to power a gas turbine. The heat available in the turbine exhaust is recuperated in the heat recovery section, before the gases are sent to the stack. Heat-recovery and clean-up sections will be described shortly.

As said in Chapter 1, the air-compression step involves an intercooler (a boiler in the present design). Intercooling is an important part of the process and deserves some more attention. Intercooling was originally designed to maintain the compressed-air temperature below the maximum operating temperature of the compressor. It also results in a reduction of the overall work of compression. From the standpoint of the system performance however, it has been shown that this reduction is only beneficial when the hot water produced by the intercooling can be efficiently used (Higdon, 1988). If that is not the case, the gain represented by the decrease of compression work is offset by the loss of low-level heat in the hot cooling water leaving the system. An important feature of the IHRM is that it can advantageously use this low level heat in the heat-recovery section. A large fraction of the cooling water leaving the boiler/intercooler is indeed sent to the heat-recovery section, where

Figure 3-2: Intercooling Efficiency



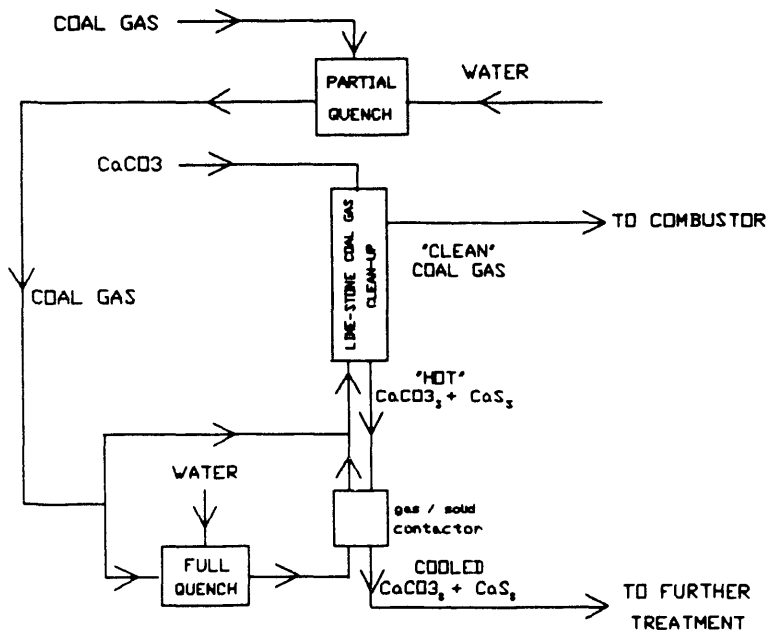
it is used to recover the heat available in the turbine exhaust gases. Intercooling is related to an important operating parameter, which is the work-load split between the two stages of

compression. This split greatly affects the overall work of compression, as shown in Figure 3-2. The intercooling efficiency is defined as the relative difference between the minimum amount of work required to compress a given quantity of air and the compression work required for a different work split. The minimum amount of work would be reached for an even split (50%-50%) if the air leaving the intercooler were at the same temperature as the air entering the first stage of compression C-1. In practice, the boiler approach temperature is set to 25°F; in other words, the air entering C-2 is 25°F hotter than the temperature of the boiler feed water. This shifts the split for the minimum work requirement to 53%-47%. By definition, this minimum corresponds to a 100% intercooling efficiency, which is then reached for a 53% fraction of compression work in C-1, as shown in Figure 3-2. As this fraction varies away from 53%, the overall compression work increases. As we will see later in the study, the intercooling efficiency has a dominant impact on the system thermal efficiency, which accounts for the special attention given to it.

3.2 Clean-Up Section

As was said in the overview of the clean-up method (Section 1.3), the primary function of this part of the process is to remove the coal-gas pollutants. At this point in the discussion, we are more concerned with the design aspects of the high-temperature clean-up. As shown in Figure 3-3, this section has other functions in addition to the clean-up itself: its first task is to cool the coal gas to the allowable clean-up inlet temperature. Typical operating temperatures are in the range of 1800° to 2400°F for the coal gas entering the system and around 1500°F for the allowable clean-up temperature. Cooling is performed by evaporating water into the hot coal gas, which is achieved in a partial quench. Quench water is provided by the intercooling water exiting the boiler. The cooled coal gas thus obtained is sent to the clean-up vessel, "cleaned" and directed to the combustor. The clean-up operation generates hot solids (CaCO_3 and CaS) that need to be cooled prior to their disposal, which offers an

Figure 3-3: Clean-Up Section

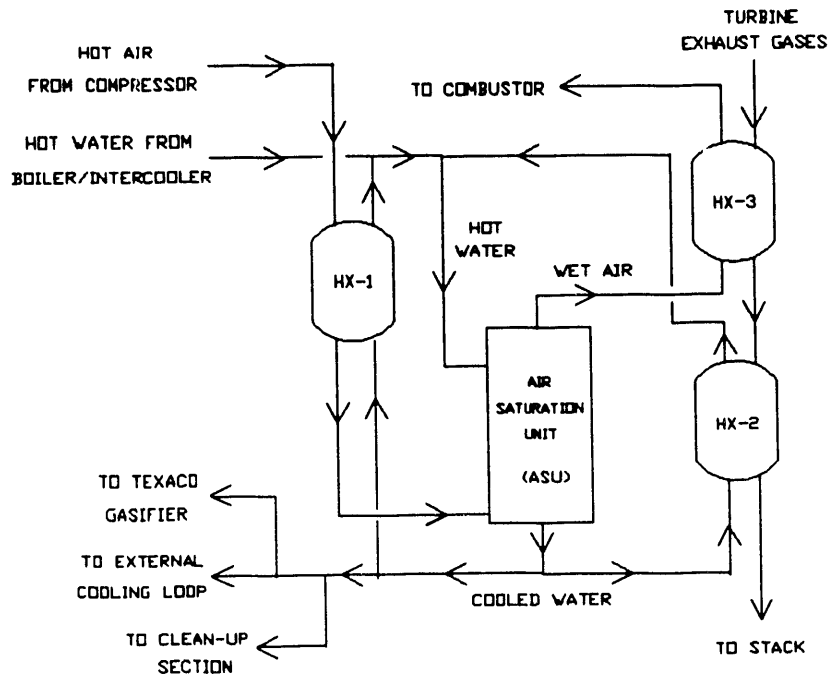


opportunity for heat recovery. Heat available in the hot solid stream is recovered in the gas/solid contactor, where the sensible heat is transferred between the hot solid and cool gas streams. The gas stream is obtained by diverting and quenching a small fraction of the coal-gas stream (typically less than 1%). This operation takes place in the full-quench unit, where the coal gas is cooled to its adiabatic saturation temperature. Quench water is provided by the heat-recovery section of the process. The contactor and the full quench are, like the partial quench, part of the heat-recovery procedure since they all use heat available to increase the flow of the coal-gas stream

3.3 Heat-Recovery Section

From the point of view of the whole study, this section is the most important part of the process since it includes the main features of the IHRM. The basics of the IHRM were disclosed in section 1.4 and are needed to understand the design presented in Figure 3-4. Our main goal is to recover the low-level as well as the high-level heats available in the process,

Figure 3-4: Heat-Recovery Section



mainly from the turbine exhaust gases and the intercooling water. This is achieved in several steps: the recoverable heat of the turbine exhaust is first used to raise the temperature of the humid air stream exiting the ASU, prior to its entrance in the combustor. This operation is achieved in heat exchanger HX-3. The remaining heat available for recovery from the turbine exhaust is then used to raise the temperature of the Air Saturation Unit feed water, which is performed in HX-2. The cold stream for the heat exchange is provided by the cooled water leaving the ASU. This design also uses advantageously the heat available in the intercooling water, since the boiler/intercooler provides the totality of the water required by the heat-recovery section.

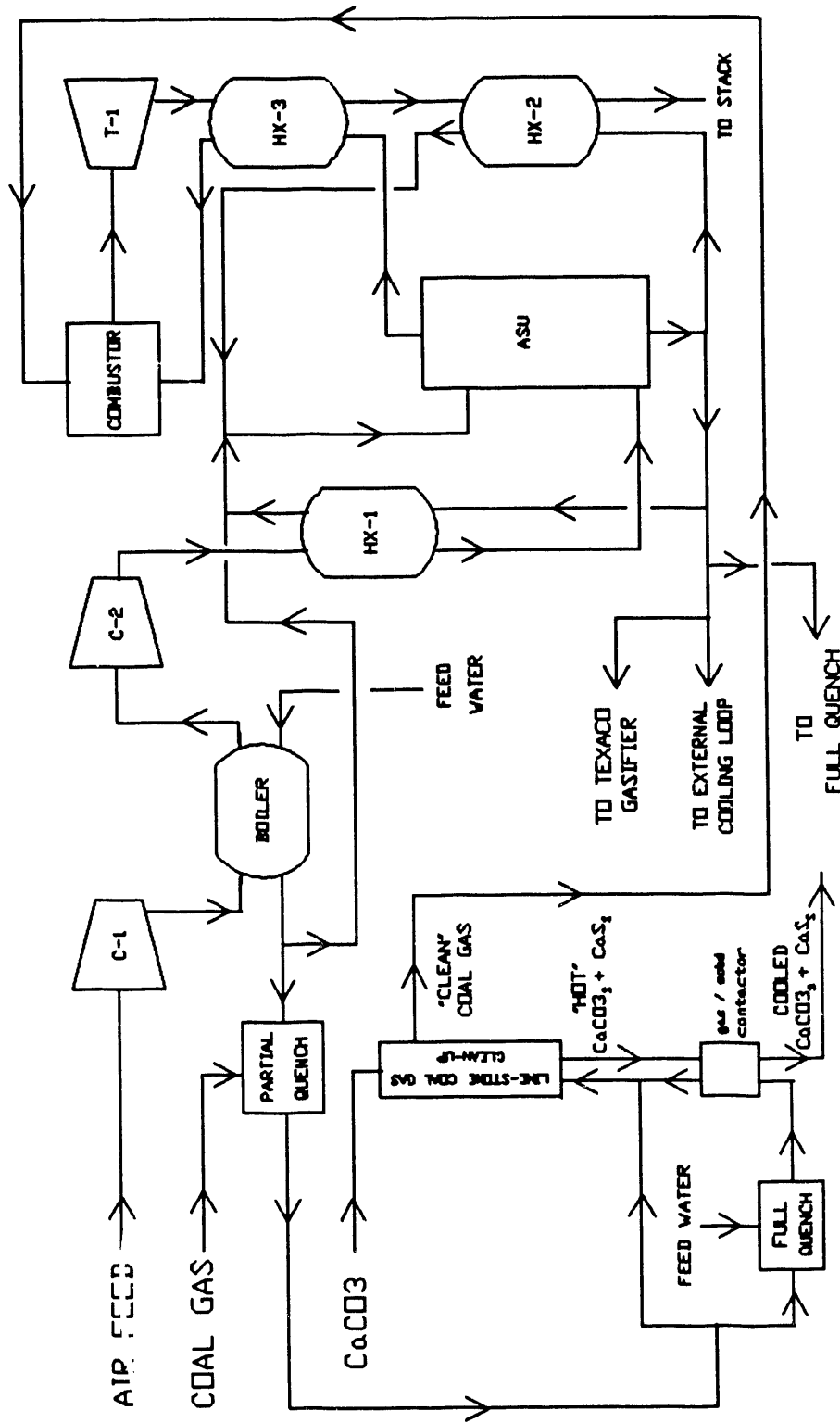
The ASU is the cornerstone of the IHRM. The heat and mass transfer that take place in the ASU are in fact what "recycles" the heat recovered from the intercooler and the turbine exhaust. The low-level heat available in the hot water streams is used to vaporize a substantial amount of water into the air stream fed to the combustor, thus reducing the excess compressed air needed to control the firing temperature. By the same token, the water that has not been

vaporized is cooled to its adiabatic saturation temperature. This ability to recover some of the low-level heat available in the system is the predominant characteristic of the ASU in the present design. The amount of water vaporized increases with the sensible heat content of the ASU feed water (*i.e.*, its temperature and flow rate). This heat content can be advantageously increased by using the heat available in the compressed air. This is achieved in HX-1, the cold source for the heat exchange being provided by the ASU water outlet. The amount of water leaving the ASU usually exceeds the water requirements of heat exchangers HX-1 and HX-2. A small fraction of this excess water is used by the clean-up section (full quench), while the remaining amount is either sent to the gasifier (for the Texaco-type gasifier) or to a cooling loop.

The function of the Heat Recovery Section can be expressed in a slightly different manner: it is also a way to minimize the heat content of the streams leaving the system (*i.e.*, water and stack gas), and therefore the energy losses that they represent.

Figure 3-5 shows a flow sheet of the whole system. This flow sheet has been obtained by assembling the three sections described earlier in this chapter. The design displayed has been developed for a power plant involving a Texaco-like gasifier. Flow sheets for different gasifying systems are very similar to the one shown here. Details of the corresponding designs will be discussed in Chapter 6.

Figure 3-5:
Improved Heat Recovery Method for Coal-Gas Combustion
Turbine Systems using Texaco Gasifying Process



CHAPTER 4: PRELIMINARY STUDIES

It was necessary to perform several analyses prior to generating the data presented in this study. The purpose of these analyses was both to secure the accuracy of the results and to make sure that the computer models developed provide an acceptable approximation of reality. The object of this chapter is to discuss the procedures used in the preliminary analyses and the results that they yielded.

4.1 Computation of the System Thermal Efficiency

Thermal efficiency was defined (Section 1.4) as the fraction of the energy content of the coal that is converted to electricity. It is a crucial process parameter, since it really characterizes the performance of the system. In the present work, "system efficiency" (or "efficiency") refers to a thermal efficiency based on the High Heating Value (HHV) of the coal, unless a different basis is specified. A good approximation efficiencies based on the Lower Heating Value (LHV) of the coal can be obtained by adding increments to HHV-based efficiencies. Those increments are 1.70 and 1.80 percentage points for the Texaco-type and the fluidized-bed gasifiers respectively, and give values of LHV-based efficiencies accurate to 0.05 percentage point.

To calculate the system efficiency, we had to determine what fraction of the power (*i.e.*, shaft work) generated by the turbine is actually converted to electricity available for external use. To do so, we identified and quantified the important power consumers of the process as well as the significant energy losses. The main energy losses encountered in the process were divided into "radiant" and "shaft", depending on their origins. Losses due to radiative heat transfers and others heat leakages were assumed to be 1.0% of the coal HHV. Shaft losses include inefficiencies in the generator and were estimated to be 3% of the turbine net output (*i.e.*, turbine work output minus compressor work). The main power consumers

are, in order of importance, the compressors, the oxygen plant and the gasifier. Their energy consumption represents 35, 6 and 0.4 % of the turbine power output respectively. Energy requirements of smaller users, *eg.* pumps, were neglected. The compressors are directly powered by the turbine, which improves the efficiency of their energy use. This is not the case for the gasifier and the oxygen plant, which are powered by the electricity produced by the generator. Their energy consumptions are therefore aggravated by the generator inefficiencies. The function of the oxygen plant is to provide the oxygen necessary to the coal gasification process and is involved in two of the three designs studied (Texaco-type and oxygen-blown fluidized-bed gasifiers). The determination of its power consumption is quite complex and is thoroughly discussed in section 5.2. Gasifiers' energy requirements are easier to compute since they mainly related to coal handling and slurry preparation prior to gasification. These requirements have been estimated to be 22.9 kW-hr/ton of coal for a Texaco-type gasifier (EPRI, 1984). Fluidized-bed gasifiers will be assumed to have similar requirements. The system efficiency can therefore be expressed as follows:

$$EFF = \frac{TURBwork - COMPwork - SHAFT LOSSES - O2PLANTwork - GASIFIERwork}{COAL HHV}$$

where . TURBwork = Shaft work generated by the turbine (including radiant losses)

. COMPwork = Total work of compression

. O2PLANTwork = Energy consumption of the oxygen plant

. GASIFIERwork = Energy consumption of the gasifier

4.2 Oxygen Plant Energy Requirements

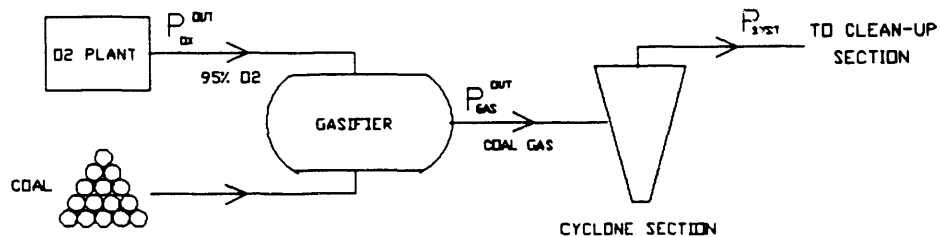
Energy consumptions and losses are either directly computed by the simulation (*eg.*, compressor work, shaft losses) or input to it (*eg.*, O2PLANTwork, GASIFIERwork, radiant losses). All inputs but one are constant: O2PLANTwork is system-pressure dependent and must therefore be dealt with separately. Because of the magnitude of its impact on the system

efficiency, O₂PLANTwork must be accurately computed. Doing so is the purpose of this analysis.

A model was developed to simulate the oxygen-plant power consumption, since very scanty data were available. Most of this power is required to compress air prior to the cryogenic separation and for the subsequent compression of the oxygen to a specified outlet pressure. The whole compression process was modelled (intercooling included) according to the specifications given by EPRI, and the results obtained were very satisfactory (EPRI, 1984). The power consumption predicted by this model differs from the experimental values available by less than 1%. O₂PLANTwork depends on the oxygen-plant outlet pressure. This pressure is imposed by the system pressure and relating these two parameters is the next problem we are going to address.

A simplified diagram of the pressures upstream of the system studied is shown in Figure 4-1. Data given by EPRI indicate a large difference between the oxygen-plant outlet

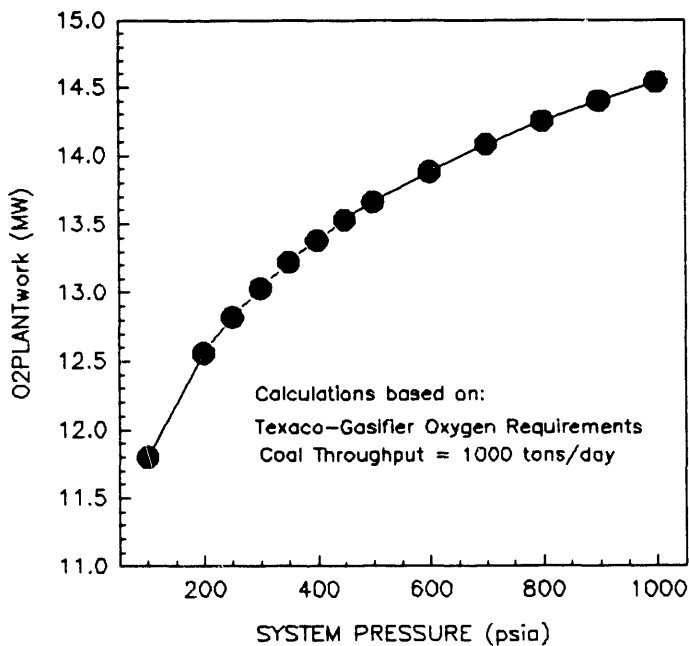
Figure 4-1: Pressures Upstream of the System



pressure (P_{ox}^{out}) and the gasifier outlet pressure (P_{gas}^{out}): $P_{ox}^{out} - P_{gas}^{out} = 119$ psia for a system pressure (P_{sys}) of 615 psia (EPRI, 1984). This pressure drop is imposed by process control and technical considerations (eg., oxygen and coal gas mixing). Pressure drop through the gasifier is negligible under these conditions. A rough cyclone design showed that pressure drop through the cyclone section is less than 0.05 psia and can consequently be neglected too. We chose to keep a constant the value of the ratio $P_{ox}^{out}/P_{gas}^{out}$ over the range of system

pressures we are going to work with (from 200 to 700 psia): $P_{ox}^{out}/P_{gas}^{out} = P_{ox}^{out}/P_{syst} = 1.194$. Using this relation between P_{ox}^{out} and P_{syst} along with the procedure described earlier, we can compute O2PLANTwork for any system pressure. The results of these computations are shown in Figure 4-2.

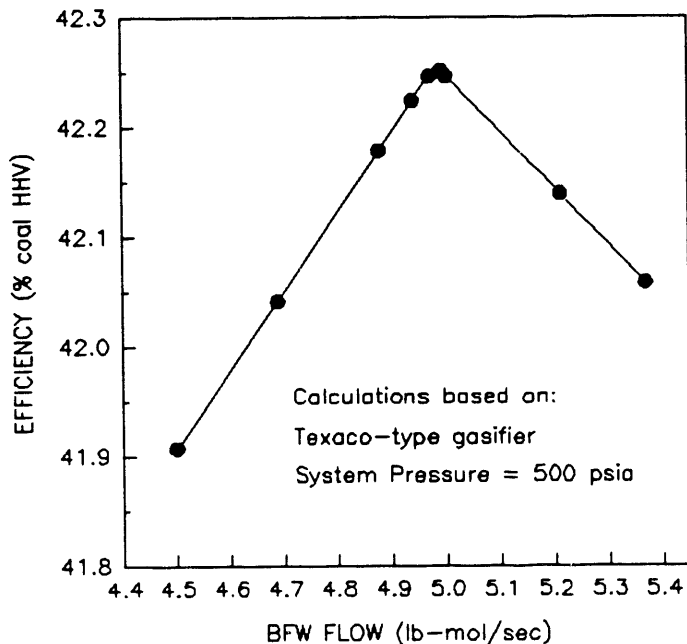
Figure 4-2: Energy Consumption of the Oxygen Plant and System Pressure



4.3 Optimization of the cooling water flows

As was said in Chapter 2, the goal of the work presented is to estimate the potential of the Improved Heat Recovery Method. To achieve this goal, it is essential to determine the optimum efficiency attainable for a given design, which is precisely what sections 4.2 to 4.5 are aiming at. Most process parameters are computed by the simulation. A few of them can be chosen however, as the cooling-water flows (to the boiler and to heat exchangers HX-1 and HX-2). The purpose of the optimization procedure presented here is to make sure that the values chosen for those flows yield the optimum efficiency. Figure 4-3 shows how efficiency is affected by the flow of cooling water through the boiler/intercooler. The system efficiency

Figure 4-3: Effect of Boiler Feed-Water Flow on System Efficiency



reaches a maximum when the heat capacities of the air and cooling-water streams are equal. Flows larger than the optimum value cause a drop of the cooling-water outlet temperature, which lowers the level of heat available for recovery and reduces the system efficiency. On the other hand, below the optimum flow, the cold-stream heat capacity is too small to cool the compressed-air stream to its specified outlet temperature. This increases the work of compression and therefore penalizes the efficiency. Results shown in Figure 4-3 exemplify the basic principle of the optimization procedure, which is to match the heat capacity of the cooling-water stream with that of the hot gas stream. An optimization loop was added to the boiler and heat exchanger modules to achieve this "heat capacity match". The flow-rates optimization increases the efficiency by as much as 0.2 percentage point, which represents a substantial difference. Three-fourths of this increase is related to the optimization of the boiler feed-water flow.

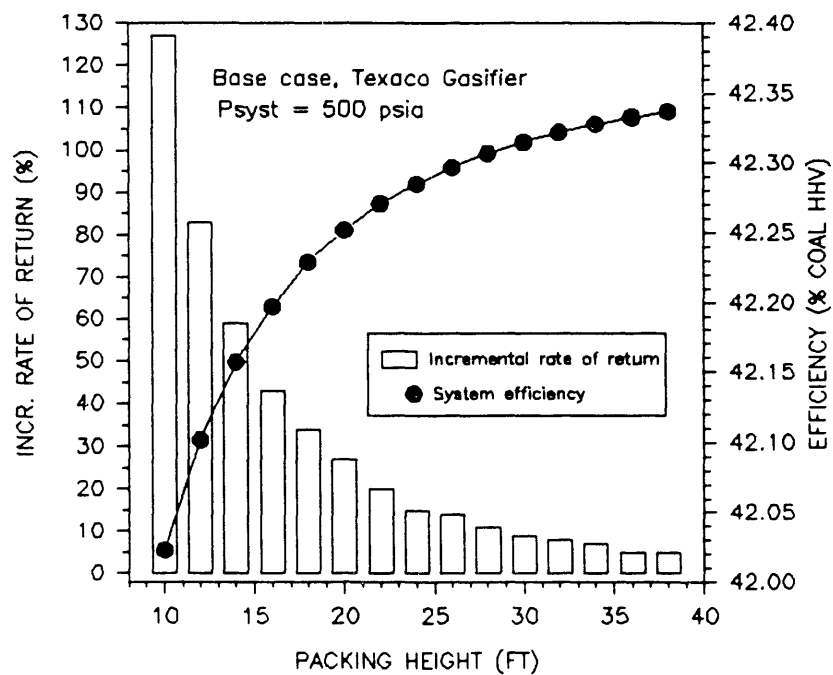
4.4 Optimization of the ASU Number of Theoretical Stages

We saw in Chapter 3 that the Air Saturation Unit is a major part of the process. We can therefore expect the system efficiency to be affected by its characteristics and more specifically by its packing height (directly related to the number of theoretical stages). For example, going from 5 to 10 theoretical stages results in a substantial 0.23 percentage-point increase in efficiency. It is therefore important to chose the packing height with care, because it will be used as a basis for all the simulations involved in this study. Determining the optimum packing height is the purpose of this section.

To do so, we performed an incremental rate-of-return analysis involving the capital investment for the ASU on the one hand, and the value of the electricity on the other hand. Determining the cost of the ASU required a rough design of the unit. The design was performed according to the procedure described by Eckert, for a Texaco-gasifier-based power plant operating under 450 psia (Eckert, 1970). The diameter is chosen so that the gas velocity is 60% of its value at flooding, as determined by the correlation from Eckert. The study showed that a 13-foot diameter column packed with 2-inch pall rings gives a good tray efficiency, with an HETP (Height Equivalent to a Theoretical Plate) close to two feet. This was therefore the design adopted to calculate the ASU capital cost. Bases for the calculation are the ones used by Higdon in his work (Higdon, 1988). The ASU bare module capital was then computed for different packing heights, using a Chemical Engineering Index of 360 for 1990 (Chemical Engineering, Nov. 1990). A 20-foot packing height ASU would for instance have a \$2.55 million (1990) bare module capital. The other part of the analysis was to relate the system efficiency to the profits generated by the sales of the electricity produced. This would indeed give us a way to correlate profits and packing height, from where we could easily determine the desired rate of return. Our profit estimation is based on a 6.5 cent per kW-hr sale price (at the plant outlet). For a 130 MW power plant and the range of efficiencies we are dealing with, this represents a \$1.78 million profit increase per additional

percentage point of efficiency. We now have all the information necessary to perform the incremental cost analysis, the results of which are shown in Figure 4-4. The system efficiency is also plotted with respect to the packing height. These results indicate that, depending on the criterion of profitability considered, the optimum packing height varies between 20 and 24 feet. This corresponds to incremental rates of return ranging from 27 to 15 %. From this observation, a conservative choice of a 20-foot packing height (or 10 theoretical stages) was adopted for the rest of the study. According to correlations found in literature, this corresponds to a pressure drop of 0.4 psia through the ASU (Eckert, 1970).

Figure 4-4: Optimization of the ASU Packing Height



4.5 Other Optimizations

A large number of process variables are computed by iterative procedures. It is for instance the case for certain temperatures (in almost every module) and flows (in boiler, heat exchanger and quench modules). Besides, the simulation itself is based on a convergence scheme. Each iterative procedure is governed by a convergence criterion, which fixes the

degree of approximation in the results. For most convergence procedures, computing time is negligible and a very high accuracy can therefore be easily attained. Convergence criteria can then be set without excessive care, since large numbers of iterations are allowed. For some convergence procedures however, high accuracy is obtained at the expense of a large computation time. It is then necessary to determine the criteria that give both the smallest computing time and the desired accuracy, which is the purpose of the work presented in this section. The trade-off chosen to achieve this optimization is the following: A convergence criterion is considered optimized when its value affects the system efficiency by less than 0.01 percentage point. This optimization procedure ensures an accuracy better than 0.05 percentage points for the value of the system efficiency (when compared to the result obtained for a very large number of iterations and a great accuracy).

One of the optimization procedure consisted of determining the optimum number of calculation stages in the compressor and turbine modules. Using the same "0.01 % rule" as before, we found that the optimum number of stages is close to 50, as it was mentioned in Section 2.5.3 ("Compressor Module").

The down-side of the optimization procedures described in this chapter is the doubling of the computing time that they induce. Most of this increase is due to the optimization of the cooling-water flows and of the number of calculation stages in the compressor and turbine subroutines.

4.6 Water-Gas-Shift Reaction

The main concern of this last preliminary study is to provide a realistic model of the power plants investigated. As it was mentioned in the description of the Shift Module (Section 2.5.2), the coal-gas composition is such that the effects of the water-gas-shift reaction can be expected to be important. We developed a computer model of the reaction to take these effects into account and included it in the simulation. The study showed that

ignoring the water-gas-shift reaction results in an overestimation of the system efficiency of 0.35 percentage points. Neglecting it would therefore greatly diminish the accuracy of the simulation. The study also showed that the drop in efficiency results because the overall effect of the reaction is to lower the quality of the coal gas as a fuel: part of the CO reacts with water to give H₂, which has a lower heat of combustion and is therefore not as good a fuel.

ANALYSES OF THE RESULTS OBTAINED FOR EACH GASIFYING PROCESS

The purpose of this section is to present the flowsheets and base-case outputs for each of the three designs studied. Approximations and assumptions used in the simulations of the different designs are presented prior to the discussion of the results.

5.1 Assumptions and Approximations Used in the Simulations Base Cases

It was necessary to make a number of assumptions to run the computations. These assumptions concern a wide range of operating parameters and pieces of equipment, and define what we call the "base case" of the simulations (*i.e.*, the reference on which the comparisons, sensitivity analyses and conclusions will be based on). The selection of the base case assumptions shown in Table 5-1 is aimed at simulating typical situations encountered in the power industry. Important assumptions and parameters will be further analyzed in later chapters.

5.2 Design Based on a Texaco-Type Gasifier

This design has been thoroughly described in Chapter 3, since its flowsheet was used in the example developed. The flowsheet is shown again in Figure 5-1, the only difference being that stream numbers have been added to ease the quantitative discussion that follows. An example of the complete output given by the simulation for this design is shown in Tables 5-2-a, 5-2-b and 5-2-c, for a system pressure of 500 psia. Those tables present the values of the process and operating parameters for each stream (Table 5-2-a) and each piece of equipment (Table 5-2-b). Table 5-2-c deals with the energy outputs and consumptions for the whole power plant. A few basic remarks can be made about these results. We can for instance note in Table 5-2-a that stream 36 (water directed to a cooling loop) is zero, which indicates that the system (gasifier included) uses all the water available in the process.

Table 5-1
Assumptions for Base Case Simulations

Ambient temperature: 60°F

Feed air to compressor: 14.4 psia, 56% relative humidity

Compressor polytropic efficiency: 86.6% efficiency

Turbine polytropic efficiency: 88.0% efficiency

Effective turbine inlet temperature: 2100°F (corresponds approximately to an actual inlet temperature of 2400°F)

Number of stages of calculations involved in the compressor and turbine subroutines: 50 stages

Fuel: Coal, Illinois #6; HHV for coal is 12,774 Btu/lb, dry basis

Gasifier : 100% gasification efficiency with equilibrium amounts of CO,CO₂,H₂, and H₂O produced

Combustor: 100% combustion efficiency, with CO₂ and H₂O produced.

Heat exchangers: 25°F minimum approach temperature

heat transfer coefficient (unit: Btu per hour square-foot°F):
 70 for gas-liquid and 50 for gas-gas heat exchanges

Air saturation unit: 10 theoretical stages

Clean-up maximum allowable temperature: 1500°F

Pressure drops: heat exchangers and boiler: high pressure gas: 2.0 psia
 low pressure gas: 0.5 psia
 water: 5.0 psia

combustor: 8.0 psia
 air saturation unit: 1.0 psia
 partial and full quenches: 0.0 psia
 contactor: 0.0 psia
 clean-up unit: 5.0 psia

Heat losses: radiant losses and other heat leakages: 1% HHV for coal
 shaft losses (including generator): 3% of turbine net output

Energy consumptions: gasifier: 0.956 kW per ton of coal gasified per day
 oxygen plant: modeled (see section 4.2)

Electricity output: based on 1000 tons of coal per day

Simulation: assumes that each piece of equipment is ideally designed to fit the operating conditions

Convergence criterion: 0.01% for each process parameter

Figure 5-1: Flowsheet, IHRM for Coal-Gas Fired Combustion Turbine Systems Using a Texaco-Like Gasifying Process

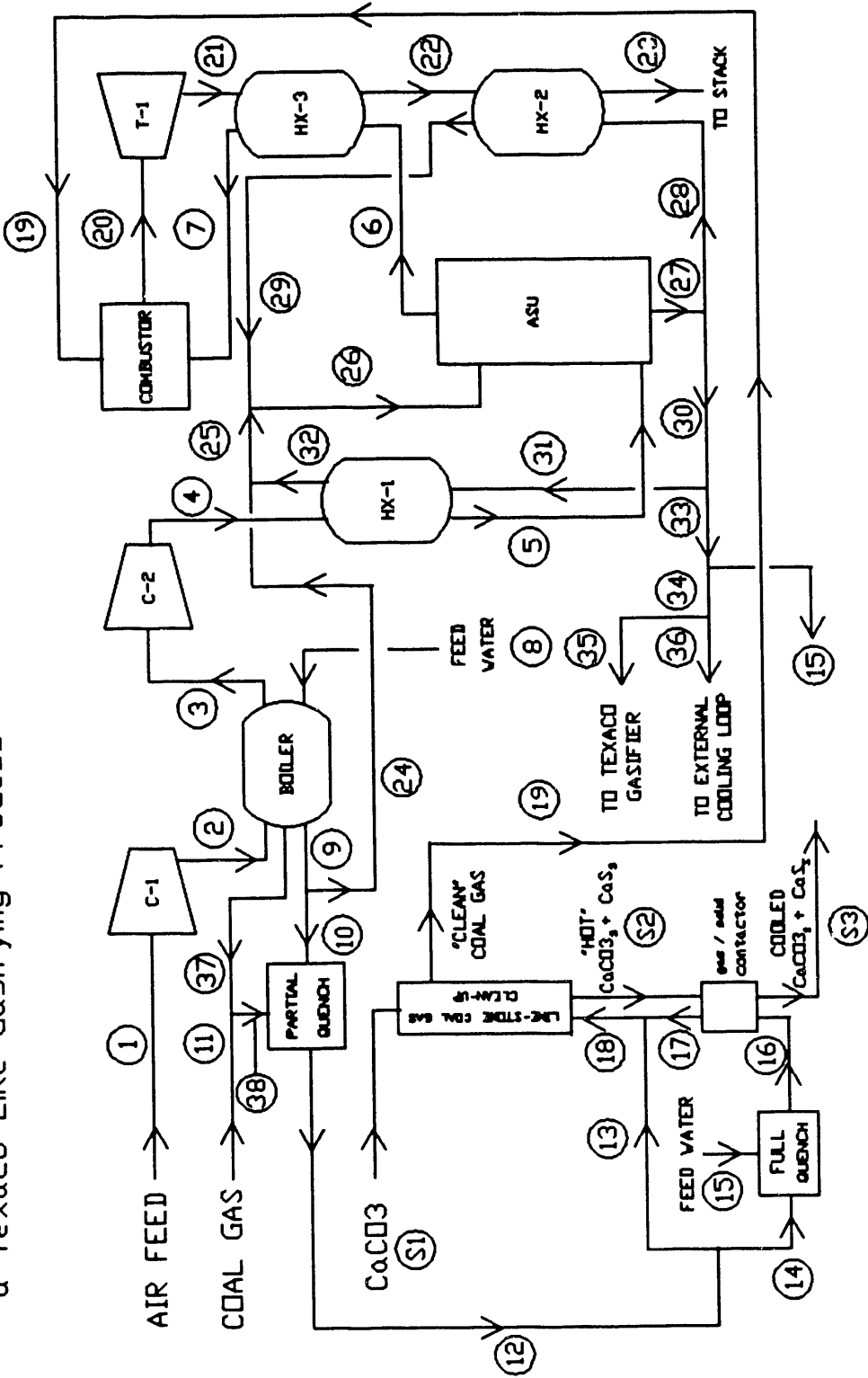


Table 5-2-a
Output, Improved Heat Recovery Method Using a Texaco-Type of Gasifier

SIMULATION OUTPUT (BASED ON 1000 SHORT TONS OF COAL / DAY)										STREAM MOLE FRACTIONS						
STREAM NUMBER	TEMP (°F)	PRESS (psia)	FLOW (lbmol/sec)	ENTHALPY (Btu/sec)	CH4	C2H6	CO2	H2Ov	N2	O2	Ar	CO	H2	H2S	NH3	H2Oliq
1	60.00	14.4	13.143	-1597.	.00000	.00000	.00033	.00990	.77311	.20739	.00925	.00000	.00000	.00000	.00000	
2	544.35	110.0	13.143	43346.	.00000	.00000	.00033	.00990	.77311	.20739	.00925	.00000	.00000	.00000	.00000	
3	85.00	108.0	13.143	431.	.00000	.00000	.00033	.00990	.77311	.20739	.00925	.00000	.00000	.00000	.00000	
4	431.23	500.0	13.143	32358.	.00000	.00000	.00033	.00990	.77311	.20739	.00925	.00000	.00000	.00000	.00000	
5	226.93	498.0	13.143	12943.	.00000	.00000	.00033	.00990	.77311	.20739	.00925	.00000	.00000	.00000	.00000	
6	321.28	497.0	16.478	26401.	.00000	.00000	.00027	.21029	.61665	.16542	.00738	.00000	.00000	.00000	.00000	
7	811.56	495.0	16.478	89271.	.00000	.00000	.00027	.21030	.61665	.16542	.00738	.00000	.00000	.00000	.00000	
8	60.00	505.0	4.994	-96023.	.00000	.00000	.00000	.00000	.00000	.00000	.00000	.00000	.00000	.00000	.00000	
9	466.58	500.0	4.628	-53836.	.00000	.00000	.00000	.00000	.00000	.00000	.00000	.00000	.00000	.00000	.00000	
10	466.58	500.0	.927	-10778.	.00000	.00000	.00000	.00000	.00000	.00000	.00000	.00000	.00000	.00000	.00000	
11	2400.00	500.0	2.625	51380.	.00080	.00000	.10790	.16450	.00680	.00000	.00910	.39620	.30260	.00170	.00000	
12	1500.00	500.0	3.917	47673.	.00054	.00000	.16376	.34894	.00456	.00000	.00610	.17405	.29423	.00670	.00114	
13	1500.00	500.0	3.881	47237.	.00054	.00000	.16376	.34894	.00456	.00000	.00610	.17405	.29423	.00670	.00114	
14	1500.00	500.0	.036	437.	.00054	.00000	.16376	.34894	.00456	.00000	.00610	.17405	.29423	.00670	.00114	
15	201.93	500.0	.019	-322.	.00000	.00000	.00000	.00000	.00000	.00000	.00001	.00000	.00000	.00000	.99968	
16	399.90	500.0	.055	115.	.00035	.00000	.10643	.57684	.00296	.00000	.00396	.11312	.19123	.00436	.00074	
17	1473.31	500.0	.055	670.	.00035	.00000	.10643	.57684	.00296	.00000	.00396	.11312	.19123	.00436	.00074	
18	1500.66	500.0	3.937	47933.	.00053	.00000	.16364	.35145	.00453	.00000	.00607	.17250	.29347	.00667	.00113	
19	1437.83	495.0	3.967	46093.	.00053	.00000	.17373	.35060	.00506	.00000	.00602	.16643	.29762	.00000	.00000	
20	2100.00	487.0	19.525	336013.	.00000	.00000	.06944	.30941	.52144	.09224	.00745	.00000	.00000	.00000	.00000	
21	836.56	15.4	19.525	115442.	.00000	.00000	.06944	.30941	.52144	.09224	.00745	.00000	.00000	.00000	.00000	
22	433.70	14.9	19.525	52577.	.00000	.00000	.06944	.30941	.52144	.09224	.00745	.00000	.00000	.00000	.00000	
23	226.93	14.7	19.525	21603.	.00000	.00000	.06944	.30941	.52144	.09224	.00745	.00000	.00000	.00000	.00000	
24	466.58	497.0	3.702	-43058.	.00000	.00000	.00000	.00000	.00000	.00000	.00000	.00000	.00000	.00000	.1.00000	
25	429.30	497.0	8.902	-110257.	.00000	.00000	.00000	.00000	.00000	.00006	.00012	.00000	.00000	.00000	.99981	
26	417.58	497.0	17.090	-215655.	.00000	.00000	.00000	.00000	.00000	.00016	.00008	.00000	.00000	.00000	.99975	
27	201.93	498.0	13.755	-229114.	.00000	.00000	.00000	.00000	.00000	.00021	.00001	.00000	.00000	.00000	.99968	
28	201.93	502.0	8.188	-136389.	.00000	.00000	.00000	.00000	.00000	.00021	.00010	.00000	.00000	.00000	.99968	
29	404.62	497.0	8.188	-105415.	.00000	.00000	.00000	.00000	.00000	.00021	.00010	.00000	.00000	.00000	.99968	
30	201.93	498.0	5.567	-92725.	.00000	.00000	.00000	.00000	.00000	.00021	.00010	.00000	.00000	.00000	.99968	
31	201.93	498.0	5.200	-86615.	.00000	.00000	.00000	.00000	.00000	.00021	.00010	.00000	.00000	.00000	.99968	
32	402.12	493.0	5.200	-67200.	.00000	.00000	.00000	.00000	.00000	.00021	.00010	.00000	.00000	.00000	.99968	
33	201.93	498.0	.367	-6110.	.00000	.00000	.00000	.00000	.00000	.00021	.00010	.00000	.00000	.00000	.99968	
34	201.93	498.0	.347	-5788.	.00000	.00000	.00000	.00000	.00000	.00021	.00010	.00000	.00000	.00000	.99968	
35	201.93	498.0	.347	-5788.	.00000	.00000	.00000	.00000	.00000	.00021	.00010	.00000	.00000	.00000	.99968	
36	.00	.00	.00	0.	.00000	.00000	.00000	.00000	.00000	.00000	.00000	.00000	.00000	.00000	.00000	
37	466.58	500.0	.366	827.	.00000	.00000	.1.00000	.00000	.00000	.00000	.00000	.00000	.00000	.00000	.00000	
38	2137.70	500.0	2.91	52208.	.00070	.00000	.09471	.26702	.00597	.00000	.00799	.34775	.26560	.00878	.00149	

Table 5-2-b
Output (Continued), Improved Heat Recovery Method Using a Texaco-Type of Gasifier

RESULTS FOR THE SOLID STREAMS IN THE CLEAN-UP SECTION FOR A $\text{CaCO}_3/\text{H}_2\text{S}$ RATIO = 1.25:1

STREAM NUMBER	TEMP ($^{\circ}\text{F}$)	MOLAR FLOW (lbmol/sec)	MASS FLOW (lb/sec)	ENTHALPY (Btu/sec)	MOLE FRACTIONS	WEIGHT FRACTION CaCO_3	WEIGHT FRACTION CaS
S1	60.0	.033	3.281	-11.	1.00	0.00	1.00
S2	1500.7	.033	2.546	701.	.20	.80	.26
S3	399.9	.033	2.546	146.	.20	.80	.26

OPERATING PARAMETERS FOR EACH PIECE OF EQUIPMENT:

COMBUSTOR OUTPUT:

AIRRATIO = 3.3 moles of dry air/mole of fuel
 FUEL INLET TEMPERATURE = 1437.8 $^{\circ}\text{F}$

WATER CONTENT (OUT) = 30.9 moles %
 WET AIR INLET TEMPERATURE = 811.6 $^{\circ}\text{F}$
 TURBINE INLET TEMPERATURE = 2100.0 $^{\circ}\text{F}$

TURBINE OUTPUT:

EXPANSION RATIO = 31.62 TURBINE EFFICIENCY = .880

TURBINE WORK = 220596. Btu/sec, OR 232.729 MW

COMPRESSOR # 1:

PRESSURE RATIO = 7.64 COMPRESSOR EFFICIENCY = .868

WORK OF COMPRESSION = 45050. Btu/sec

COMPRESSOR # 2:

PRESSURE RATIO = 4.63 COMPRESSOR EFFICIENCY = .868

WORK OF COMPRESSION = 32464. Btu/sec

TOTAL WORK OF COMPRESSION = 77514. Btu/sec, or 81.777 MW

AIR SATURATION UNIT (ASU):

NUMBER OF STAGES = 10 PRESSURE DROP = 1.0 psia
 WATER EVAPORATED IN ASU = 3.34 lb-moles/sec

WATER CONTENT (IN) = .010 mole %
 NO SIDESTREAM

WATER CONTENT (OUT) = .266 mole %

HEAT EXCHANGER # 1

CALCULATED UA = 718.9 BTU/sec $^{\circ}\text{F}$ APPR. TEMP. AT HOT INLET = 29.1 $^{\circ}\text{F}$ APPR. TEMP. AT HOT OUTLET = 25.0 $^{\circ}\text{F}$
 DELTA T (HOT STREAM) = 204.3 $^{\circ}\text{F}$ DELTA T (COLD STREAM) = 200.2 $^{\circ}\text{F}$ HOT STREAM DELTA P = 2.0 psia
 COLD STREAM DELTA P = 5.0 psia

HEAT EXCHANGER # 2

CALCULATED UA = 1147.6 BTU/sec $^{\circ}\text{F}$ APPR. TEMP. AT HOT INLET = 29.1 $^{\circ}\text{F}$ APPR. TEMP. AT HOT OUTLET = 25.0 $^{\circ}\text{F}$
 DELTA T (HOT STREAM) = 206.8 $^{\circ}\text{F}$ DELTA T (COLD STREAM) = 202.7 $^{\circ}\text{F}$ HOT STREAM DELTA P = .2 psia
 COLD STREAM DELTA P = 5.0 psia

HEAT EXCHANGER # 3

CALCULATED UA = 1081.1 BTU/sec $^{\circ}\text{F}$ APPR. TEMP. AT HOT INLET = 25.0 $^{\circ}\text{F}$ APPR. TEMP. AT HOT OUTLET = 112.4 $^{\circ}\text{F}$
 DELTA T (HOT STREAM) = 402.9 $^{\circ}\text{F}$ DELTA T (COLD STREAM) = 490.3 $^{\circ}\text{F}$ HOT STREAM DELTA P = .5 psia
 COLD STREAM DELTA P = 2.0 psia

Table 5-2-c
Output (continued), Improved Heat Recovery Method Using a Texaco-Type of Gasifier

BOILER OUTPUT	APPR. TEMP. AT HOT OUTLET = 25.0°F	APPR. TEMP. AT HOT INLET = 77.8°F	APPR. TEMP. AT THE BOILER TEMP. PINCH = 25.4°F
AIR-SIDE PRESSURE DROP = 2.0 psia	WATER-SIDE PRESSURE DROP = 5.0 psia	STEAM FLOW = 7.32 % of the boiler feed water flow	
P-QUENCH WATER FLOW = 18.55 % of the boiler water flow	WATER FLOW TO THE HEAT RECOVERY SECTION: 74.12 % of the boiler feed water flow		
PARTIAL QUENCH OUTPUT			
TEMP. DROP THROUGH THE QUENCH = 637.7°F	COAL GAS INLET TEMP. = 2137.7°F	QUENCH WATER INLET TEMP. = 466.6°F	
QUENCH OUTLET TEMP. = 1500.0°F	WATER VAPORIZED = .93 lb-mol/sec	WATER CONTENT (IN) = 26.7 mol %	WATER CONTENT (OUT) = 34.9 mol %
FULL QUENCH OUTPUT			
TEMP. DROP THROUGH THE QUENCH = 1100.1°F	COAL GAS INLET TEMP. = 1500.0°F	QUENCH WATER INLET TEMP. = 201.9°F	
QUENCH OUTLET TEMP. = 399.90°F	WATER VAPORIZED = .019 lb-mol/sec	WATER CONTENT (IN) = 34.9 mol %	WATER CONTENT (OUT) = 57.7 mol %
COAL GAS QUENCHED = .9 % of main coal gas stream			
CONTACTOR OUTPUT			
GAS INLET TEMP. = 399.90°F	GAS OUTLET TEMP. = 1473.31°F	SOLIDS INLET TEMP. = 1500.7°F	SOLIDS OUTLET TEMP. = 399.9°F
CLEANUP OUTPUT			
ASSUMING COMPLETE REMOVAL OF H ₂ S AND NH ₃	CLEAN-UP TEMP. = 1469.2°F	PRESSURE DROP = 5.0 psia	CaCO ₃ /H ₂ S RATIO = 1.25:1
INLET COAL GAS TEMP. = 1500.7°F	OUTLET GAS TEMP. = 1437.8°F	INLET LIMESTONE TEMP. = 60.0°F	OUTLET SOLIDS TEMP. = 1500.7°F
LIMESTONE FLOW = .033 lb-mol/sec	RATE OF H ₂ S REMOVAL = .026 lb-mol/sec	RATE OF NH ₃ REMOVAL = .004 lb-mol/sec	
SYSTEM OUTPUT:			
BASIS OF STUDY : 1000.0 short tons of moisture free Illinois coal No.6 / day; COAL HHV (dry) = 12,774 Btu/lb , LHV (dry) = 12,284 btu/lb			
NUMBER OF GLOBAL ITERATIONS REQUIRED TO REACH CONVERGENCE = 18			
FRACTION OF TOTAL COMPRESSION WORK ACCOMPLISHED IN COMPRESSOR C-1 = 58.12 %			
ENERGY REQUIRED BY THE OXYGEN PLANT = 1294.7. Btu/sec or 13.66 MW			ENERGY REQUIRED BY THE GASIFIER = 906. Btu/sec or .96 MW
HEAT LOSS THROUGH THE GASIFIER = .69 % of HHV for coal		RADIANT HEAT LOSS (COMBUSTOR SECTION) = 1.00 % of HHV for coal	
SHAFT LOSSES (INCLUDING GENERATOR) = 3.00 % of turbine net work output			
TURBINE NET WORK OUTPUT = 143082. Btu/sec or 150.96 MW		SYSTEM ELECTRIC POWER OUTPUT = 124936. Btu/sec or 131.81 MW	
HEAT RATE = 8076. Btu / kWhr (based on HHV for coal)			
SYSTEM CORRECTED EFFICIENCY (HEAT LOSS IN THE GASIFIER NOT INCLUDED) = 42.56 % (based on HHV for coal)			[= 45.08 % (LHV)]
OVERALL SYSTEM EFFICIENCY (INCLUDING THE HEAT LOSS OCCURRING IN THE GASIFIER) = 42.25 % (based on HHV for coal)			[= 43.94 % (LHV)]

An important consequence of this point is that the large capital investment for a cooling water can be avoided in this design. Table 5-2-c shows that a typical efficiency for the "Texaco design" is 42.2%.

5.3 Design Based on an Oxygen-Blown Fluidized-Bed Gasifier

This design, shown in Figure 5-2, is very similar to the "Texaco design". The main difference is that the gasifying process requires steam instead of water. Some of the steam generated by the boiler/intercooler is diverted to purpose. We will see later that this imposes certain constraints on the operating conditions for the boiler, which has to provide a minimum amount of steam. Another difference is that the amount of oxygen required for the gasification is 32% lower in the oxygen-blown fluidized-bed gasifier than in the Texaco type, which reduces both the energy consumption of the oxygen plant and the CO_2 produced by the gasifier. These reductions account for a large part of the significant increase in the system efficiency observed, 44.5% (plus 2.3 percentage points over the Texaco-based design efficiency).

As before, a complete output of the simulation is shown in Tables 5-3-a, 5-3-b and 5-3-c. We note that, unlike in the Texaco-type design, the system does not use all the water available: stream 38 (Table 5-3-a) has a flow rate equal to 1.6 lb-moles/sec (which approximately corresponds to 207 gallons per minute) and a cooling loop is therefore required in this design. In addition to the fact that the gasifying process does not use liquid water, the magnitude of stream 38 be explained by the difference in coal-gas inlet temperatures between the "oxygen design" and the "Texaco design" (1850°F and 2400°F respectively): because of this difference, it takes 70% less water to quench the coal-gas in the former design than in the latter. Another point is that the amount of air required by the system is substantially higher in the "oxygen design" (plus 20%). This is due to the higher CO to H_2 ratio in the coal-gas produced by the fluidized-bed gasifier: $\text{CO}/\text{H}_2 = 1.97$, instead of 1.30 for the Texaco

Figure 5-2: Flowsheet, IHRM for Coal-Gas Fired Combustion Turbine Systems Using an Oxygen-Blown Fluidized-Bed Gasifying Process

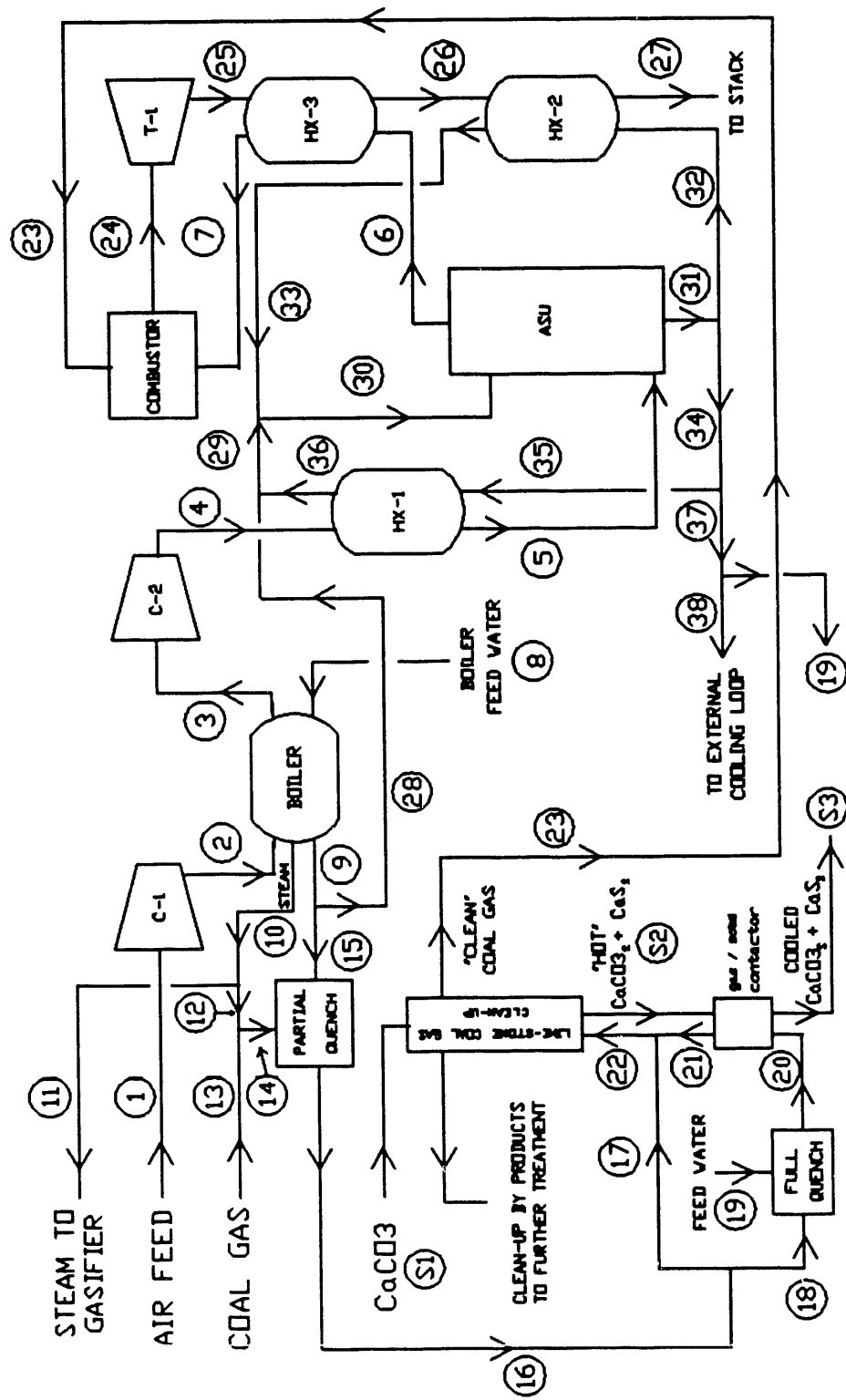


Table 5-3-a
output, Improved Heat Recovery Method (IHRM) Using an Oxygen-Blown Fluidized-Bed Gasifier

SIMULATION OUTPUT (BASED ON 1000 SHORT TONS OF COAL / DAY)									
STREAM NUMBER	TEMP (°F)	PRESS (psia)	FLOW (lbmol/sec)	ENTHALPY (Btu/sec)	CH4	C2H6	CO2	H2Ov	N2
1	60.00	14.4	15.731	-1912.	.00000	.00000	.00033	.00990	.77311
2	514.53	100.0	15.731	48498.	.00000	.00000	.00033	.00990	.77311
3	85.00	98.0	15.731	549.	.00000	.00000	.00033	.00990	.77311
4	459.53	500.0	15.731	41961.	.00000	.00000	.00033	.00990	.77311
5	227.47	498.0	15.731	15553.	.00000	.00000	.00033	.00990	.77311
6	318.85	497.0	19.546	31024.	.00000	.00000	.00027	.00925	.20739
7	795.47	495.0	15.546	103325.	.00000	.00000	.00027	.00925	.20739
8	60.00	505.0	5.974	-114875.	.00000	.00000	.00000	.00000	.00000
9	466.58	500.0	5.786	-67303.	.00000	.00000	.00000	.00000	.00000
10	466.58	500.0	.188	373.	.00000	.00000	.00000	.00000	.00000
11	466.58	500.0	.154	306.	.00000	.00000	.00000	.00000	.00000
12	466.58	500.0	.034	77.	.00000	.00000	.00000	.00000	.00000
13	1850.00	500.0	2.048	29554.	.05800	.00000	.04700	.00400	.00730
14	1833.26	500.0	2.082	29849.	.05705	.00000	.05225	.00363	.00718
15	466.58	500.0	.359	-4179.	.00000	.00000	.00000	.00000	.00000
16	1500.00	500.0	2.441	28826.	.04866	.00000	.11874	.00612	.00612
17	1500.00	500.0	2.404	28385.	.04866	.00000	.11874	.00612	.00612
18	1500.00	500.0	.037	441.	.04866	.00000	.11874	.00612	.00612
19	202.47	500.0	.020	-328.	.00000	.00000	.00000	.00000	.00000
20	773.86	500.0	.057	112.	.03184	.00000	.07769	.042337	.423337
21	1490.41	500.0	.057	688.	.03184	.00000	.07769	.042337	.423337
22	1503.84	500.0	2.461	29184.	.04827	.00000	.12040	.12317	.00607
23	1408.91	495.0	2.488	27497.	.04775	.00000	.13797	.12439	.06061
24	2100.00	487.0	21.195	359104.	.00000	.00000	.06421	.25026	.57451
25	820.47	15.4	21.195	121009.	.00000	.00000	.06421	.25026	.57451
26	385.89	14.9	21.195	48713.	.00000	.00000	.06421	.25026	.57451
27	227.47	14.7	21.195	23356.	.00000	.00000	.06421	.25026	.57451
28	466.58	497.0	5.427	-63124.	.00000	.00000	.00000	.00000	.00000
29	447.12	497.0	11.611	-139658.	.00000	.00000	.00000	.00005	.00011
30	408.24	497.0	20.547	-263068.	.00000	.00000	.00000	.00015	.00007
31	202.47	498.0	16.752	-278539.	.00000	.00000	.00000	.00021	.00010
32	202.47	502.0	8.937	-148768.	.00000	.00000	.00000	.00010	.00000
33	356.26	497.0	8.937	-123410.	.00000	.00000	.00000	.00021	.00010
34	202.47	498.0	7.795	-129771.	.00000	.00000	.00000	.00021	.00010
35	202.47	502.0	6.184	-102943.	.00000	.00000	.00000	.00001	.00000
36	429.78	497.0	6.184	-76535.	.00000	.00000	.00000	.00010	.00000
37	202.47	498.0	1.612	-26828.	.00000	.00000	.00000	.00000	.00000
38	202.47	498.0	1.592	-26500.	.00000	.00000	.00000	.00021	.00010

Output (Continued), IHRM Using an Oxygen-Blown Fluidized-Bed Gasifier

PROCESS PARAMETERS FOR THE SOLID STREAM IN THE CLEAN-UP SECTION FOR A $\text{CaCO}_3/\text{H}_2\text{S}$ RATIO = 1.25:1						
STREAM NUMBER	TEMP (°F)	MOLAR FLOW (lbmol/sec)	MASS FLOW (lb/sec)	ENTHALPY (Btu/sec)	MOLE FRACTIONS CaCO_3	WEIGHT FRACTION CaCO_3
S1	60.0	.033	3.328	-11.	1.00	0.00
S2	1503.8	.033	2.583	713.	.20	.80
S3	373.9	.033	2.583	135.	.20	.80

OPERATING PARAMETERS FOR EACH PIECE OF EQUIPMENT:

COMBUSTOR OUTPUT:
 AIR:RATIO = 6.3 moles of dry air/mole of fuel
 FUEL INLET TEMPERATURE = 1408.9°F

WATER CONTENT (OUT) = 25.0 lb-moles %
 WET AIR INLET TEMPERATURE = 795.5°F

PRESSURE DROP = 8.0 psia
 TURBINE INLET TEMPERATURE = 2100.0°F

TURBINE OUTPUT:
 EXPANSION RATIO = 31.62

TURBINE EFFICIENCY = .880

TURBINE WORK = 238125. Btu/sec, or 251.22 MW

COMPRESSOR # 1:
 PRESSURE RATIO = 6.94

COMPRESSOR EFFICIENCY = .868

WORK OF COMPRESSION = 50532. Btu/sec

COMPRESSOR # 2:
 PRESSURE RATIO = 5.10

COMPRESSOR EFFICIENCY = .868

WORK OF COMPRESSION = 42033. Btu/sec

TOTAL WORK OF COMPRESSION = 92566. Btu/sec, or 97.657 MW

AIR SATURATION UNIT (ASU):
 NUMBER OF STAGES = 10
 PRESSURE DROP = 1.0 psia
 WATER EVAPORATED IN ASU = 3.82 lb-moles/sec

H2ORATIO(IN) = .010
 NO SIDESTREAM

H2ORATIO(OUT) = .255

HEAT EXCHANGER # 1:
 CALCULATED UA = 967.1 BTU/sec°F APPR. TEMP. AT HOT INLET = 29.8°F APPR. TEMP. AT HOT OUTLET = 25.0°F
 DELTA T (HOT STREAM) = 232.1°F DELTA T (COLD STREAM) = 227.3°F HOT STREAM DELTA P = 2.0 psia

COLD STREAM DELTA P = 5.0 psia

HEAT EXCHANGER # 2:
 CALCULATED UA = 930.3 BTU/sec°F APPR. TEMP. AT HOT INLET = 29.6°F APPR. TEMP. AT HOT OUTLET = 25.0°F
 DELTA T (HOT STREAM) = 158.4°F DELTA T (COLD STREAM) = 153.8°F HOT STREAM DELTA P = .2 psia

COLD STREAM DELTA P = 5.0 psia

HEAT EXCHANGER # 3:
 CALCULATED UA = 1696.3 BTU/sec°F APPR. TEMP. AT HOT INLET = 25.0°F APPR. TEMP. AT HOT OUTLET = 67.0°F
 DELTA T (HOT STREAM) = 434.6°F DELTA T (COLD STREAM) = 476.6°F HOT STREAM DELTA P = .5 psia

COLD STREAM DELTA P = 2.0 psia

Table 5-3-C
Output (continued), IHRM Using an Oxygen-Blown Fluidized-Bed Gasifier

BOILER OUTPUT: APPR. TEMP. AT HOT OUTLET = 25.0°F AIR-SIDE PRESSURE DROP = 2.0 psia P-QUENCH WATER FLOW = 6.01 % of the boiler feed water flow	APPR. TEMP. AT HOT INLET = 48.0°F WATER-SIDE PRESSURE DROP = 5.0 psia WATER FLOW TO THE HEAT RECOVERY SECTION = 90.83 % of the boiler feed water flow	APPR. TEMP. AT THE BOILER TEMP. PINCH = 25.4°F STEAM FLOW = 3.15 % of the boiler feed water flow
PARTIAL QUENCH OUTPUT TEMP. DROP THROUGH THE QUENCH = 333.3°F QUENCH OUTLET TEMP. = 1500.0°F	COAL GAS INLET TEMP. = 1833.3°F WATER VAPORIZED = .36 lb-mol/sec	QUENCH WATER INLET TEMP. = 466.6°F WATER CONTENT (IN) = 5.4 mol % WATER CONTENT (OUT) = 11.9 mol %
FULL QUENCH OUTPUT TEMP. DROP THROUGH THE QUENCH = 1126.1°F QUENCH OUTLET TEMP. = 373.86°F COAL GAS QUENCHED = 1.5 % of main coal gas stream	COAL GAS INLET TEMP. = 1500.00°F WATER VAPORIZED = .020 lb-mol/sec	QUENCH WATER INLET TEMP. = 202.47°F WATER CONTENT (IN) = 11.9 mol % WATER CONTENT (OUT) = 42.3 mol %
CONTACTOR OUTPUT GAS INLET TEMP. = 373.86°F	GAS OUTLET TEMP. = 1490.41°F	SOLIDS INLET TEMP. = 1503.8°F SOLIDS OUTLET TEMP. = 373.9°F
CLEANUP OUTPUT ASSUME COMPLETE REMOVAL OF H ₂ S AND NH ₃ LIMESTONE FLOW = .033 lb-mol/sec INLET COAL GAS TEMP. = 1503.8°F	CLEAN-UP TEMP. = 1456.4°F RATE OF H ₂ S REMOVAL = .027 lb-mol/sec OUTLET GAS TEMP. = 1408.9°F	PRESSURE DROP = 5.0 psia RATE OF NH ₃ REMOVAL = .0001 lb-mol/sec INLET LIMESTONE TEMP. = 60.0°F OUTLET SOLIDS TEMP. = 1503.8°F
SYSTEM OUTPUTS:		
BASIS OF THE STUDY : 1000.0 short tons of moisture free Illinois coal No.6 / day;	COAL HHV (dry) = 12,774 Btu/lb , COAL LHV (dry) = 12,284 btu/lb	
NUMBER OF GLOBAL ITERATIONS REQUIRED TO REACH CONVERGENCE = 16		
FRACTION OF TOTAL COMPRESSION WORK ACCOMPLISHED IN COMPRESSOR NO.1 = 54.59 %		
ENERGY REQUIRED BY THE OXYGEN PLANT = 8752. Btu/sec or 9.23 MW	ENERGY REQUIRED BY THE GASIFIER = 906. Btu/sec or .96 MW	
HEAT LOSS THROUGH THE GASIFIER = .69 % of coal HHV SHAFT LOSSES (INCLUDING GENERATOR) = 3.00 % of turbine net work output	RADIENT HEAT LOSS (COMBUSTOR SECTION) = 1.00 % of coal HHV	
TURBINE NET WORK OUTPUT = 145559. Btu/sec or 153.57 MW	SYSTEM ELECTRIC POWER OUTPUT = 131534. Btu/sec or 138.78 MW	
HEAT RATE = 7671. Btu / kw-hr (based on HHV for coal)		
SYSTEM CORRECTED EFFICIENCY (HEAT LOSS IN THE GASIFIER NOT INCLUDED) = 44.84 % (based on HHV for coal)	[= 47.46 % (LHV)]	
SYSTEM THERMAL EFFICIENCY (INCLUDING THE HEAT LOSS OCCURRING IN THE GASIFIER) = 44.48 % (based on HHV for coal)	[= 46.26 % (LHV)]	

gasifier. Since CO has a higher heat of combustion than H₂, the amount of air required for the control of the firing temperature increases with increasing values of the CO to H₂ ratio. The larger flow of compressed air also contributes to the increased amount of excess water in the system, since more water is needed for intercooling.

5.4 Design Based on an Air-Blown Fluidized-Bed Gasifier

The flowsheet developed for this design is shown in Figure 5-3 and can be easily related to the previous flowsheet (Figure 5-2). Both fluidized-bed gasifying processes require steam, which is provided by the intercooler (boiler) in the two designs. The steam requirements are however 50% larger in the air-blown design, which aggravates the limitations on the operating conditions of the boiler mentioned in the previous section.

The main difference between the two designs is that the oxygen required by the gasification is provided by a compressor (air) instead of being provided by an oxygen plant (95% O₂). Compressed air for gasification is obtained by diverting some of the air from compressor C-2 to compressor C-3 (stream 41). In addition to decreasing the amount of energy required to provide the oxygen necessary for the gasification by 23%, using compressed air increases the flow of gasifier gas by 105 % and thereby reduces the amount of excess air required to control the firing temperature in the combustor. This results in a decrease of the energy requirements of the plant while the work of compression remains roughly constant, since the total amount of compressed air in both fluidized-bed designs are comparable. For process control reasons (among others), the pressure of the air stream fed to the gasifier is significantly higher than the system pressure: typically 550 psia for a system pressure of 500 psia. As we already did in a similar situation (oxygen plant, Section 4.2), we chose to relate the two pressures by a constant ratio (equal to 1.1 in this case).

Tables 5-4-a, 5-4-b and 5-4-c provide a complete output of the simulation of the design. The efficiency obtained for this design is close to 45.8%.

Figure 5-3:
Flowsheet, IHRM for Coal-Gas Fired Combustion Turbine Systems Using an Air-Blown Fluidized-Bed Gasifying Process

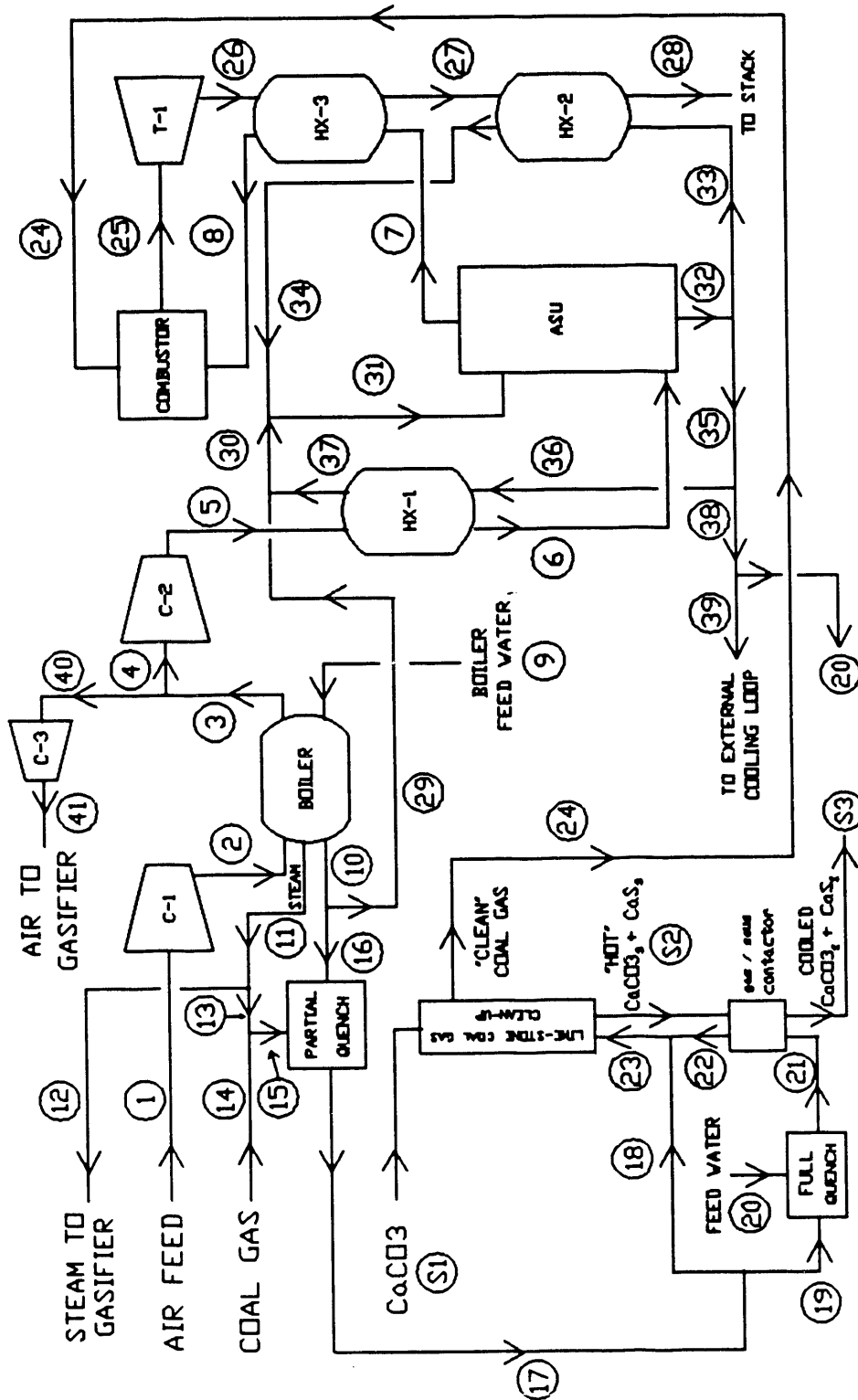


**Table 5-4-a
Output, Improved Heat-Recovery Method (IHRM) Using an Air-Blown Fluidized-Bed Classifier**

SIMULATION STREAM NUMBER	TEMP (°F)	PRESS (psia)	FLOW (lbmol/sec)	ENTHALPY (Btu/sec)	STREAM MOLE FRACTIONS								
					CO ₂	C2H ₆	CH ₄	N ₂	O ₂	Ar	CO	H ₂	H ₂ S
1	60.00	14.4	15.687	-1907.	.00000	.00033	.00990	.77311	.20739	.00925	.00000	.00000	.00000
2	559.52	115.0	15.687	53346.	.00000	.00033	.00990	.77311	.20739	.00925	.00000	.00000	.00000
3	85.00	113.0	15.687	502.	.00000	.00033	.00990	.77311	.20739	.00925	.00000	.00000	.00000
4	85.00	113.0	13.066	414.	.00000	.00033	.00990	.77311	.20739	.00925	.00000	.00000	.00000
5	418.33	500.0	13.066	30945.	.00000	.00033	.00990	.77311	.20739	.00925	.00000	.00000	.00000
6	230.63	498.0	13.066	13216.	.00000	.00033	.00990	.77311	.20739	.00925	.00000	.00000	.00000
7	326.61	497.0	16.728	27347.	.00000	.00026	.00026	.22671	.60383	.16198	.00722	.00000	.00000
8	781.86	495.0	16.728	86902.	.00000	.00026	.00026	.22670	.60384	.16198	.00722	.00000	.00000
9	60.00	505.0	5.963	-114659.	.00000	.00000	.00000	.00000	.00000	.00000	.00000	.00000	.00000
10	466.58	500.0	5.409	-62914.	.00000	.00000	.00000	.00000	.00000	.00000	.00000	.00000	.00000
11	466.58	500.0	.554	1098.	.00000	.00000	.00000	.00000	.00000	.00000	.00000	.00000	.00000
12	466.58	500.0	.231	459.	.00000	.00000	.00000	.00000	.00000	.00000	.00000	.00000	.00000
13	466.58	500.0	.323	731.	.00000	.00000	.00000	.00000	.00000	.00000	.00000	.00000	.00000
14	1850.00	500.0	4.200	52826.	.01000	.00000	.03800	.04100	.20600	.00000	.27500	.26880	.15600
15	1755.17	500.0	4.523	55572.	.00929	.00000	.06085	.08392	.19129	.00000	.25536	.22336	.17043
16	466.58	500.0	.497	-5782.	.00000	.00000	.00000	.00000	.00000	.00000	.00000	.00000	.00000
17	1500.00	500.0	5.020	53196.	.00837	.00000	.09376	.13569	.17235	.00000	.23008	.16225	.19248
18	1500.00	500.0	4.980	52774.	.00837	.00000	.09376	.13569	.17235	.00000	.23008	.16225	.19248
19	1500.00	500.0	.040	423.	.00837	.00000	.09376	.13569	.17235	.00000	.23008	.16225	.19248
20	205.63	500.0	.019	-314.	.00000	.00000	.00000	.00000	.00021	.00010	.00001	.00000	.00000
21	372.06	500.0	.059	108.	.00567	.00000	.06355	.41418	.11682	.00000	.15594	.10997	.13046
22	1477.66	500.0	.059	653.	.00567	.00000	.06355	.41418	.11682	.00000	.15594	.10997	.13046
23	1501.23	500.0	5.039	53502.	.00833	.00000	.09426	.13809	.17170	.00000	.22921	.16079	.19261
24	1449.16	495.0	5.064	51812.	.00829	.00000	.10150	.13965	.17085	.00000	.22807	.15726	.19438
25	2100.00	487.0	20.903	349319.	.00000	.00000	.06490	.26638	.52464	.08302	.06104	.00000	.00000
26	806.86	15.4	20.903	115581.	.00000	.00000	.06490	.26638	.52464	.08302	.06104	.00000	.00000
27	440.21	14.9	20.903	56029.	.00000	.00000	.06490	.26638	.52464	.08302	.06104	.00000	.00000
28	230.63	14.7	20.903	23227.	.00000	.00000	.06490	.26638	.52464	.08302	.06104	.00000	.00000
29	466.58	497.0	4.912	-57132.	.00000	.00000	.00000	.00000	.00011	.00005	.00000	.00000	.00000
30	427.21	497.0	10.111	-125636.	.00000	.00000	.00000	.00000	.00015	.00007	.00000	.00000	.00000
31	419.88	497.0	18.645	-234427.	.00000	.00000	.00000	.00000	.00015	.00007	.00000	.00000	.00000
32	205.63	498.0	14.982	-248558.	.00000	.00000	.00000	.00000	.00021	.00010	.00001	.00000	.00000
33	205.63	502.0	8.534	-141581.	.00000	.00000	.00000	.00000	.00021	.00010	.00001	.00000	.00000
34	411.12	497.0	8.534	-108779.	.00000	.00000	.00000	.00000	.00021	.00010	.00001	.00000	.00000
35	205.63	498.0	6.448	-106977.	.00000	.00000	.00000	.00000	.00021	.00010	.00001	.00000	.00000
36	205.63	502.0	5.199	-86254.	.00000	.00000	.00000	.00000	.00021	.00010	.00001	.00000	.00000
37	388.94	497.0	5.199	-68525.	.00000	.00000	.00000	.00000	.00021	.00010	.00001	.00000	.00000
38	205.63	498.0	1.249	-20722.	.00000	.00000	.00000	.00000	.00021	.00010	.00001	.00000	.00000
39	205.63	498.0	1.230	-20408.	.00000	.00000	.00000	.00000	.00021	.00010	.00001	.00000	.00000
40	85.00	113.0	2.621	83.	.00000	.00033	.00990	.77311	.20739	.00925	.00000	.00000	.00000
41	445.09	550.0	2.621	6710.	.00000	.00033	.00990	.77311	.20739	.00925	.00000	.00000	.00000

Table 5-4-b
Output (Continued) , IHRM Using an Air-Blown Fluidized-Bed Gasifier

RESULTS FOR THE SOLID STREAMS IN THE CLEAN-UP SECTION FOR A $\text{CaCO}_3/\text{H}_2\text{S}$ RATIO = 1.25:1

STREAM NUMBER	TEMP (°F)	MOLAR FLOW (lbmo/sec)	MASS FLOW (lb/sec)	ENTHALPY (Btu/sec)	MOLE FRACTIONS CaCO_3	WEIGHT FRACTION CaCO_3
S1	60.0	.032	3.150	10.	1.00	0.00
S2	1501.2	.032	2.444	673.	.20	.80
S3	372.1	.032	2.444	127.	.20	.80

OPERATING PARAMETERS FOR EACH PIECE OF EQUIPMENT:

COMBUSTOR OUTPUT AIR RATIO = 2.6 moles of dry air/mole of fuel
 FUEL INLET TEMPERATURE = 1449.2°F

TURBINE EXPANSION RATIO = 31.62
 TURBINE EFFICIENCY = .880
 TURBINE WORK = 233774. Btu/sec, OR 246.632 MW

COMPRESSOR # 1
 PRESSURE RATIO = 7.99
 COMPRESSOR # 2
 PRESSURE RATIO = 4.42
 COMPRESSOR # 3
 PRESSURE RATIO = 4.87
 COMPRESSOR EFFICIENCY = .868
 WORK OF COMPRESSION = 6743. Btu/sec

TOTAL WORK OF COMPRESSION = 93197. Btu/sec, or 98.328 MW

AIR SATURATION UNIT (ASU)
 NUMBER OF STAGES = 10
 ADDITIONAL WATER EVAPORATED IN ASU = 3.66 lb-moles/sec
 PRESSURE DROP = 1.0 psia
 WATER CONTENT (IN) = .010 mol % WATER CONTENT (OUT) = .293 mol %
 NO SIDESTREAM

HEAT EXCHANGER # 1
 CALCULATED UA = 653.4 BTU/sec°F
 DELTA T (HOT STREAM) = 187.7°F
 APPR. TEMP. AT HOT INLET = 29.4°F APPR. TEMP. AT HOT OUTLET = 25.0°F
 DELTA T (COLD STREAM) = 183.3°F HOT STREAM DELTA P = 2.0 psia COLD STREAM DELTA P = 5.0 psia

HEAT EXCHANGER # 2
 CALCULATED UA = 1215.1 BTU/sec°F
 DELTA T (HOT STREAM) = 209.6°F
 APPR. TEMP. AT HOT INLET = 29.1°F APPR. TEMP. AT HOT OUTLET = 25.0°F
 DELTA T (COLD STREAM) = 205.5°F HOT STREAM DELTA P = .2 psia COLD STREAM DELTA P = 5.0 psia

HEAT EXCHANGER # 3
 CALCULATED UA = 1017.5 BTU/sec°F
 DELTA T (HOT STREAM) = 366.7°F
 APPR. TEMP. AT HOT INLET = 25.0°F APPR. TEMP. AT HOT OUTLET = 113.6°F
 DELTA T (COLD STREAM) = 455.3°F HOT STREAM DELTA P = .5 psia COLD STREAM DELTA P = 2.0 psia

**Table 5-4-C
Output (Continued), IHRM Using Air-Blown Fluidized-Bed Gasifier**

BOILER OUTPUT	APPR. TEMP. AT WATER INLET = 25.0°F	APPR. TEMP. AT WATER OUTLET = 91.9°F	APPR. TEMP. AT BOILER TEMP. PINCH = 25.4°F
AIR SIDE PRESSURE DROP = 2.0 psia	WATER SIDE PRESSURE DROP = 5.0 psia	STEAM MOLAR FLOW RATE = 9.30 % of the boiler feed water flow	
P-QUENCH MOLAR WATER FLOW = 8.34 % of the boiler feed water flow	WATER TO THE HEAT RECOVERY SECTION = 82.37 % of the boiler feed water molar flow		
 PARTIAL QUENCH OUTPUT			
TEMP. DROP THROUGH THE QUENCH = 265.2°F	COAL GAS INLET TEMP. = 1765.2°F	QUENCH WATER INLET TEMP. = 466.6°F	
QUENCH OUTLET TEMP. = 1500.0°F	WATER VAPORIZED = .50 lb-mol/sec	WATER CONTENT (IN) = 8.4 mole %	WATER CONTENT (OUT) = 13.6 mole %
 FULL QUENCH OUTPUT			
COAL GAS QUENCHED = .8 % of main coal gas stream	TEMPERATURE DROP THROUGH THE QUENCH = 1127.9°F		
COAL GAS INLET TEMP. = 1500.00°F	QUENCH WATER INLET TEMP. = 205.63°F	QUENCH OUTLET TEMP. = 372.06°F	
WATER VAPORIZED = .019 lb-mol/sec	WATER CONTENT (IN) = 13.6 mole %	WATER CONTENT (OUT) = 41.4 mole %	
 CONTACTOR OUTPUT			
GAS INLET TEMP. = 372.06°F	GAS OUTLET TEMP. = 1477.66°F	SOLIDS INLET TEMP. = 1501.2°F	SOLIDS OUTLET TEMP. = 372.1°F
 CLEANUP OUTPUT			
ASSUMING COMPLETE REMOVAL OF H ₂ S AND NH ₃	CLEAN-UP TEMP. = 1475.2°F	PRESSURE DROP = 5.0 psia	CaCO ₃ /H ₂ S RATIO = 1.25:1
INLET COAL GAS TEMP. = 1501.2°F	OUTLET GAS TEMP. = 1449.2°F	INLET LIMESTONE TEMP. = 60.0°F	OUTLET SOLIDS TEMP. = 1501.2°F
LIMESTONE FLOW = .032 lb-mol/sec	RATE OF H ₂ S REMOVAL = .025 lb-mol/sec	RATE OF NH ₃ REMOVAL = .0001 lb-mol/sec	
 SYSTEM OUTPUT:			
BASIS OF THE STUDY : 1000.0 short tons of moisture free Illinois coal No.6 / day; HHV for coal (dry) = 12,774 Btu/lb, LHV (dry) = 12,284 Btu/lb			
NUMBER OF GLOBAL ITERATIONS REQUIRED TO REACH CONVERGENCE = 17			
FRACTION OF TOTAL COMPRESSION WORK ACCOMPLISHED IN COMPRESSOR NO.1 = 59.42 %			
ENERGY REQUIRED BY THE OXYGEN PLANT = 0. Btu/sec or .00 MW ENERGY REQUIRED BY THE GASIFIER = 906. Btu/sec or .96 MW			
HEAT LOSS THROUGH THE GASIFIER = .69 % of HHV for coal		RADIANT HEAT LOSS (COMBUSTOR SECTION) = 1.00 % of HHV for coal	
SHAFT LOSSES (INCLUDING GENERATOR) = 3.00 % of turbine net work output			
TURBINE NET WORK OUTPUT = 140577. Btu/sec or 148.32 MW		SYSTEM ELECTRIC POWER OUTPUT = 135456. Btu/sec or 142.91 MW	
HEAT RATE = 7449. Btu / kW-hr (based on HHV for)			
SYSTEM CORRECTED EFFICIENCY (HEAT LOSS IN THE GASIFIER NOT INCLUDED) = 46.18 % (based on HHV for coal) [= 48.87 % (LHV)]			
OVERALL SYSTEM EFFICIENCY (INCLUDING THE HEAT LOSS OCCURRING IN THE GASIFIER) = 45.81 % (based on HHV for coal) [= 47.64 % (LHV)]			

CHAPTER 6: SENSITIVITY ANALYSES

Our goal is to explore and quantify the dependence of the system performance on a number of operating parameters and assumptions. For that, we performed sensitivity analyses similar to the one discussed in Section 4.4, where we examined the variations of the efficiency with the packing height of the air saturation unit for the "Texaco design". The presentation of the results of the sensitivity analyses is divided between Chapters 6 and 7. Chapter 6 deals with the major operating parameters: compression-work split, system pressure, clean-up and turbine maximum allowable temperatures.

The "base case" that we will be constantly referring to was defined in section 5.1 (Table 5.1). Cost estimations (*i.e.*, profits) are based on the assumptions discussed in section 4.4; with those assumptions, a gain of efficiency of one percentage point results in a \$1.78 million increase in yearly profit.

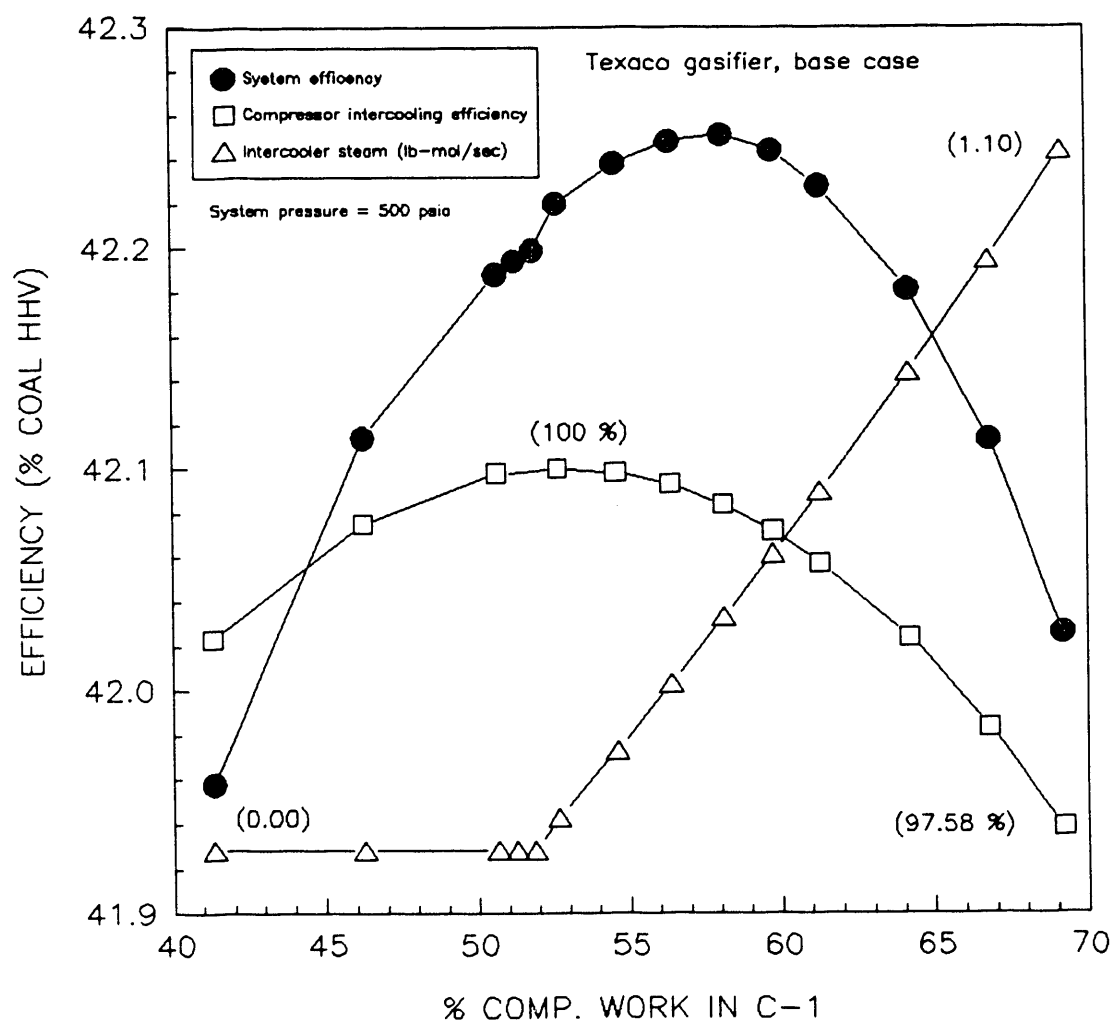
6.1 Efficiencies and Compression-Work Split

Section 3.1 introduced the effect of intercooling on system efficiency: the amount of work required to compress a given amount of air varies with the way the work is split between the two stages of compression. This indicates that this parameter is likely to have an important impact on the system efficiency and accounts for the sensitivity analyses devoted to it.

6.1.1 Design Based on the Texaco-Type Gasifying Processes

Figure 6-1 shows the dependence of the system efficiency on the fraction of the total work of compression performed in the first stage of compression, which is a convenient way to express the work split. The curve has an interesting feature: a secondary minimum appears for a compression work fraction close to 53%, which corresponds to the optimum intercooling efficiency. The notion of intercooling efficiency was discussed in Section 3-1. Intercooling

Figure 6-1:
Efficiency and Compression-Work Split



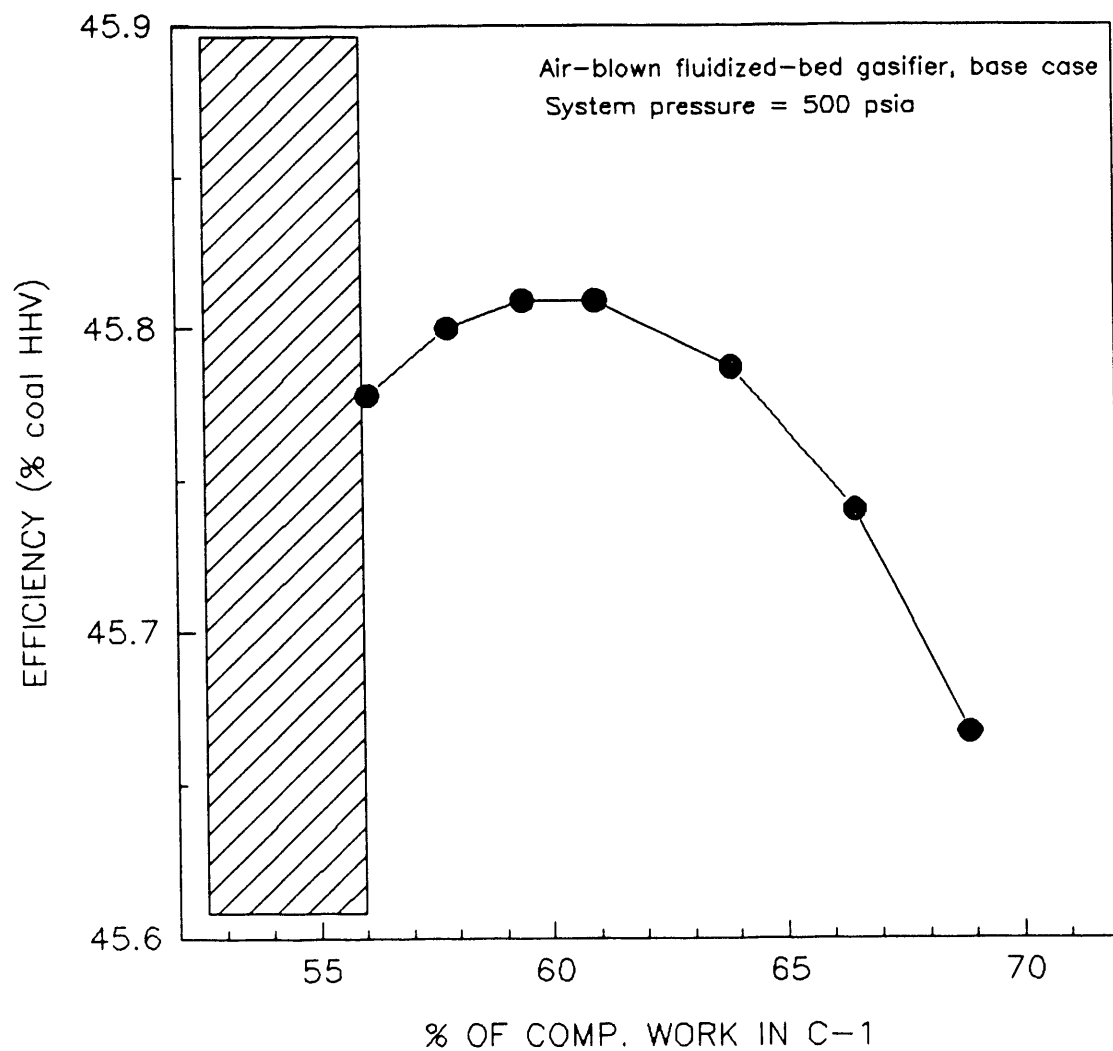
therefore accounts for the increase of efficiency in the absence of steam. If no steam were produced, the efficiency curve would follow the intercooling efficiency and their optima would be located at the same position. Steam generation hence accounts for the continuing increase in efficiency beyond the secondary minimum. Its effect is to reduce the amount of excess air required to control the firing temperature in the combustor and to decrease the work of compression. For fractions of compression work in C-1 higher than 58%, the benefits of an increase in the steam flow are off-set by a rapidly decreasing intercooling efficiency, and results in a lower system efficiency. Extrema values for the intercooling efficiency and the steam flow are reported in Figure 6-1 to somewhat quantify the variations experienced by those two parameters. It is important to note that, because of the magnified scale of efficiency in Figure 6-1, actual variations in efficiency are not as large as they appear to be on the graph. This remark also holds for the two other designs (Figures 6-2 and 6-3). Besides the peculiar shape of the curve, the conclusion of this sensitivity analysis is that the compression-work split is an important operating parameter, since a 20% change in it alters the system efficiency by as much as 0.3 percentage points, which represents a \$540,000 yearly difference in the profits generated by the plant.

6.1.2 Design Based on the Air-Blown Fluidized-Bed Gasifying Process

Sensitivity analyses similar to the one described for the "Texaco design" were performed for the "fluidized-bed designs". Figure 6-2 shows the dependence of the system efficiency with the work split for the "air-blown design", which will be the first fluidized-bed gasifier examined. We can notice that the efficiency curves shown in Figures 6-1 and 6-2 are very similar: in both cases, the location of the optimum system efficiency is determined by the amount of steam generated by the boiler/intercooler and by the intercooling efficiency. The effects of these two parameters are discussed above.

As mentioned in Section 5.2, the steam requirements of the fluidized-bed gasifiers put some constraints on the operating parameters of the compression section. These constraints

Figure 6-2:
Efficiency and Compression-Work Split



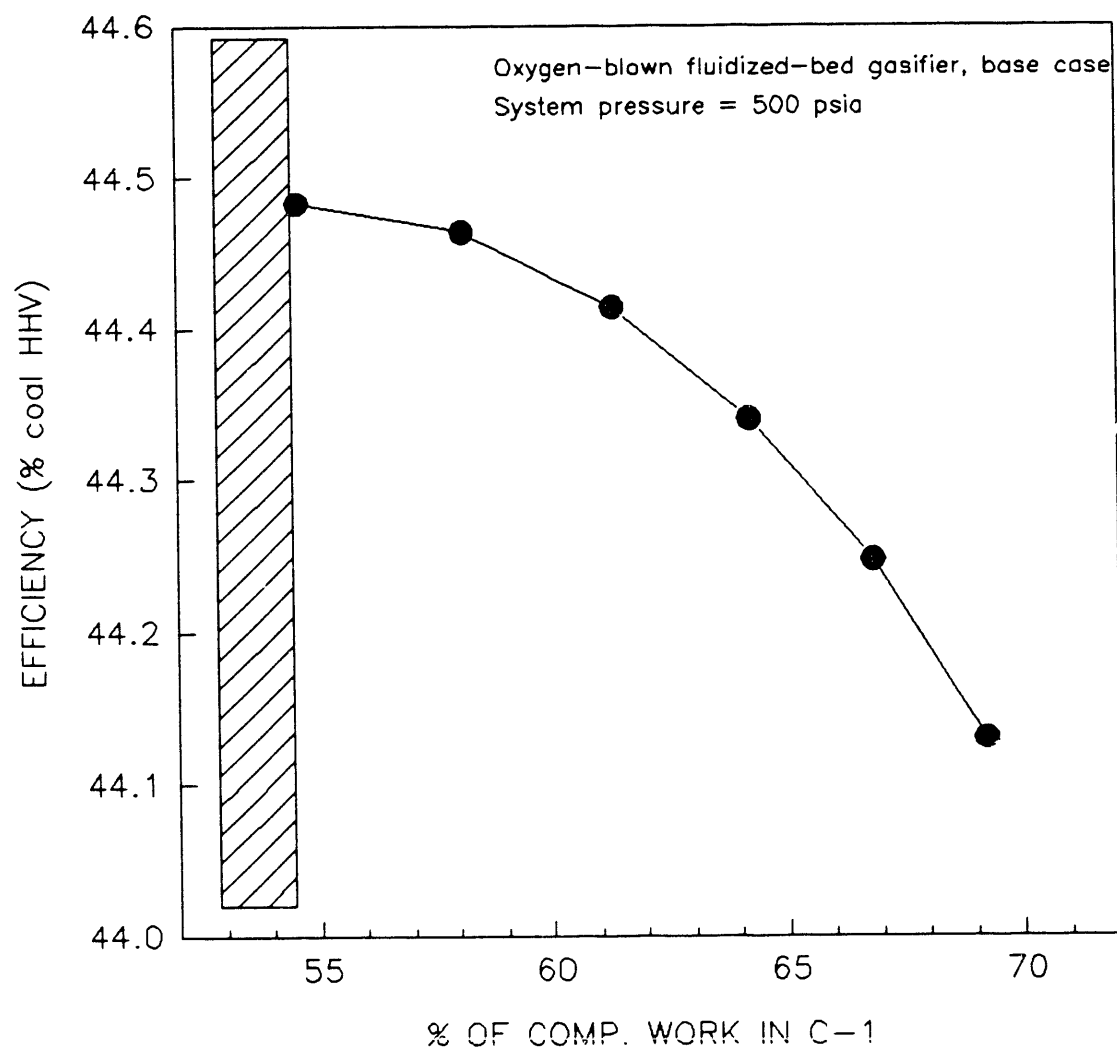
appear clearly in Figure 6-2, which shows the presence of a minimum allowable value for the fraction of compression work in C-1 (hatched area); below this value, the boiler cannot generate enough steam for the gasifier.

6.1.3 Design Based on the Oxygen-Blown Fluidized-Bed Gasifying Process

The "oxygen design" is the second "fluidized-bed design" examined. Both designs require steam for the gasifying processes involved, which accounts for the minimum allowable value of the compression-work split observed again in Figure 6-3 (hatched area).

We can observe a major difference between the system-efficiency curve shown in Figure 6-3 and the curves obtained for the two designs discussed previously: the efficiency does not reach a maximum in the range of work splits considered. This can be explained by the relatively low temperature and flow of the coal-gas stream produced by the oxygen-blown fluidized-bed gasifier: 1850°F for a flow equal to 2.05 lb-mol/sec. This should be compared with the 2400°F and the 4.20 lb-mol/sec for the coal-gas streams respectively produced by the Texaco and the air-blown gasifiers. Indeed, high temperatures and large flows (e.g. in the "Texaco" and "Air" designs) result in large amounts of water vaporized in the coal-gas stream in the partial quench; in that situation the quantity of steam generated by the boiler marginally affects the equilibrium composition of the gas (determined by the water-gas-shift reaction). An increase in the steam flow then chiefly results in a higher water content of the coal-gas and therefore in a reduction of the compression work, since it reduces the amount of excess air required to control the combustor firing temperature. Conversely, for coal-gas streams with lower flows and temperatures (e.g. in the oxygen design), an increase of the steam flow affects the amount of water evaporated in the partial quench to a much greater extent than in the previous cases; the equilibrium composition is in turn affected substantially, and the reduction of compression work resulting from the higher water content is offset by the decrease in the CO-to-H₂ ratio in the coal gas. Overall, an increase of steam flow has thus a very slight effect on the system performance, and the system-efficiency curve

Figure 6-3
Efficiency and Compression-Work Split



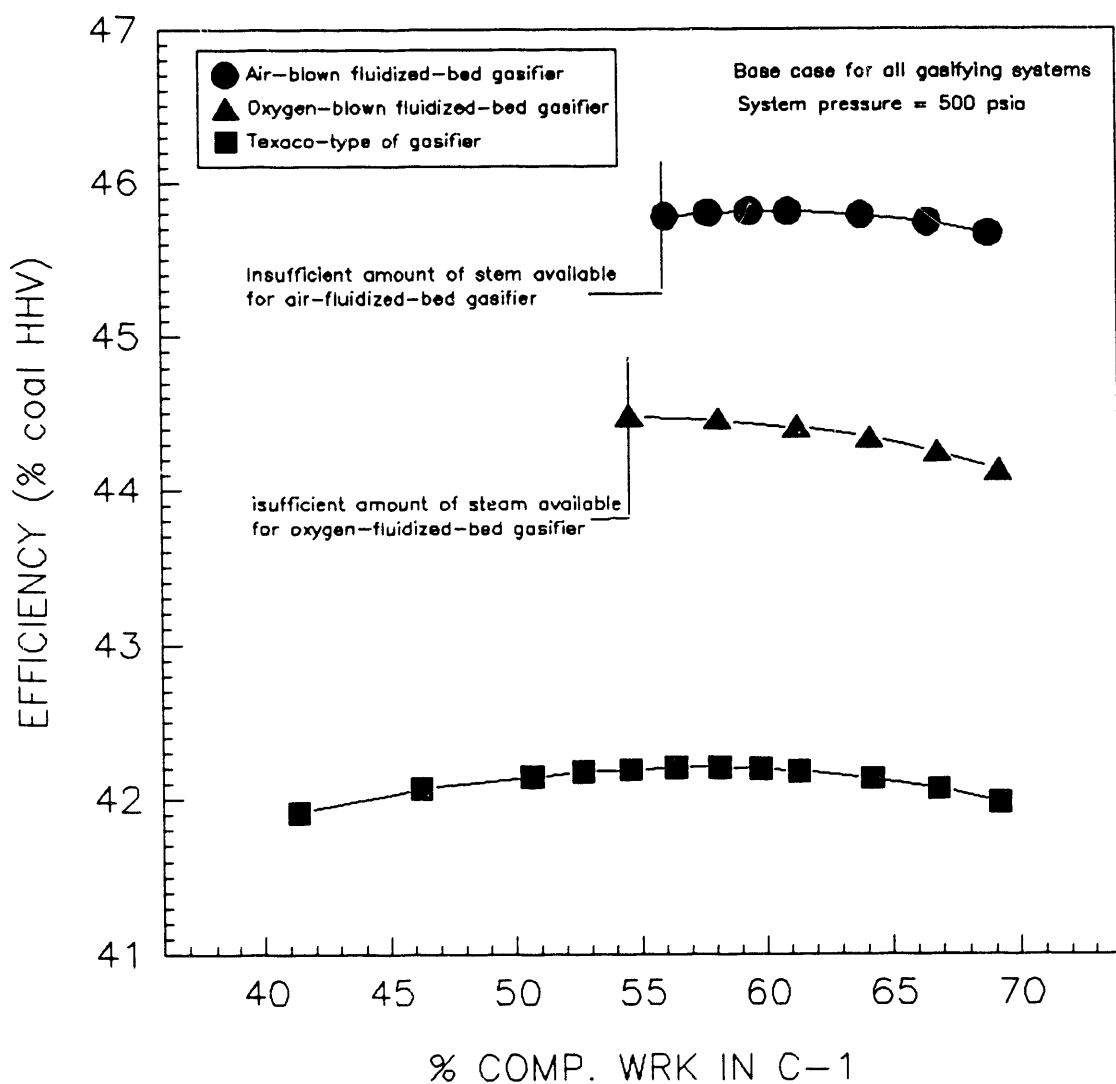
is mostly determined by the intercooling efficiency (which is optimum for "% COMP. WORK IN C-1 = 53%"). This accounts for the location of the optimum in the "oxygen design".

6.1.4 Comparison of the Results for the Three Designs

Figure 6-4 summarizes the results obtained in the different sensitivity analyses discussed in Section 6-1. The scale chosen here is 15-fold larger than the scale used in the individual figures presented earlier. As we can see, the system efficiency is a relatively weak function of the compression-work split, since the curves present little variations with this parameter. However, this by no means implies that the optimization of the compression-work split should not be performed carefully. The throughput and profits involved are indeed tremendous and a slight increase in the system efficiency generates large amounts of money in terms of yearly profits: 0.1 percentage point in efficiency represents a \$178,000 difference in the yearly profits. Figure 6-4 also offers a direct comparison of the performances of the different designs. The fluidized-bed gasifying technologies are very significantly more efficient than the Texaco-type of gasification: plus 2.3 and plus 3.6 percentage points for the oxygen and the air-blown fluidized-bed gasifiers respectively, which represents yearly gains of \$4.1 and \$6.4 millions. These differences are due to the fact that the coal-gas produced by the fluidized-bed gasifiers is richer in CO and H₂ than the gas produced by the Texaco process, and is in other words a better fuel. This naturally results in the higher efficiency observed. The sensitivity analysis also demonstrates that the "air-blown design" has a better efficiency than the "oxygen-blown design". The large energy consumption of the oxygen-plant involved in the latter design appeared to be the main reason for this difference: the "air-blown design" uses compressed air instead of 95% oxygen, which overall requires less energy.

All the remarks and conclusions of the study presented above are based on the results obtained for a system pressure of 500 psia and a maximum allowable clean-up temperature of 1500°F. The object of the next sensitivity analyses is to examine the dependence of the

Figure 6-4:
Efficiencies and Compression-Work Split



system performance on these parameters.

6.2 Efficiency and System Pressure

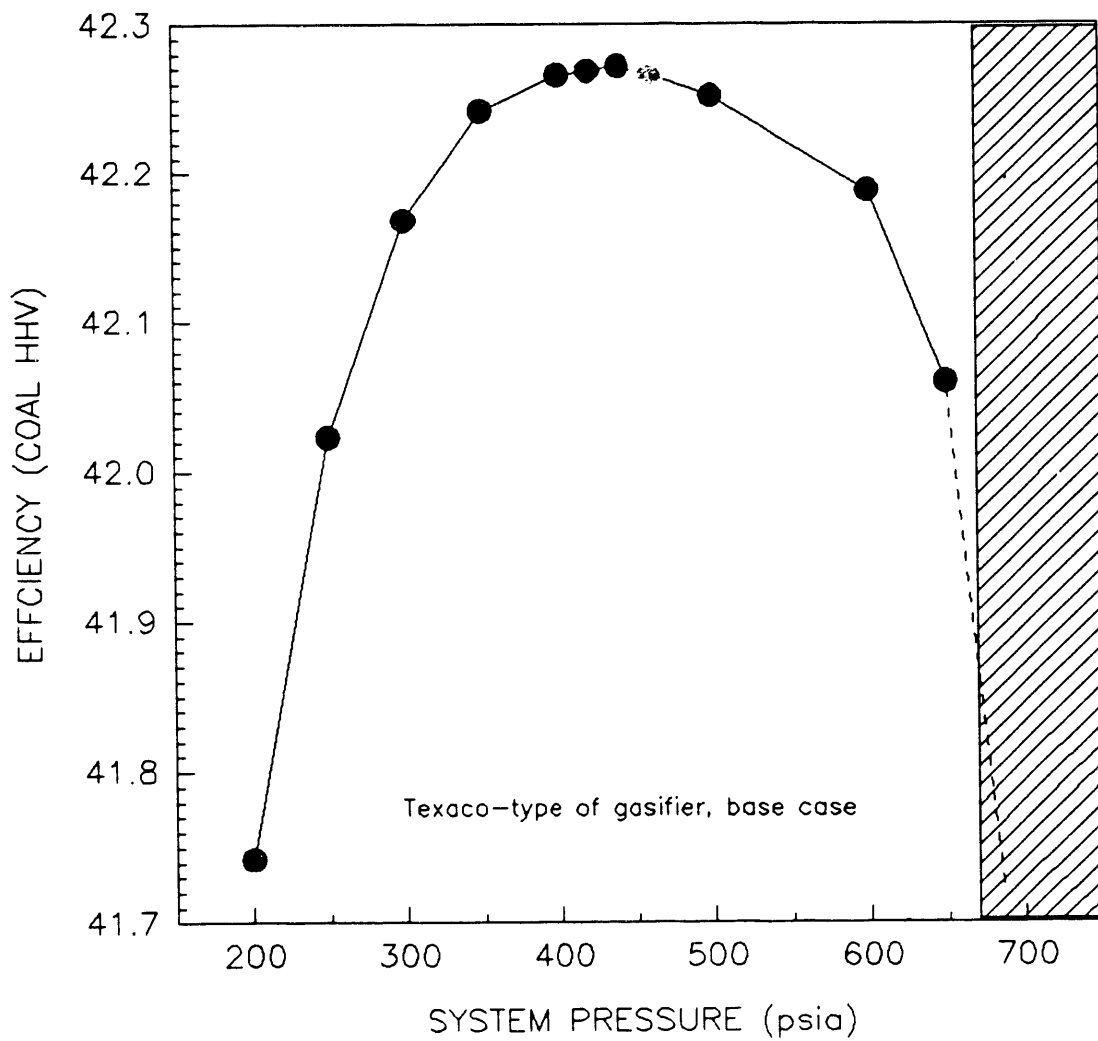
The main effect of a change of system pressure is to modify the expansion ratio of the turbine and the total work of compression. The fact that those two parameters have a major effect on the design performance naturally raises the question of the pressure dependence of the system efficiency. The object of the present section is to quantify this dependence for the different designs studied, and to examine the eventual existence of an optimum operating pressure.

6.2.1 Design Based on The Texaco Gasifying Process

Figure 6-5 details the variations of the efficiency with respect to the system pressure. Note the greatly expanded scale. The efficiencies shown on the graph are the optimum values obtained for each pressure, which usually correspond to a 58% fraction of the work of compression in C-1. It is interesting to note the insensitivity of the system efficiency to the pressure over a wide range of pressures (from 350 to 550 psia). The maximum efficiency is obtained for a system pressure close to 440 psia, which indicates that the 500 psia chosen for our base case simulation provides a good estimation of the optimum performance of the "Texaco design". Outside this plateau, variations in efficiency are more significant: reducing the system pressure from 440 to 250 psia results in a 0.25 percentage point drop in efficiency, which represents a \$360,000 reduction of the yearly profits.

As mentioned above, the evolution of the system efficiency can be explained by the way pressure affects the compression work and the expansion ratio. This ratio is a crucial operating parameter since it determines the turbine exhaust temperature. Large expansion ratios (*i.e.*, high pressures) result in low turbine-exhaust temperatures, which in turn reduces the temperature of the air stream fed to the gasifier. Less excess air is then required to control the firing temperature of the combustor, which reduces both the positive (*i.e.*, increase

Figure 6-5
Efficiency and System Pressure



of the turbine output) and the negative effects (*i.e.*, increase of the compression work) caused by higher system pressures. Conversely, low pressures result in high turbine-outlet temperatures, and hence in smaller air requirements, which has the exactly opposite effect on the turbine output and the compression work. It appears that the global effect of the heat recovery section is to mitigate the consequences of a change in the system pressure, which results in a quite limited pressure dependence of the efficiency. The location of the optimum pressure depends on the specifics of the design considered (*e.g.*, flow of excess air), but the same reasoning holds for each of the three designs involved in the study.

A study of the location of the optimum pressure in the case of the "Texaco design" showed that the position of the optimum pressure is determined by the energy consumption of the oxygen plant in addition to the parameters mentioned before. Because of the large pressure drop occurring between its outlet and the gasifier inlet (Section 4.2), the oxygen-plant power requirements increase at a higher rate than the work of compression, which shifts the optimum pressure towards lower values. The impact of this parameter is very limited however, because of the small pressure-dependence of the efficiency over this range of pressures. The design in this base case has a maximum operating pressure, as shown in the hatched area in Figure 6-5. This limit is due to the rapid diminution of the flow of intercooling water as pressure increases, caused by decreasing requirement for excess air. For pressures higher than 670 psia, there is not enough water available in the system to perform normally. This limitation could obviously be easily overcome by increasing the boiler/intercooler feed-water flow. As explained in Section 4-3, such an increase would result in a steep drop of the a system efficiency, and is therefore not worth examining in our sensitivity analysis.

6.2.2 Designs Based on the Fluidized-Bed Gasifying Processes

The efficiency curves obtained for these designs are shown in Figures 6-6 and 6-7. The optimum pressures are lower than in the "Texaco design": 200 and 250 psia for the oxygen

Figure 6-6:
Efficiency and system pressure

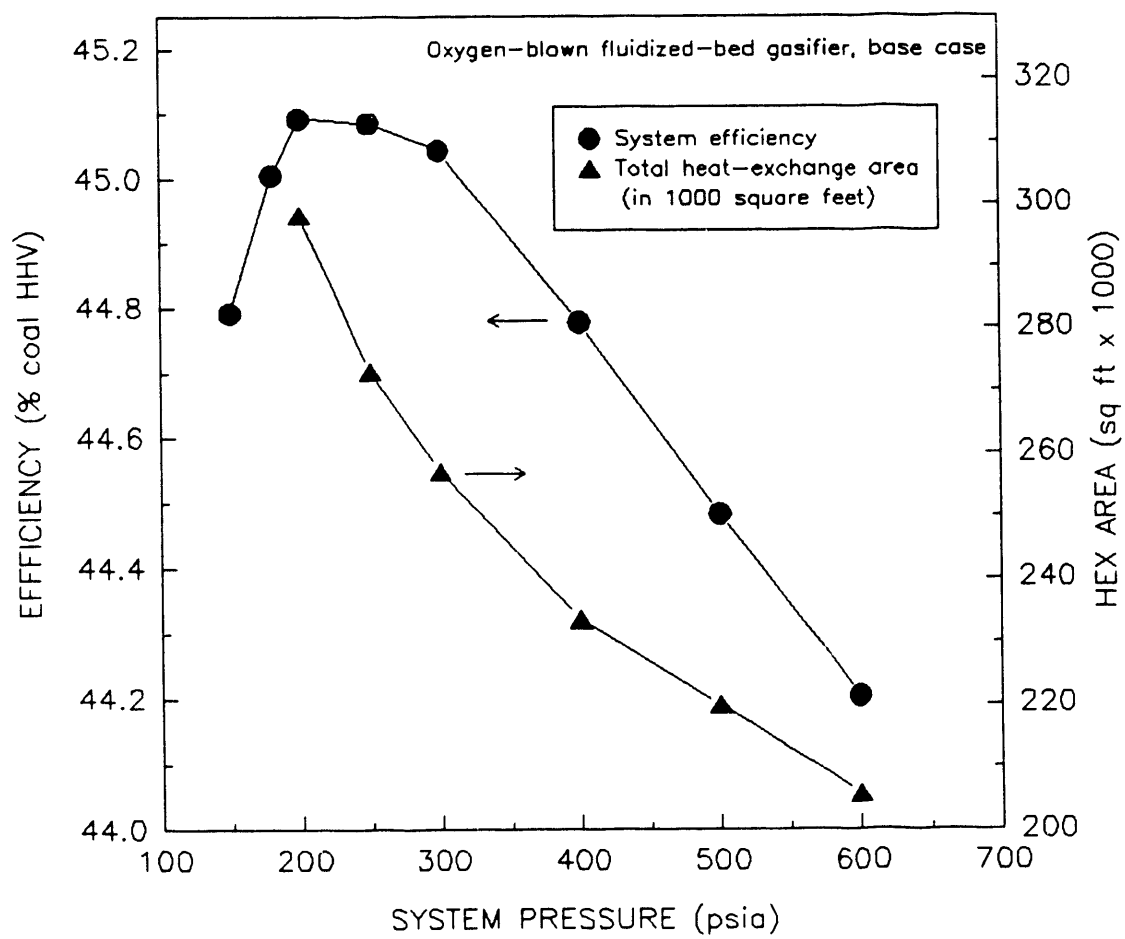
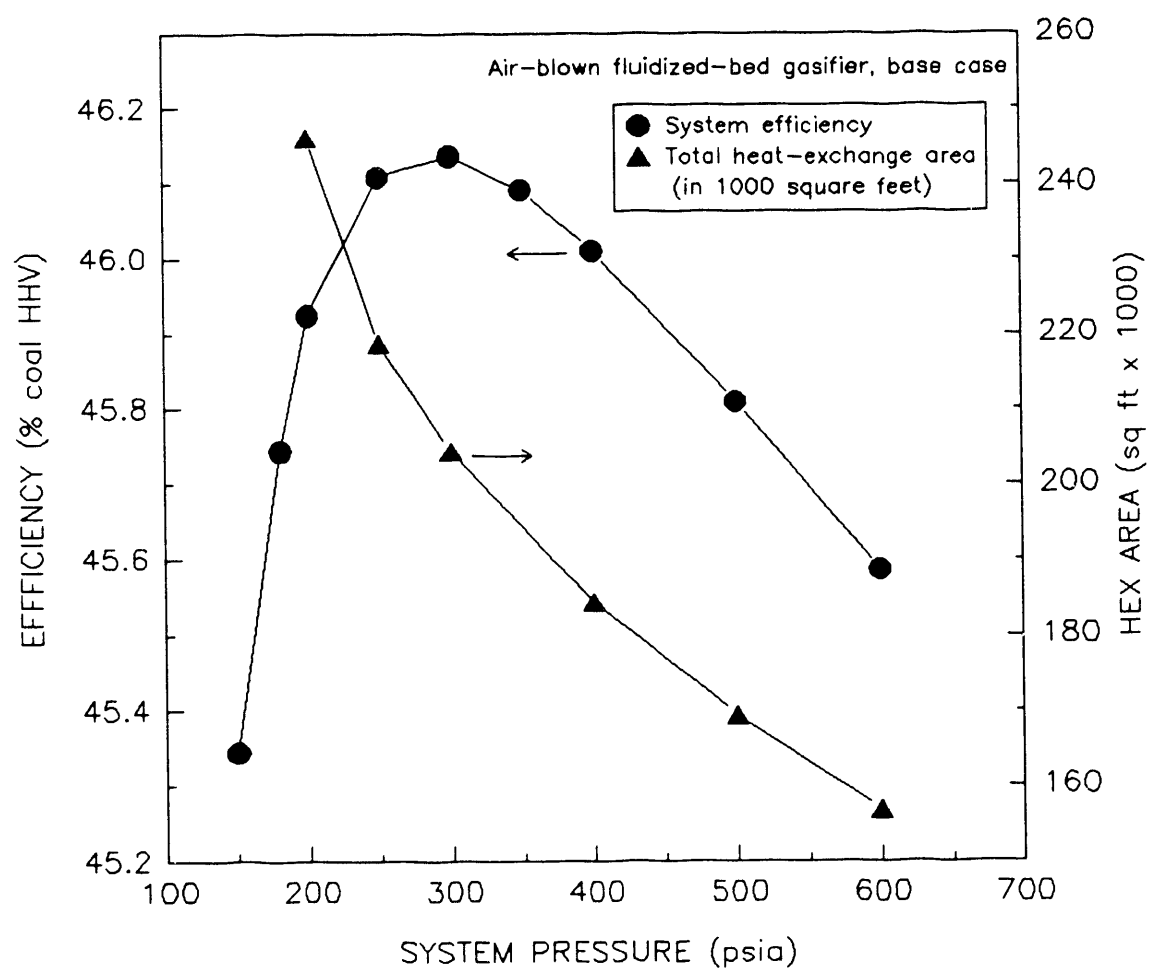


Figure 6-7
Efficiency and System Pressure



and air designs respectively instead of the 440 psia observed in the previous case. The relatively low values of these pressures become a problem when cost optimization is taken into account. At such pressures the total heat-exchange area required for each of the designs becomes really prohibitive, as shown on the same figures. Changing the system pressure from 500 to 200 psia increases the total heat exchange areas by 35 to 45% depending on the design. Considering the order of magnitude of the areas involved (from 180 to 300 thousand ft² total), this will obviously have to be taken into account in an optimization of the designs. The resulting optimum system pressure is likely to be in the range of 400 to 500 psia, as in the "Texaco design". This study also shows that there is a substantial difference between the total heat-exchange areas required in the "fluidized-bed designs". This area is approximately 25% greater in the "oxygen design" than it is in the "air design", which represents a notable difference in the capital investment of the power plant. The main reason for this difference is the disparity in the amounts of excess air required in each design, the excess-air requirement for the "oxygen design" being typically 20% greater than for the "air design".

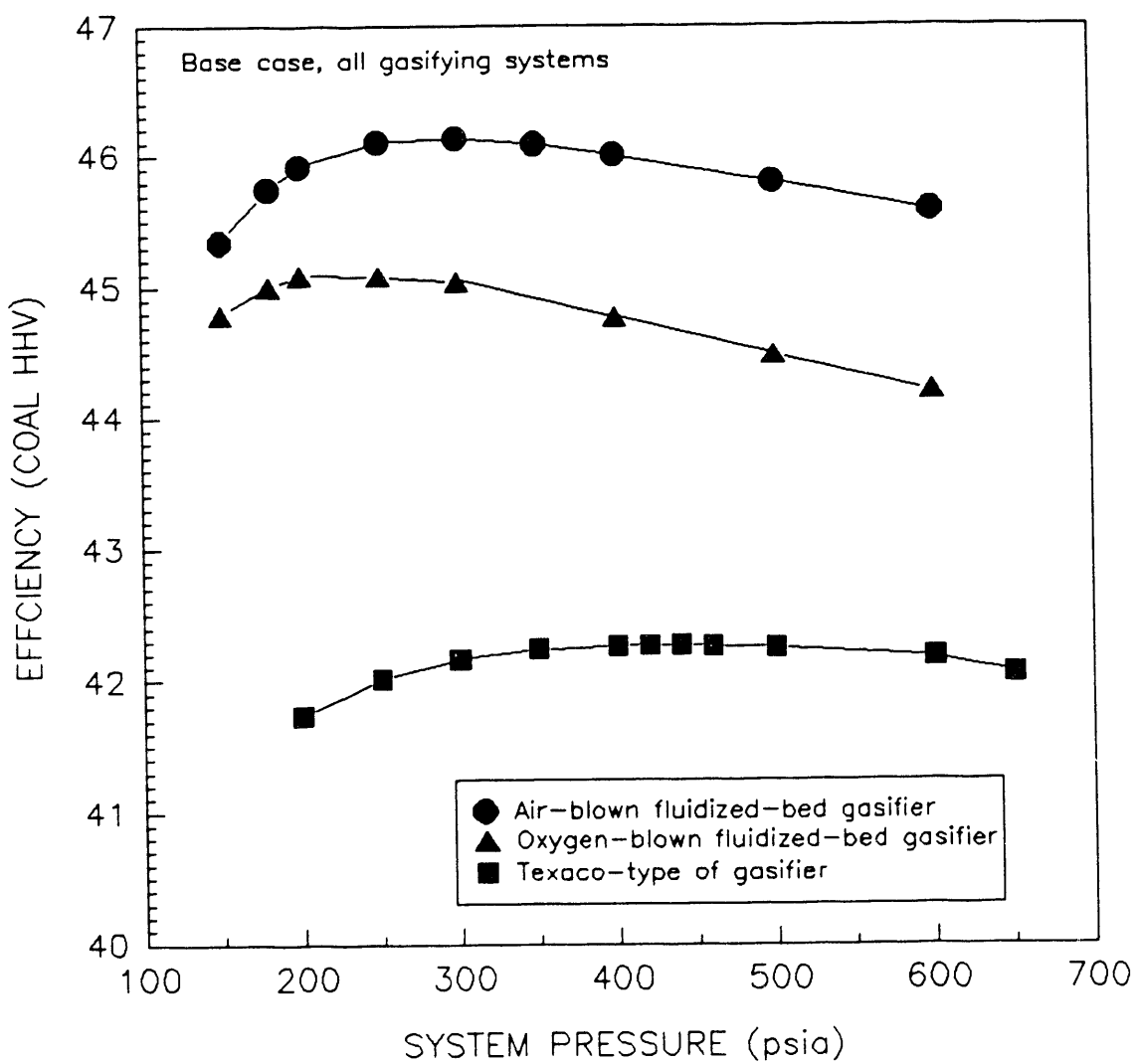
6.2.3 Comparison of the Results Obtained for the Different Designs

The efficiency curves individually examined above are reported on a single graph in Figure 6-8. As mentioned above, an important conclusion of the study is that the system performance is not very sensitive to the pressure, which would be an important consideration in a comprehensive cost optimization. The "fluidized-beds designs" are however slightly more pressure-dependent than the Texaco one.

6.3 Efficiency and Clean-Up Temperature

The maximum allowable clean-up temperature determines the amount of water vaporized in the clean-up section for the coal-gas quench and we can therefore expect the system efficiency to be a strong function of this parameter. The purpose of this section is to investigate and quantify this dependence.

Figure 6-8
Efficiencies and System Pressure



The clean-up temperatures considered cover a 600°F-wide range around the base-case value of 1500°F.

6.3.1 Design Based on the Texaco-Type Gasifying Process

The results obtained for this design are displayed in Figure 6-9. This design has the characteristic of requiring a design modification for a certain range of clean-up temperatures: for temperatures below 1380°F, the amount of water necessary for quenching the coal-gas exceeds the water available in the system, which is normally provided by the boiler feed-water. Below this temperature, the additional water required by the partial quench can be directly provided after being preheated in an economizer located at the cold end of heat exchanger HX-2. The purpose of this economizer is to recover some of the heat available in the stack gas.

The study shows that the system efficiency gains an average of 0.25 percentage point per 100°F increase of the clean-up temperature, which approximately represents a \$450,000 improvement in the annual profit. The system performance depends therefore strongly on this parameter, as anticipated. In addition to the efficiency curve, Figure 6-9 also shows the flow of water leaving the heat-recovery section. As shown in Figure 5-2, this stream is used for two things: it provides the water to the full-quench as well as to the gasifier. In case the amount of water leaving the heat-recovery section exceeds those requirements, the remaining water is sent to a cooling loop. Note that the water requirement for the system (gasifier included) is exceeded for clean-up temperatures higher than 1580°F. For these temperatures, a cooling loop is hence required since there is a net flow of hot water leaving the system. The flow of water directed towards the cooling tower increases by 29 gallons per minute per 100°F increase in the clean-up temperature.

6.3.2 Designs Based on the Fluidized-Bed Gasifying Processes

Similar sensitivity analyses have been performed for the two other designs studied, and the results obtained are shown in Figure 6-10 and 6-11. Because of the large excess of water

Figure 6-9:
Efficiency and Clean-Up Temperature

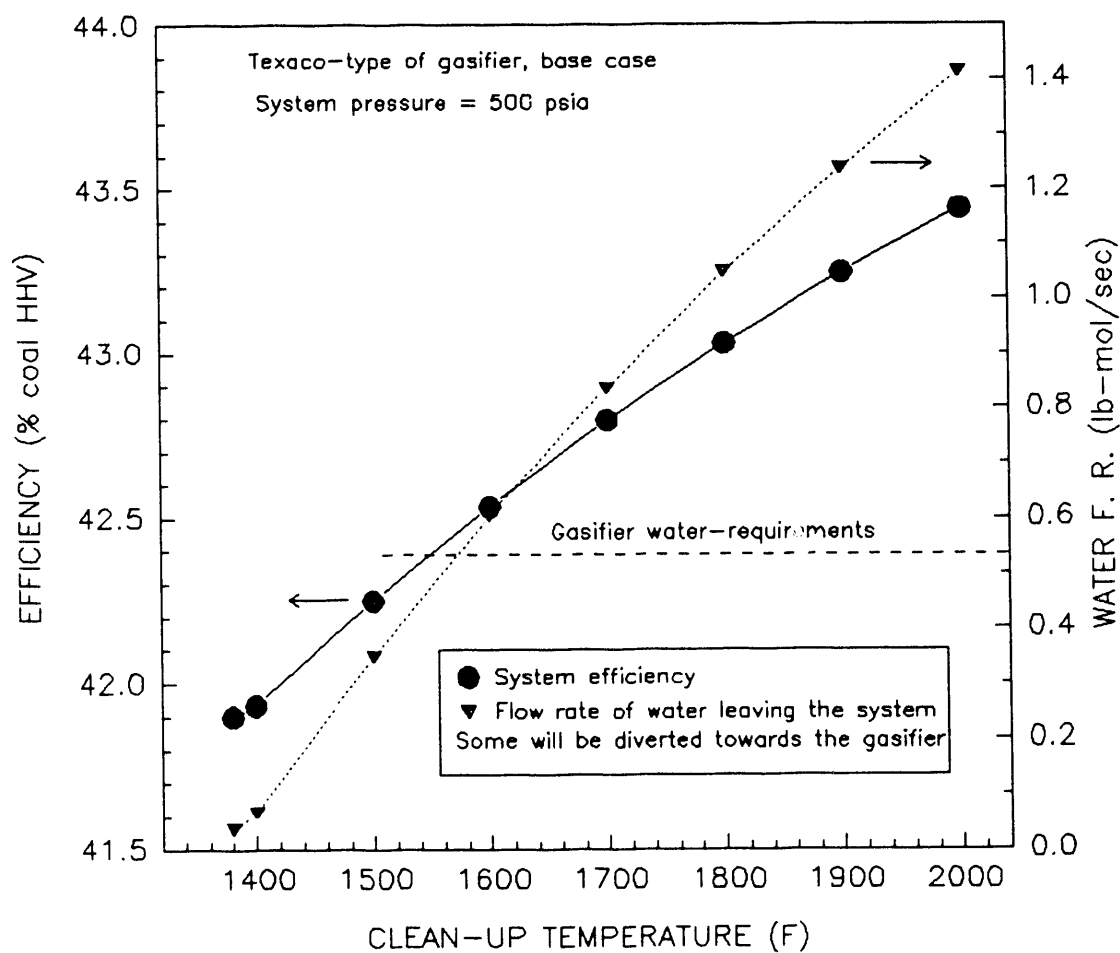


Figure 6-10:
Efficiency and Clean-up Temperature

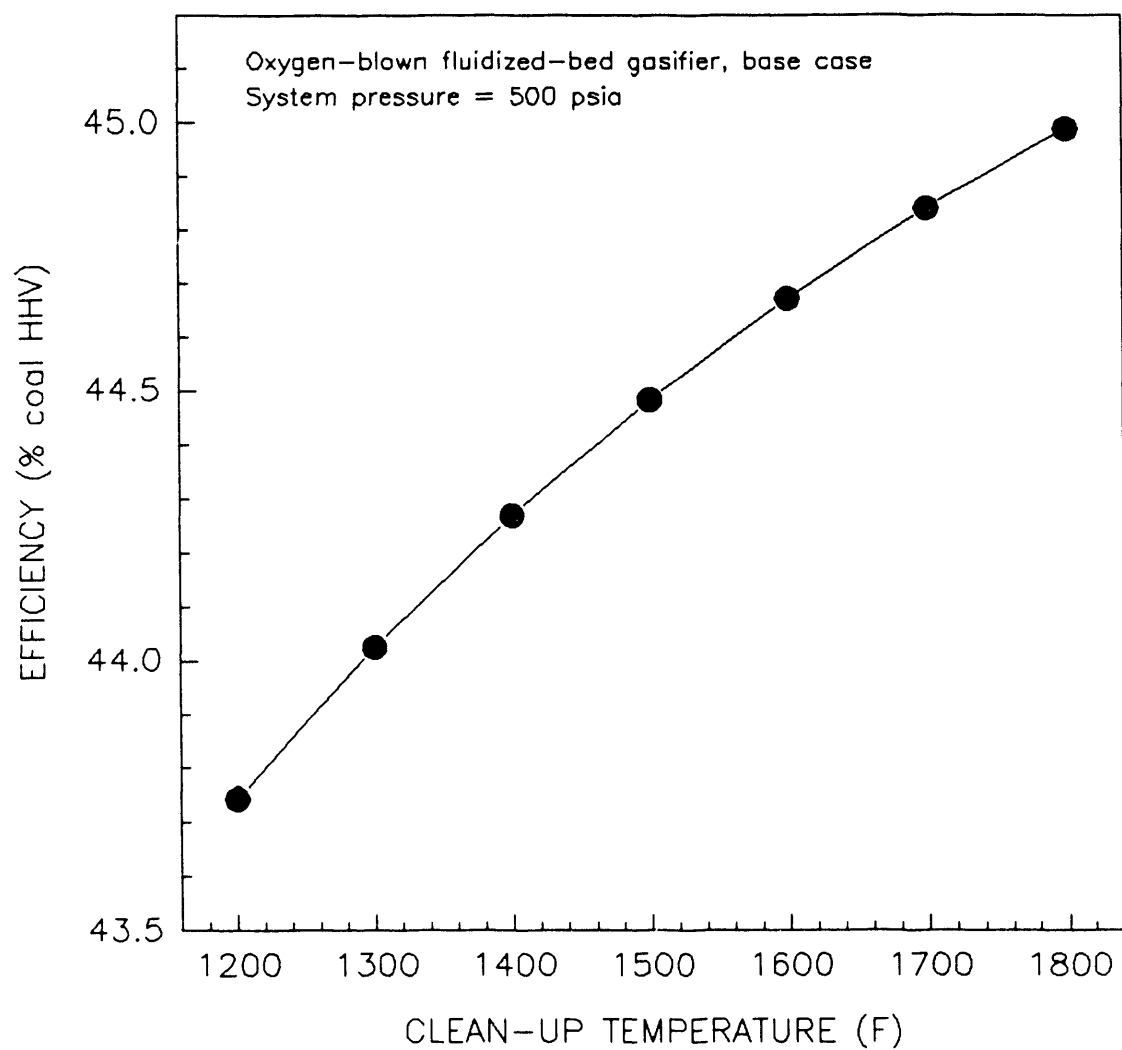
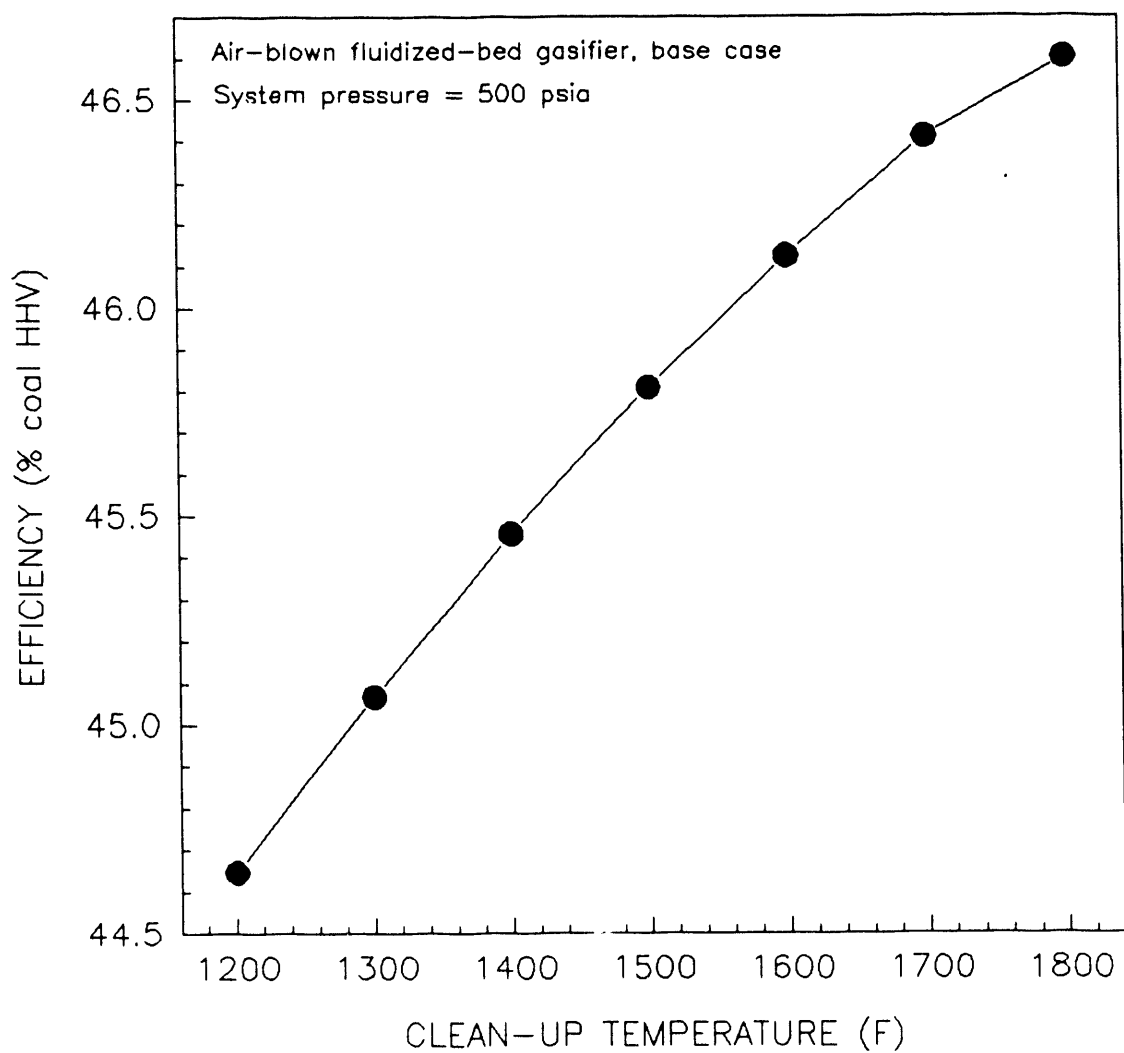


Figure 6-11
Efficiency and Clean-Up Temperature



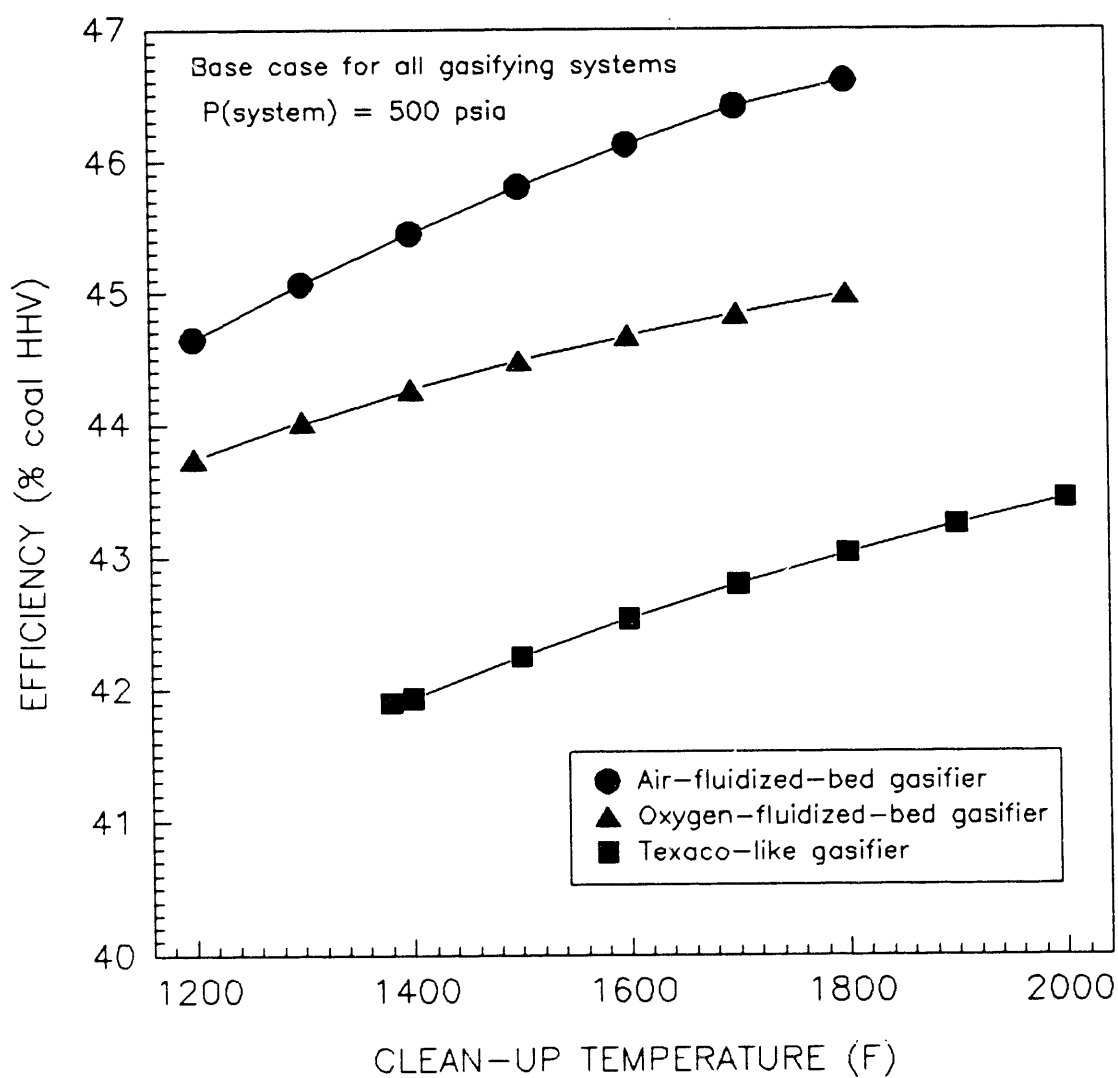
available in the system, no minimum allowable clean-up temperature is observed in the "fluidized-bed designs". The upper limit of the range of temperatures studied is imposed by the coal-gas inlet temperature (1850°F). The system efficiencies shown in the two figures are also strong functions of the clean-up temperature: plus 0.20 and 0.33 percentage points per additional 100°F in the clean-up temperature for the "oxygen" and the "air" designs respectively.

6.3.3 Comparison of the Results Obtained for the Three Designs

Figure 6-12 summarizes the results of the sensitivity analyses for the clean-up temperature. It is interesting to note that the three efficiency curves have different average slopes: 0.23 for the "Texaco design", 0.20 for the "oxygen design" and 0.33 for the "air design" (units: percentage point of efficiency per 100°F of clean-up temperature). This disparity is related to the magnitude of the coal-gas flows in each design: 3.92 in the "Texaco design", 2.44 in the "oxygen design" and 5.02 in the "air design" for a clean-up temperature of 1500°F (units: lb-mol/sec). The bigger the flow, the more a change in its temperature affects the whole system. We can therefore expect the slope of the efficiency curves to vary from one design to the other according to the values of the coal-gas flows entering the combustor, which is exactly what is observed.

Figure 6-12 also gives a clear picture of the incentive for raising the maximum allowable clean-up temperature: going from 1500°F to 1800°F increases the annual profits by \$1.4 million as an average for the three designs. The actual value of the maximum allowable clean-up temperature will however be set by kinetic and physical considerations. These aspects are currently under investigation.

Figure 6-12:
Efficiency and Clean-Up Temperature



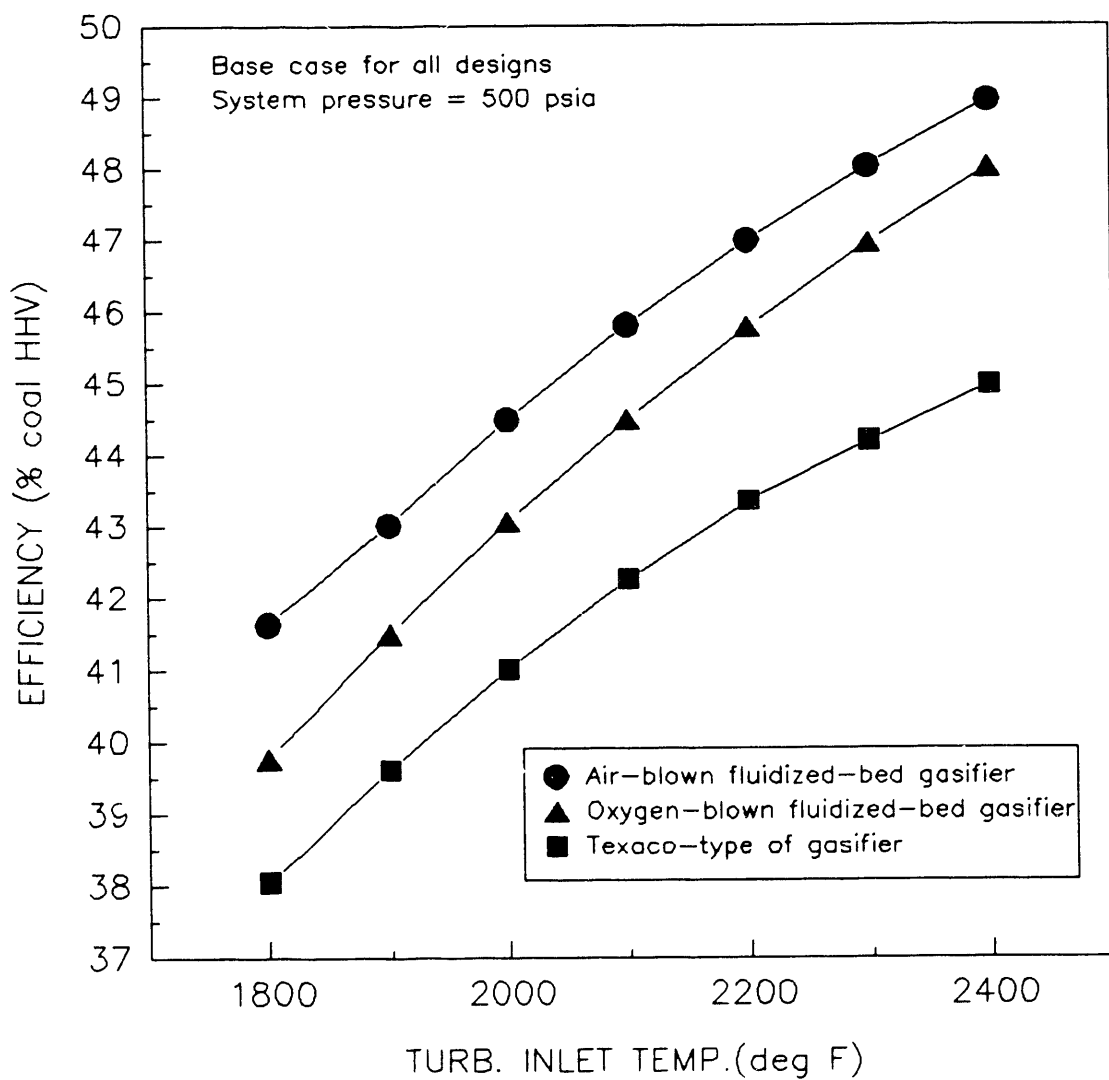
6.4 Efficiencies and Effective Turbine-Inlet Temperature

As explained in Section 2.5.4, a way to simplify the modeling of sophisticated turbines is to use an effective inlet temperature, which was the approach chosen in this work. The purpose of this section is to analyze the sensitivity of the system performance to this parameter. The results of such an analysis can be used to anticipate the increase in system efficiency that would result from advances in turbine technology involving higher maximum-allowable inlet temperatures. They can also be useful to estimate the design performances under different operating conditions and assumptions.

Figure 6-13 presents the results obtained for the three designs investigated in the study. The system efficiencies turn out to be very sensitive to the turbine-inlet temperature: the average slope of the efficiency curves are 1.32, 1.37 and 1.26 (units: percentage points per 100°F) for the "Texaco", "oxygen" and "air" designs respectively, which is approximately five times more important than what was observed for the clean-up temperature. The magnitude of this temperature dependence appears even larger when translated in terms of profits: a 100°F increase in the maximum allowable effective inlet temperature would indeed result in an approximate \$2.35 million yearly gain. It is then easy to understand why tremendous amounts of money are currently being invested in turbine technology.

The major impact of a higher turbine-inlet temperature on the system efficiency can be explained by the combination of three effects. The first effect is to decrease the amount of excess air required to control the firing temperature in the combustor, and hence to reduce the work of compression. The second effect is to raise the temperature of the turbine exhaust gase, which enables a more efficient heat recovery and contributes to enhancing the performance of the design. The third results from the increased work produced by expanding a hotter gas through the turbine. These effects have a very similar impact on the system performance of the three designs, which accounts for the comparable slopes observed. There is however a singularity in the efficiency curve obtained for the "Texaco design", which

Figure 6-13: Efficiencies and Maximum-Allowable Effective Turbine-Inlet Temperature



manifests itself as a change in the slope of the curve for temperatures above 2200°F. Above this temperature, the water requirements of the system exceed the amount of water needed by the boiler/intercooler. It is then necessary to provide additional water to the partial quench to meet these requirements, which penalizes the efficiency and results in a lower slope.

CHAPTER 7: OTHER SENSITIVITY ANALYSES

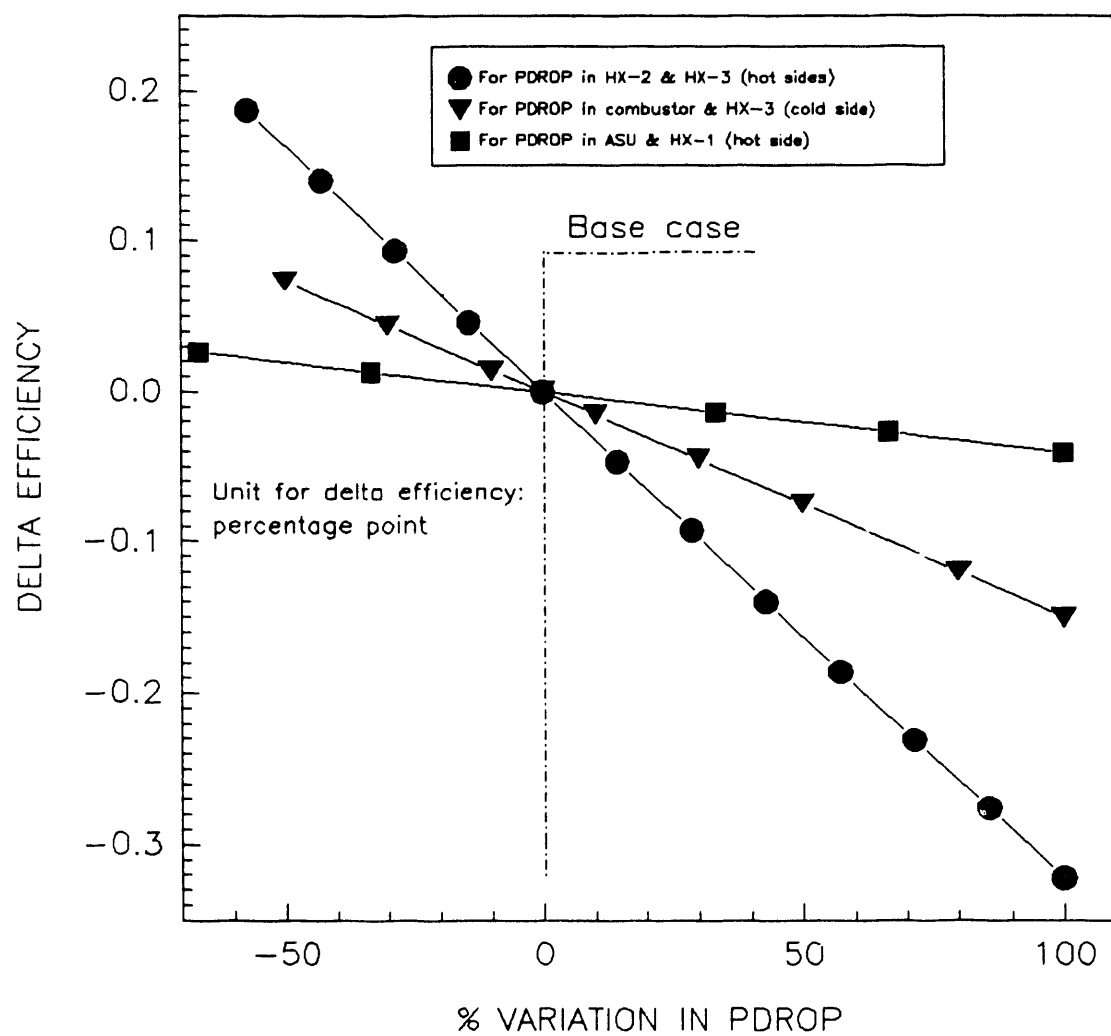
Sensitivity analyses are not limited to the major operating parameters presented in Chapter 6: important assumptions and minor design modifications were also the object of a similar treatment. The purpose of the present chapter is to discuss the results brought by these analyses.

7.1 Efficiency and Pressure Drops

Although they were carefully chosen, the base-case values for the numerous pressure drops involved in the design are quite approximate. Because of the complexity of the design of certain pieces of equipment (*e.g.* large heat exchangers HX-1 and HX-2, combustor) it is indeed difficult to determine most pressure drops with a good accuracy. In some cases (*e.g.* clean-up section), it is even impossible to do so since the actual design of the section is currently under investigation. For those reasons, the approach chosen in the study is to examine the sensitivity of the system performance to the different pressure drops encountered in the design.

The system pressure is defined as the air-stream pressure at the outlet of the second stage of compression. The pressures in the other streams are adjusted by the simulation to match the system pressure set by the user. An important consequence of this set-up is that the pressure drops relative to the air stream have a much larger impact on the system efficiency than those relative to other streams: they indeed directly affect the turbine inlet and outlet pressures (*i.e.*, the expansion ratio), and hence the turbine output. Results of the sensitivity analyses relative to these pressure drops are shown in Figure 7-1 and involves the hot sides of heat-exchanger HX-1 and HX-2, both sides of HX-3, the combustor and the air saturation unit. It might be useful to review the position of those elements in the overall process using one of flowsheets shown in Chapter 5. Figure 7-1 presents a convenient way

Figure 7-1:
Efficiency and Pressure Drops



to examine the dependence that we are interested in: The pieces of equipment involved are grouped when possible and the variations of pressure drops are expressed in percent instead of absolute values. The study revealed that the way pressure drops affect the systems strongly depends on the position of the pieces of equipment relatively to the turbine and to the air saturation unit, which accounts for the grouping shown in Figure 7-1. We will shortly come back to this point in more detail.

The main conclusion of the analysis is that the system efficiency is only very slightly sensitive to changes in pressure drops: a fifty-percent difference in the two most critical pressure drops results in less than a 0.17 percentage point difference in the efficiency. Since the values used in the base case are unlikely to vary more than that from the actual values, the effects of possible errors in the assumptions should be less than 0.2 percentage point in efficiency. In addition, errors are likely to be made in both directions (*i.e.*, under and over-evaluations), which should also minimize their overall effect. The analysis of the results shown in Figure 7-1 also raises interesting points regarding the relative effects of the pressure drops reported. The slopes of the three curves examined are respectively 0.17, 0.08 and 0.02 for $\{HX-2_{hot} + HX-3_{hot}\}$, $\{\text{combustor} + HX-3_{cold}\}$ and $\{\text{ASU} + HX-1_{hot}\}$; the units of these slopes are: percentage points in efficiency per 50% variation of the sum of the pressure drops related to the pieces of equipment given in the brackets; the subscripts "hot" and "cold" refer to the side of the heat exchanger considered. As it was mentioned earlier, the significantly higher slope obtained for $\{HX-2_{hot} + HX-3_{hot}\}$ is due to the downstream position of these heat exchangers relatively to the turbine. This can be explained by the expressing the variations of the turbine expansion ratio as follows:

$$\frac{\Delta ER}{ER} = \frac{\Delta P_{out}}{P_{out}} + \frac{\Delta P_{in}}{P_{in}}$$

where ER is the expansion ratio and P_{in} and P_{out} respectively the inlet and outlet turbine

pressures. This expression shows that, because of their different magnitudes ($P_{in} \approx 500$ psia while $P_{out} \approx 15$ psia), similar changes in P_{in} and P_{out} induce very different variations of expansion ratio. For instance, a 100% change in pressure drop affects ER by 2.0% if it occurs upstream of the turbine (thus affecting P_{in}) and by 4.5% if it does downstream (thus affecting P_{out}), hence the effects observed on the efficiency. The ASU brings a minor additional effect to the one mentioned above, which accounts for the different slopes observed for {combustor + HX-3_{cold}} and {ASU + HX-1_{hot}}. It mitigates the consequences of a change in pressure induced by different upstream pressure drops: larger pressure drops result in a lower pressure in the ASU, where slightly more water is then evaporated, thus reducing the work of compression while the turbine output drops for the reason explained earlier. The decrease in efficiency is therefore somewhat reduced by the effect of the ASU, hence the slopes observed.

Pressure drops relative to the air stream are not the only ones that have been examined. The boiler pressure drop (air side) has also been studied, since it affects the work of compression. The dependence observed is very small however: 0.04 is the slope obtained when expressed in the same units as before. We also examined the pressure drop through the clean-up section for that matter, but the sensitivity observed is even smaller. The other pressure drops (on the liquid sides of the heat exchanger and boiler) have not been studied since they only affect the work performed by the pumps, which has always been neglected in the calculations.

We can conclude that the overall effect of possible errors regarding the pressure drops values chosen in the base case is small and should not affect our assessment of the potential of the Improved Heat Recovery Method. The study presented above moreover gives the means to correct these errors if a higher accuracy is needed.

7.2 Efficiency and Compressor C-3 Outlet Pressure

A problem that we had to solve earlier in this study was to relate the system pressure to the outlet pressure of the oxygen plant or of compressor C-3 (depending on the design considered). In the case of the oxygen plant, we had some actual values to help us choose the relation between the two pressures that we are interested in here (see Section 4.2). In the case of the design based on an air-blown fluidized-bed gasifier, we don't have any actual values we can refer to since such gasifiers are not yet commercially available. The 50-psia difference between the C-3 outlet pressure and the system pressure that we assumed in the base case (Section 5.3) are based on a rough estimate given to us by the M. W. Kellogg Company (Houston). The purpose of the present study is to examine the sensitivity of the "air design" efficiency to this assumption.

Results obtained for a system pressure of 500 psia in this study are shown in Figure 7-2. The range of pressures investigated covers 100 psia around the base case value of 550 psia. The analysis shows that the system efficiency is mildly sensitive to C-3 outlet pressure: doubling the pressure difference from 50 to 100 psia results in a 0.15 percentage point drop in efficiency. This sensitivity is important enough to be taken into account if the actual pressure difference (or ratio) turns out to be substantially different from the one selected in the base case. The graph presented gives a convenient way to make such adjustments.

7.3 Efficiency and Minor Design Modifications

The original idea underlying this part of the study is to improve the design performance by means of slight modification of the flowsheet.

The first modification considered regards the layout of the flowsheet around the Air Saturation Unit (ASU) and more specifically the presence of a side-stream. Figure 7-3-a and 7-3-b show the details of the modifications. For a better understanding of the following explanation, it might be useful to go back to Figure 3-4 to review the way the ASU fits into

Figure 7-2:
Efficiency and Compressor C-3 Outlet Pressure

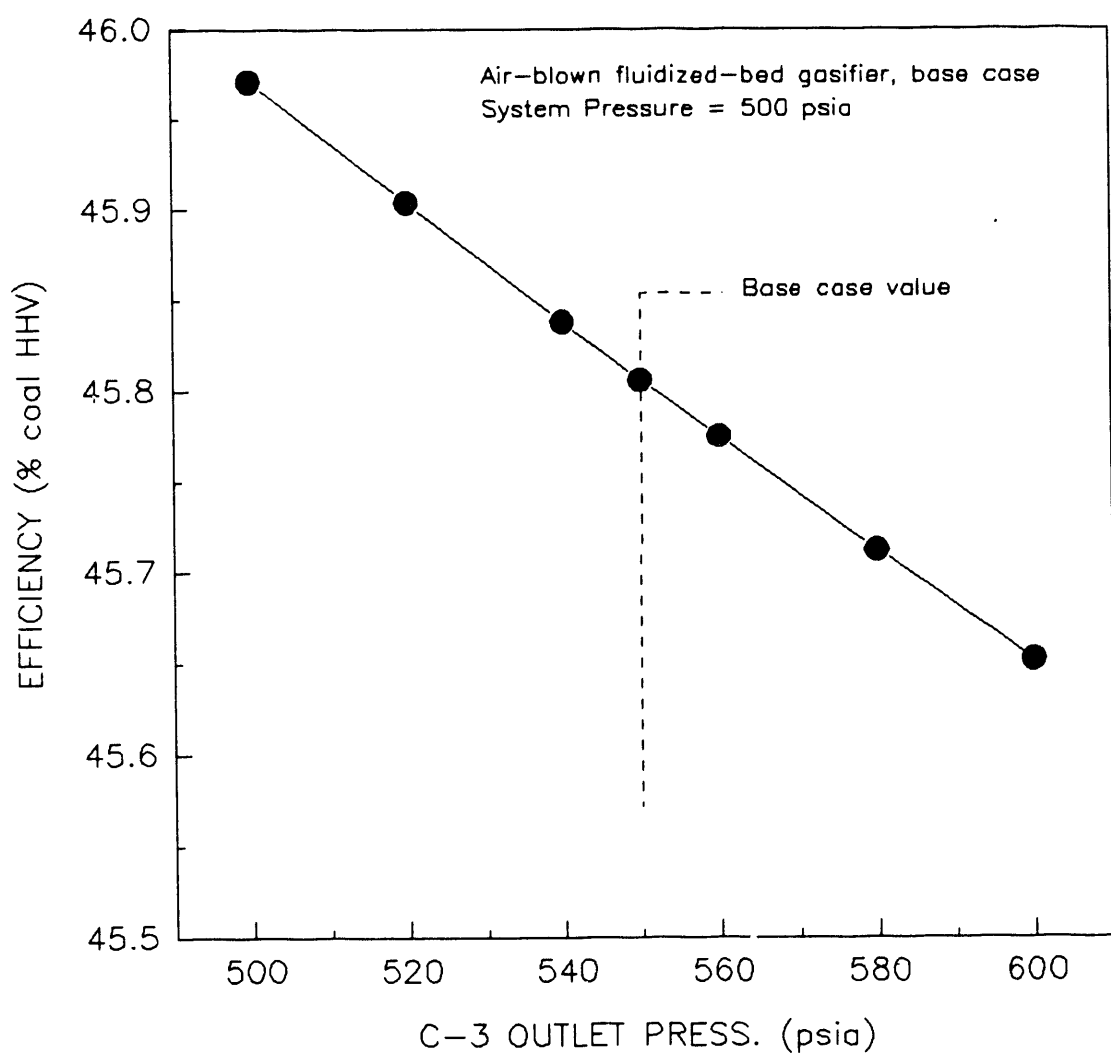


Figure 7-3-a:
Configuration without side Stream

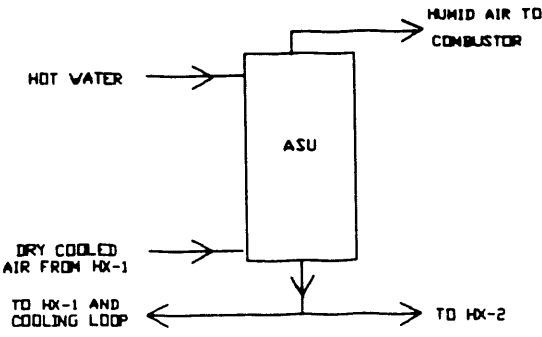
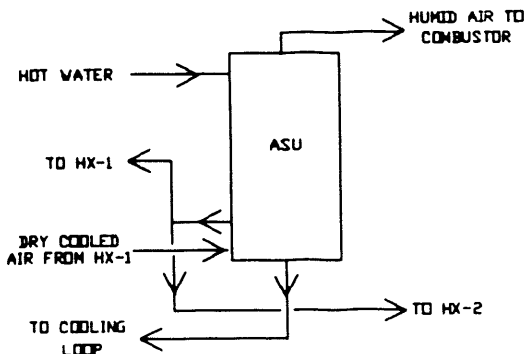


Figure 7-3-b:
Configuration with Side Stream



the heat recovery section. The basic idea involved in the modifications of the ASU is to reduce the temperature and the flow of water leaving the system. A way to do this is to use a higher temperature water in heat exchangers HX-1 and HX-2.

As is shown in Figure 7-3-b, this water may be provided by a side-stream taken from the first theoretical stage of this ASU. A higher water temperature induces larger water requirements in HX-1 and HX-2. Taking a large side stream also results in a significant decrease in the temperature of the water leaving the bottom of the ASU (approximately 7°F). On the other hand, doing so reduces the contact between the air and the water streams in the ASU and slightly lowers the amount of water evaporated per mole of air. This in turn causes a slight increase in the flow of excess air required, in the work of compression and in the boiler-feed water flow. Going from a "without side stream" to a "with side stream" configuration therefore results in two opposite effects on the system efficiency, the balance of which is difficult to foretell since it depends on the specific values of the air and water flows encountered in each design. Actual base-case computations showed that the design modifications described earlier have a negligible effect on the system performance: taking a side stream increases the efficiency by 0.04 percentage points in the "air design" while it reduces it by 0.02 percentage points in the "oxygen design". There is no point in

implementing the change in the Texaco design since all the water available is used by the system. In addition to its inconclusive improvement of the system performance, the "side stream design" is more costly because of the construction complications it induces, which makes it even less attractive. The simple "no side stream design" should therefore be kept.

The other design modification examined involves the source of water for the partial quench. In the original design, this water is provided by the stream going to the cooling loop. We tested the effect of taking the water from the boiler outlet instead, the idea being that it could result in a somewhat greater use of water in the system. The effect observed are too small to be considered since the variation of efficiency observed is smaller than 0.05 percentage point, and therefore there is no reason to modify the base-case design for this feature.

7.4 Is the Presence of HX-1 Justified?

The role of HX-1 is to increase the temperature and flow of the water stream fed to the top of the ASU by recovering heat from the hot compressed air. Doing so increases the amount of water vaporized in the ASU, which results in a reduction of compression work and in a higher efficiency. The question that we want to address here is to know very approximately whether HX-1 is justified or not from an economic point of view. For the "Texaco design" and a base case situation, suppressing HX-1 results in a 0.84 percentage point loss in efficiency, which represents an approximate \$1.5 million yearly loss. A cost estimation based on the calculations performed in a similar situation gives a total module factor of \$3.3 millions (1990) (Higdon, 1988). The rate of return on the investment represented by the heat exchanger turns out to be 45%, which tends to indicate that HX-1 is a very good investment and should figure in the design. In some extreme cases (low pressures in the "fluidized-bed designs" design for instance) the heat transfer surface area of HX-1 is so large that the investment might be questionable. A more detailed cost optimization would be then necessary.

to judge the soundness of the investment in HX-1. Other than these extreme cases, our rough estimation shows that the presence of HX-1 in the process is justified.

CHAPTER 8: CONCLUSIONS

The computer simulations discussed in this work successfully fulfilled the goals set in Section 2.1, which can be summarized as follows:

1. Develop efficient designs based on the IHRM (Improved Heat Recovery Method) and quantify their thermal efficiencies.
2. Compare the performances of the IHRM obtained for different gasifying processes.
3. Compare the performances of the IHRM with other state-of-the-art heat-recovery methods and from there assess its potential interest for industry.

1. The study showed that typical thermal efficiencies obtained with the IHRM are 45.0% and 46.0% for the designs respectively based on the oxygen-blown and air-blown fluidized-bed gasifiers, and 42.2% for the Texaco gasifier. All the efficiencies reported in this work are based on the High Heating Value of the coal (HHV) and are relative to the assumptions and operating conditions listed in Table 5-1. The study also revealed the dominant operating parameters in terms of their effects on the system performances. The efficiencies are for instance insensitive to moderate changes in the system pressure or in pressure drops, while it is substantially more dependant on the compression-work split. The operating parameters the most strongly affecting the system performance are the clean-up and the turbine-inlet temperatures. Along with the dependence of the efficiency on the different operating parameters examined, the sensitivity analyses provide useful information about optimum operating conditions encountered for each design.

2. Our analyses yielded interesting results as far as the relative performances of the three designs is concerned. It appeared that the fluidized-bed gasifying processes result in

a very significant increase of efficiency over the Texaco process: plus 3.8 and 4.8 percentage points of efficiency for the oxygen-blown and the air-blown designs respectively, which represents \$6.7 and \$8.6 millions of increased yearly revenues for the base-case calculations (130-MW power plant). Interestingly enough, there is also a significant difference (1 percentage point) between the two "fluidized-bed designs". The "air design" has remarkable advantages over the "oxygen design": Besides having a substantially higher thermal efficiency, it avoids the large capital investment of an oxygen plant in addition to requiring approximately 25% less heat-exchange surface area. However, these advantages are offset to some extent by a higher capital cost of the gasifier itself because of the higher gas flow through it, and the capital cost of the two designs can be expected to be similar.

We haven't performed an economic analysis to determine the capital cost per kW produced for each design. To be meaningful, such an analysis would require a quite accurate design of the different parts of the process, which is outside the scope of this study.

3. It is inherently very difficult to compare the performances of different power-generations systems, since they depend on operating parameters that can vary a lot from one design to the other. Given these limits, it is nonetheless possible to make a rough comparison by using estimations available in recent publications. We will limit our comparison to the most advanced technologies for coal-based power generation, since those are the ones the IHRM would have to compete with. This accounts for the fact that the ISTIG technology described in Section 1.4 is not mentioned in the comparison, since its performance is not competitive in the case of coal-gas power plants. As a landmark however, it is useful to keep in mind the 34% efficiency typically obtained in a conventionally-fired steam power plant currently in operation. The thermal efficiency of the Texaco Integrated Gasification Combined Cycle (TIGCC) is close to 35%, which is much lower than the 42% obtained with the IHRM for the same gasification process (Rodgers and Maude, 1989). The enormous

difference of 7 percentage points shows that for this type of gasifier, the IHRM indisputably represents a large improvement. However, the performances of the TIGCC are relatively poor compared to what constitute the "state of the art" in the power generation technology. The most efficient technologies currently tested are the British Coal Topping Cycle, the Kellogg Rust-Westinghouse IGCC (KIGCC) and the Pressurized Fluidized Bed Combustion (PFBC) processes. The efficiencies obtained by these processes are respectively 45.5%, 42% and 42% (Rodgers and Maud, 1989). The KIGCC uses the same gasifier as our "air design", and is therefore the most meaningful for a comparison. It seems that, with its 46% predicted efficiency, the IHRM is very competitive with the KIGCC and its 42% efficiency. Data available however indicate that the Topping Cycle and its 46% predicted efficiency would probably result in a better performance than the IHRM. Lastly, we can also compare the performance of the IHRM with the results obtained by the advanced heat recovery method developed by Lynn and Russell (Russell, 1989). This method uses a medium-temperature coal-gas clean-up. When calculated on the same bases, the efficiencies obtained with the IHRM associated with a high-temperature clean-up are substantially higher than the ones obtained with the advanced design: plus 2.1 and 1.7 percentage points respectively for the Texaco and the fluidized-bed designs. The biggest part of these differences result from a higher clean-up temperature.

In conclusion, the IHRM has the potential for being a promising alternative to the advanced technologies already in their pre-commercial testing phases. Much more work needs to be done, however, on the large-scale design, the main tasks being to evaluate the capital cost per kW generated by this process and to refine the model used in the simulation. But before this stage is reached, a crucial part of the process presented in the study has to be completed. The study revealed the large impact of the clean-up temperature on the system performance. In order to carry on the analysis of the IHRM, the characteristics of the high

temperature clean-up were assumed. The feasibility of this clean-up method however remains to be demonstrated and a process design has to be developed before the study presented in this work is truly completed. These aspects are currently under investigation. The simulation has been designed to accommodate different situations with a minimum of modification; if the final clean-up process selected were to be different from the "fictitious process" used in this study, the new system performance could therefore be easily evaluated. The sensitivity analysis presented in Section 6-3 provides a quite accurate way to estimate the new performance quickly.

REFERENCES

Barin, I., and Knacke, O., *Thermodynamics Properties of Inorganic Substances*, Springer Verlag, Berlin, 1973.

Brandt, D.E., "Heavy-Duty Turbopower: the MS7001F", *Mechanical Engineering*, 109 (7), 28-37 (1987)

Eckert, J.S., "No Mystery in Packed-Bed Design", *Oil & Gas Journal*, August 24, 1970.

EPRI (Electric Power Research Institute), "Cost and Performance for Commercial Applications of Texaco-Based Gasification-Combined-Cycle Plants, Volume 2: Design Details", *EPRI Report AP-3486*, Chapter 2, 1984.

Fulkerson, W., Judkins, R.R., Sanghvi, M.K., "Energy from Fossile Fuels", *Scientific American*, September 1990.

Higdon, C.R., Louks, B.M., and Lynn, S., "A Novel Heat-Recovery Process for Improving the Thermal Efficiency of Gas Turbines in Electric Power Generation", presented to the 52nd Annual American Power Conference, Chicago, April 23-25, 1990.

Higdon, C.R., *A Novel Heat Recovery Process for Improving the Thermal Efficiency of Gas Turbines in Electric Power Generation*, Master Thesis, Department of Chemical Engineering, UC Berkeley, CA, 1988.

Irvine, T.F., and Liley, P.E., *Steam and Gas Tables with Computer Equations*, Academic Press, Inc., New York, 1984, pp 21-50.

King, J.C., *Separation Processes*, McGraw Hill Book Company, Inc., New York, 1980, pp 480-481, 811-824

Kirk, R. and Othmer, D., *Encyclopedia of Chemical Technology*, second edition, volume one, The Interscience Encyclopedia Inc., New York.

Louks, B.M., Project Manager, Advanced Power System Division, Electric Power Research Institute, Palo Alto, California, personal communication, June 18, 1987.

Newman, J.S., "Numerical Solution of Coupled, Ordinary Differential Equations", *Industrial and Engineering Chemistry: Fundamentals*, 7, 514-517 (1968).

Prausnitz, J.M., Lichtenhaler, R.N., and de Azevedo, E.G., *Molecular Thermodynamics of Fluid-Phase Equilibria*, Second Edition, Prentice Hall, Inc., Englewood Cliffs, New Jersey, 1986, pp. 93-137.

Rodger, B.R., Maude, C.M., "Comparison of Advanced Power Generation Technologies Using Computer Simulation", presented at the American Institute of Chemical Engineers, Annual Meeting, San Francisco, California, November 5-10, 1989.

Russell, J.V., *Development and Evaluation of a Superior Heat Recovery Design for Gas-Turbine Systems Using Gasified Coal*, Master Thesis, UC Berkeley, CA, 1989.

APPENDIX

The Appendix to this report, a 119-page description and listing of the computer code used to simulate the flow configurations discussed above, is available upon request from:

**Professor Scott Lynn
Dep[artment of Chemical Engineering
University of California
Berkeley, CA 94720-9989**

END

**DATE
FILMED**

12/10/1911

